

**Proceedings of the 1973 Workshop
on
Naval Applications of Superconductivity**

**November 28-29, 1973
Naval Research Laboratory
Washington, D.C.**

Sponsored by

CHIEF OF NAVAL RESEARCH AND NAVAL RESEARCH LABORATORY

October 30, 1974



**NAVAL RESEARCH LABORATORY
Washington, D.C.**

Approved for public release; distribution unlimited.

A total of nineteen papers were presented describing various on-going programs in the uses of superconducting materials and devices in the following areas of potential application:

- 1) magnetometers and gradiometers for ASW sensors and for ELF and HF antennas,
- 2) superconducting resonant circuits for HF applications,
- 3) mm and sub-mm radiation detectors,
- 4) superconducting motors and generators for ship propulsion systems,
- 5) superconducting solenoids for airborne minesweeping and underwater acoustic transducers.

Reviews of the ONR Contract Research Program in superconductivity and the NRL program in superconducting materials were also presented.

This report contains the unclassified papers presented at the Workshop, while the classified papers are contained in a separate report (NRL Report No. 7823).

PREFACE

The 1973 Workshop on Naval Applications of Superconductivity was held at the Naval Research Laboratory in Washington, D. C. on 28-29 November 1973. This workshop was co-sponsored by the Office of Naval Research and the Naval Research Laboratory and has been coordinated with the Chief of Naval Development. This was the second such workshop; the first was held on 4-6 November 1970 at the Naval Coastal Systems Laboratory in Panama City, Florida.

Since the first workshop, interest within the Navy in applications of superconductivity has increased significantly, and there are a number of pertinent research and development programs now underway. The intent of this meeting was to exchange information concerning these current programs and to discuss future plans. The meeting also provided an opportunity for administrative and Fleet personnel to become acquainted with the potential systems improvements which can result from the successful exploitation of this new technology. It is hoped that meeting of this type will encourage more effective interaction among the Naval laboratories and expedite the transfer of superconductive technology from the research and development areas into the Systems Commands and ultimately into the Fleet.

The Program and Organizing Committee consisted of the following:

M. Nisenoff, Naval Research Laboratory, Chairman

Ted G. Berlincourt, Office of Naval Research

Edgar A. Edelsack, Office of Naval Research

Richard G. Brandt, Office of Naval Research, Pasadena Office

Robert A. Hein, Naval Research Laboratory

In order to insure a free and open discussion of ideas and plans, the committee decided that attendance at this Workshop would be restricted to Naval personnel with a limited number of observers from other units of the Department of Defense.

The Organizing Committee contacted the various Naval laboratories where R&D programs in applications of superconductivity were known to be in progress and these groups were invited to present talks at the Workshop. In response to the initial announcement a number of other organizations asked if they could also present talks at the meeting. In keeping with the above objectives, a few short communications were included in the program.

The Workshop was conducted as a classified meeting so that the discussions could be as free and unencumbered as possible. However, because of security considerations, the Proceedings of the Workshop are being published in two parts; this document contains the unclassified papers while a separate document (NRL Report No. 7823) contains the classified reports.

The successful running of any Workshop can only be accomplished with a great deal of help from many people. In particular, the Committee would like to thank Mrs. Jean B. Quick who did the typing of the announcements and various mailings, and assisted in handling the replies. The assistance of Mr. H. Poole and Mr. James Gately of the Public Affairs Branch, NRL, who arranged for the auditorium, buses, signs, etc., is greatly appreciated. During the Workshop, the registration was very efficiently "manned" by Mrs. Quick, Mrs. Carolyn Hepler and Mrs. Lahni Blohm.

In conclusion, we would like to express the appreciation of the Committee to the Office of Naval Research, Code 420, for providing the necessary funds to cover the expenses of running the Workshop and for the publication of these Proceedings.

M. NISENOFF
Chairman

TABLE OF CONTENTS

PREFACE iii

WELCOMING REMARKS ix

 Capt. J.T. Geary, USN
 Naval Research Laboratory
 Washington, D.C. 20375

MAGNETOMETRY

SUPERCONDUCTING MAGNETOMETRY 1

 M. Nisenoff
 Naval Research Laboratory
 Washington, D.C. 20375

ONR SUPPORTED SUPERCONDUCTIVITY RESEARCH – 1973 39

 Edgar A. Edelsack
 Office of Naval Research
 Arlington, Virginia 22217

COMMUNICATION APPLICATIONS

HF APPLICATIONS OF SUPERCONDUCTIVITY 48

 Nancy K. Welker and Fernand D. Bedard
 National Security Agency
 Fort George G. Meade, Maryland 20755

SUPERCONDUCTING HIGH FREQUENCY RESONANT CIRCUITS 61

 C. Hobbis and L. Weinman
 Naval Research Laboratory
 Washington, D.C. 20375

SUPERCONDUCTING ANTENNAS FOR LOW FREQUENCY
COMMUNICATIONS 81

 S.A. Wolf, J.R. Davis and M. Nisenoff
 Naval Research Laboratory
 Washington, D.C. 20375

JOSEPHSON-EFFECT DETECTORS AT MILLIMETER AND SUBMILLIMETER WAVELENGTHS	83
Richard G. Brandt Office of Naval Research Pasadena, California 91106	
SUPERCONDUCTING RADIATION DETECTORS — THEIR DEVELOPMENT AND APPLICATIONS POTENTIAL	101
Douglas M. Warschauer Naval Weapons Center China Lake, California 93555	
SUPERCONDUCTING MATERIALS RESEARCH AT NRL	109
R.A. Hein and R.A. Meussner Naval Research Laboratory Washington, D.C. 20375	
SUPERCONDUCTIVITY RESEARCH IN USSR WITH COMMUNICATION APPLICATIONS (Title Only)	122
J.T. Coleman Naval Intelligence Support Center Suitland Maryland 20023	
SHIP PROPULSION	
DEVELOPMENT OF THE ACYCLIC SHAPED FIELD MOTOR	123
M. Cannell, T. Doyle, S. Raphael Naval Ship Research and Development Center Annapolis, Maryland 21402	
ACYCLIC SUPERCONDUCTIVE GENERATOR DESIGN	138
Leroy T. Dunnington, Howard O. Stevens, and Michael J. Superczynski Naval Ship Research and Development Center Annapolis, Maryland 21402	
PERFORMANCE ADVANTAGES OF SUPERCONDUCTING SHIP PROPULSION (Title Only)	166
G. Green, W.J. Levedahl, H. Robey and D.B. Steen Naval Ship Research and Development Center Annapolis, Maryland 21402	

SOLENOIDS

SUPERCONDUCTIVITY IN AIRBORNE MINESWEEPING (Title only) 167

D.A. Ross
Naval Air Systems Command
Washington, D.C. 20360

WELCOMING REMARKS

CAPT. J.T. Geary, USN
U.S. Naval Research Laboratory
Washington, D.C. 20375

UNCLASSIFIED

Good Morning. On behalf of the staff of the Laboratory, it is indeed a privilege to welcome you to this second Workshop in what we hope will be a fruitful meeting on naval applications of superconductivity.

As you know, the Workshops are co-sponsored by the Office of Naval Research and NRL. I would like to express RADM Van Orden's regrets that he could not be here, especially since he had been looking forward to attending this meeting.

The first Workshop in this series was held in 1970 at the Naval Coastal Systems Laboratory in Panama City, Florida. In this first meeting, I am told that there were but 63 attendees from the Navy. It is refreshing to note the sizeable increase in Navy interest which this current meeting represents.

I am certain the support given this conference by the Chief of Naval Development, the CNM Laboratories and the Syscoms, as well as the participation of our colleagues from the National Security Agency and the Applied Physics Laboratory will have a strong and positive influence, and is certainly indicative of increased participation in this emerging field.

The stated purposes of this Workshop are to exchange information on current programs and future plans for the Navy, and to encourage interaction among the Naval Laboratories to expedite the transfer of this technology from R & D into production and, ultimately, to the Fleet. Accordingly, the atmosphere in which our discussions take place is charged with the spirit of some urgency in solving a real problem in the translation of technology to operational systems in response to real operational needs.

The role of the Navy's laboratories is to pursue research and development work on emerging technologies which will be the basis of the next generation of Navy electronic, communications, fire control, and propulsion systems. And the R & D work of the Navy laboratories and that funded by ONR must be efficiently communicated to and coupled with the Systems Commands to insure that these technologies get into the fleet in the most direct fashion.

To me, superconductivity is a very exciting field, with yet unexploited potential for Fleet applications, especially for smaller and lighter, higher reliability systems and orders of magnitude improvement in efficiency. For example, NRL scientists studying the use of SQUIDS as H-field antennas for ELF and VLF communications systems have demonstrated 4 orders of magnitude improvement in sensitivity at 1 Hz and, with approximately equal sensitivity at 1 KHz, about 1/100 th the volume of conventional devices. The operational implications for strategic submarine communications are quite clear. This and many other examples which you will discuss during these two days may lead to revolutionary new or significantly improved capabilities.

This morning's sessions will be devoted to superconductivity magnetometers and gradiometers. This afternoon we will focus on communications applications covering the electromagnetic spectrum from LF to the millimeter wavelengths. Tomorrow we will hear how NSRDC (Annapolis) is using a superconducting alloy to build compact motor-generator systems for shipboard propulsion systems, while others will discuss applications of superconductivity to acoustic transducers and airborne mine-sweeping.

All of these applications are of great interest to the Navy. However, because superconductivity is inherently a low temperature phenomenon - although there is a great deal of speculation about superconductivity at temperatures well above 20 degrees Kelvin, the present "ceiling" - suitable refrigeration systems must be available to provide the required cryogenic environment. It is obvious that if superconductive systems are to become operational, compact and reliable cooling systems are essential. It may be premature to make such a suggestion, but possibly the next Navy-sponsored Workshop in applied superconductivity might address this very important topic.

From looking at the schedule of the Workshop, I see that you have a very full and interesting two days ahead of you. To those of you who are visiting NRL for the first time, welcome aboard, and to our old friends, we are happy to see you again. The work going on

at NRL is varied and extensive and, after the business of this Workshop is completed, I encourage you all to return to NRL and meet with our professional staff to discuss problems of mutual interest so that we all can pull together to help solve the Navy's problems.

SUPERCONDUCTING MAGNETOMETRY

M. Nisenoff

Naval Research Laboratory, Washington, D. C. 20375

INTRODUCTION

Superconductivity was discovered by Kamerlingh Onnes in 1911.¹ Although it was an interesting phenomena, it remained a laboratory curiosity for the next 50 years. In the early 1960's two developments (superconductivity in high magnetic fields and tunneling across dielectric barriers) raised hopes that superconductivity and its intriguing properties could be used in practical applications. To understand the potential uses of superconductivity, we will review some of the fundamental properties of superconductors and then concentrate on how the developments involving these properties can be used to construct a class of extremely sensitive magnetometers.

ZERO RESISTANCE

In most pure metals and alloys, as the temperature is lowered, the electrical resistance decreases and eventually levels off at some temperature-independent value. However, in a superconductor as the temperature is lowered, the resistance does not level off but at some characteristic temperature T_c abruptly drops to zero (Fig. 1). Onnes said that below T_c materials entered a new state of matter which he called the Superconducting State.¹

In the superconducting state a superconductor can support a zero-voltage current for current less than some critical current I_c ;

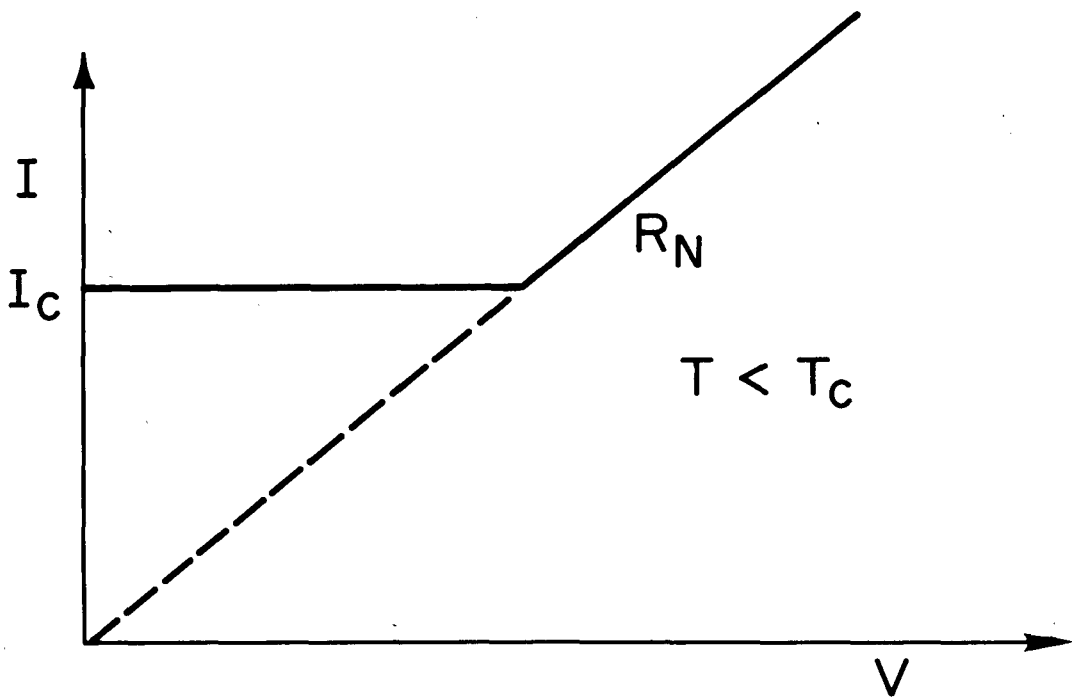
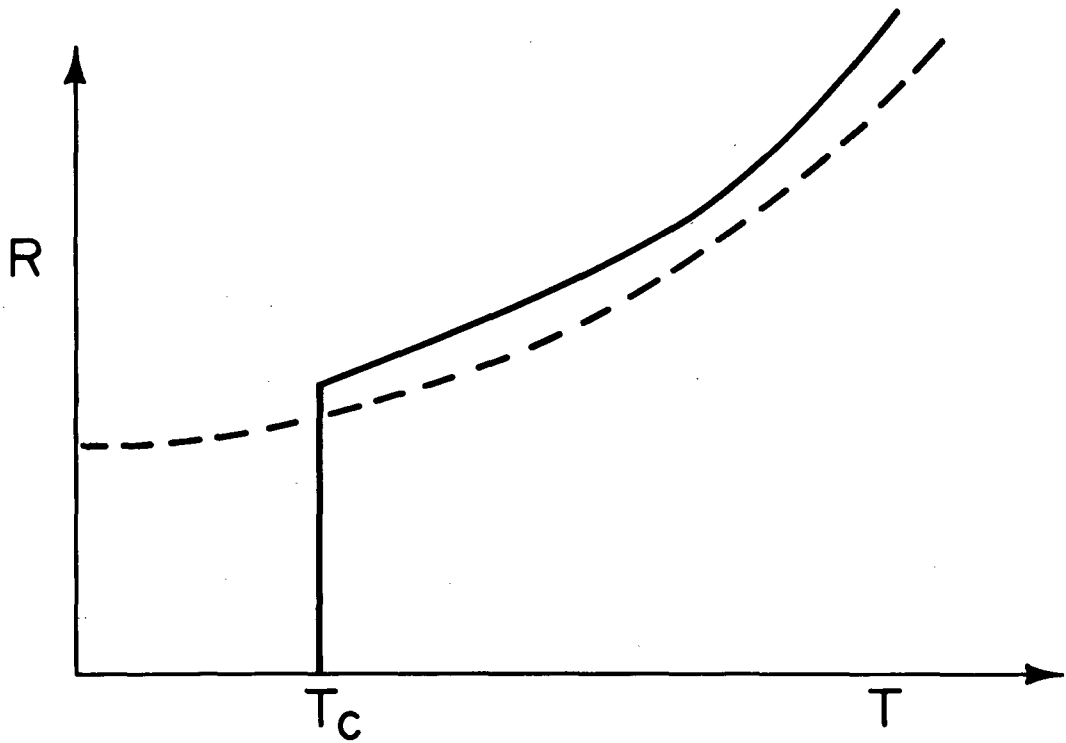


Fig. 1 — (Upper Trace) Resistance as a function of temperature for a superconductor (solid line) and that of a normal metal (dashed line). (Lower Trace) Current vs. voltage characteristic for a superconductor at temperatures less than the critical temperature. The resistance in the normal state, that is, at temperatures greater than the transition temperature T_c , is designated as R_N .

for currents in excess of I_c the sample is driven into the normal state, the state when current can flow only when there is a finite voltage drop along the sample. The superconducting-to-normal transition can either be abrupt (as shown in the lower part of Fig. 1) or gradual depending on the electrical parameters of the circuit containing the superconducting element. The critical current is a function of temperature; it is zero at the critical temperature T_c and increases as the temperature is lowered, reaching a value at $T = 0$ K corresponding to a current density of about 10^7 A/cm². If a magnetic field is applied to the superconductor, the magnitude of the critical current is depressed, and even at $T = 0$ K superconductivity can be destroyed by applying a sufficiently large magnetic field. Prior to 1960 all the known superconductors whose critical-current properties had been investigated, exhibited rather low values for I_c when exposed to magnetic fields in excess of about 1 tesla (10,000 gauss). However in 1962, Kunzler et al.² found that Nb₃Sn ($T_c = 18.2$ K) could support lossless current densities of 10^5 A/cm² in fields of 8.8 T. This development opened up the era of high-field superconducting magnets, and tomorrow you will hear about ship propulsion systems--motors and generators--that are being built using recently developed high-field superconducting materials.

JOSEPHSON EFFECTS

In 1963 a young English graduate student, Brian Josephson,³ considered the magnitude of the supercurrent (current with no IR drop)

that might flow between two superconductors separated by a thin dielectric barrier (Fig. 2). When such a barrier has zero thickness, the entire system is of course superconducting and the sample can carry a supercurrent equal in magnitude of the bulk value. However Josephson postulated on the basis of the microscopic theory of superconductivity that if the dielectric layer had nonzero thickness there would be a finite probability that a supercurrent could flow across the barrier. More specifically, for a layer up to about 50 Å thick (ten atomic layers) a nonzero supercurrent with a value less than the bulk value can flow. Josephson proposed that the supercurrent flowing across the barrier would have the functional form

$$I = I_0 \sin (\varphi_1 - \varphi_2), \quad (1)$$

where I_0 is the maximum value of this supercurrent and depends on the barrier thickness and where φ_1 and φ_2 are the quantum-mechanical phases on either side of the barrier. In quantum mechanics, evaluations of the properties of atomic systems are carried out using wave functions; that is, the various energy states of the system can be represented mathematically by a function which has an amplitude and a phase. The superconducting state can be described by the simple wave function $\psi = \psi_0 e^{i\varphi}$. The formalism of quantum mechanics is analogous to electromagnetic theory with the propagating electric and magnetic fields being represented by an amplitude function and a function of time which has the form $e^{i\omega t}$, where ω is the angular frequency of the propagating wave. In this analogy, if an electromagnetic wave is traveling in one medium and is incident on the interface with a second medium, the amount of energy that can propagate in the second medium depends on interface losses and the mode of propagation of the electromagnetic wave in

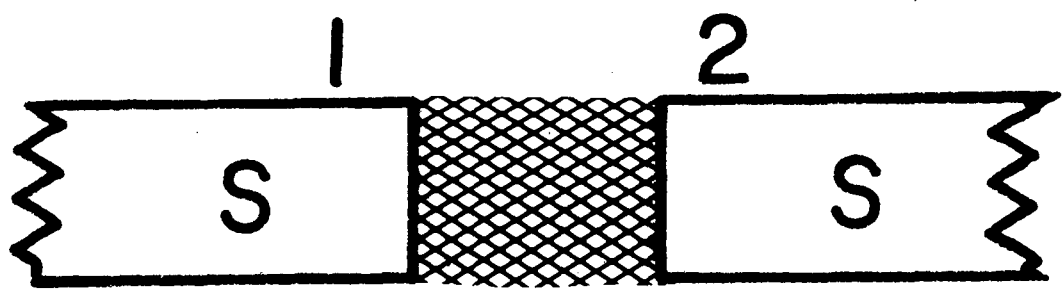


Fig. 2 — Sketch of Josephson Junction showing two superconducting regions (marked 1 and 2) separated by dielectric barrier (denoted by cross-hatching).

the second medium. If the boundary conditions in the second medium are such that the electromagnetic wave can propagate in this medium only when its E or H vector, as the case may be, is at a right angle to the E or H vector of the wave in the first medium, then the incident wave on entering the second medium cannot excite a electromagnetic disturbance in it. For this situation it is customary to say that energy cannot couple into the second medium because the propagation modes in the two media are orthogonal. If the modes of propagation are not orthogonal, then a disturbance can be excited in the second medium, with the efficiency of coupling depending on the angle between the modes.

When the concept is applied to tunneling of supercurrents through barriers(Fig. 2), if the quantum-mechanical phase in superconductor 1 is orthogonal to the phase in superconductor, 2, the superelectrons on the two sides of the barrier will be decoupled. However, if these phases are not precisely orthogonal, then there will be some coupling across the barrier, and the amplitude of the supercurrent that will flow across the barrier will be proportional to the sine of the phase difference of the superconducting electrons on either side of the barrier.

Let us consider the effect of imposing a current through the barrier. If a current imposed through the barrier is much smaller than I_0 , the current will flow through the barrier with no voltage appearing across the barrier. Furthermore, since the phase difference across the barrier is given by $\sin(\phi_1 - \phi_2) = I/I_0 < 1$, the superconducting electron on either side of the barrier will be coupled by the supercurrent that is flowing through the barrier. As the

magnitude of the imposed current is increased, the phase difference will increase until the imposed current is precisely equal to I_0 , the maximum supercurrent that the barrier is capable of supporting. For an imposed current I_0 the difference in quantum-mechanical phase across the barrier is 90 degrees, so that the wave functions describing the superconducting electrons on either side of the barrier are orthogonal and the two regions are decoupled. If, after the junction has been driven into this state, the imposed current is reduced to a value less than I_0 , the phase difference across the barrier would be less than 90 degrees, supercurrent would again be able to flow across the barrier, and the superconducting regions on the two sides of the barrier will again be coupled. Thus the two superconducting regions can be coupled and uncoupled reversibly by adjusting the magnitude of the current imposed on the barrier. This property of the Josephson junction can be used in the construction of a class of magnetic-field sensors, and the function of the barrier or weak link in these devices will be discussed in a later subsection.

A second prediction made by Josephson was that if a dc voltage denoted V_{12} , is applied across the barrier, the difference in the quantum-mechanical phase across this barrier will be a function of time according to the relation

$$\frac{d}{dt}(\varphi_1 - \varphi_2) = \frac{2e}{h/2\pi} V_{12} , \quad (2)$$

where e is the charge of the electron and h is Planck's constant. From Eq. (1) a dc voltage across a barrier

separating two regions of superconductivity will cause an alternating current to flow through the barrier, and the frequency of this current is

$$\omega_{\text{Josephson}} = \frac{2e}{h} V_{12}. \quad (3)$$

The value of $2e/h$, the ratio of Josephson frequency to voltage, has been determined to be $(483\,593.7 \pm 0.2)$ GHz/V.⁴ Thus, a dc voltage of 20 microvolts across a Josephson junction will cause a current of frequency 10 GHz to flow across the barrier. Conversely if 10 GHz radiation is coupled into a Josephson junction, a zero resistance step will appear in the I versus V curve of the device at 20 microvolts and multiples of 20 microvolts. Hence a Josephson junction can be employed as either a generator or as a detector of electromagnetic radiation. This application of Josephson junctions will be discussed in several papers to be presented at this workshop.

Equations (1) and (2) summarize the results of the work done by Josephson in 1962, for which he shared in the 1973 Nobel price in physics.

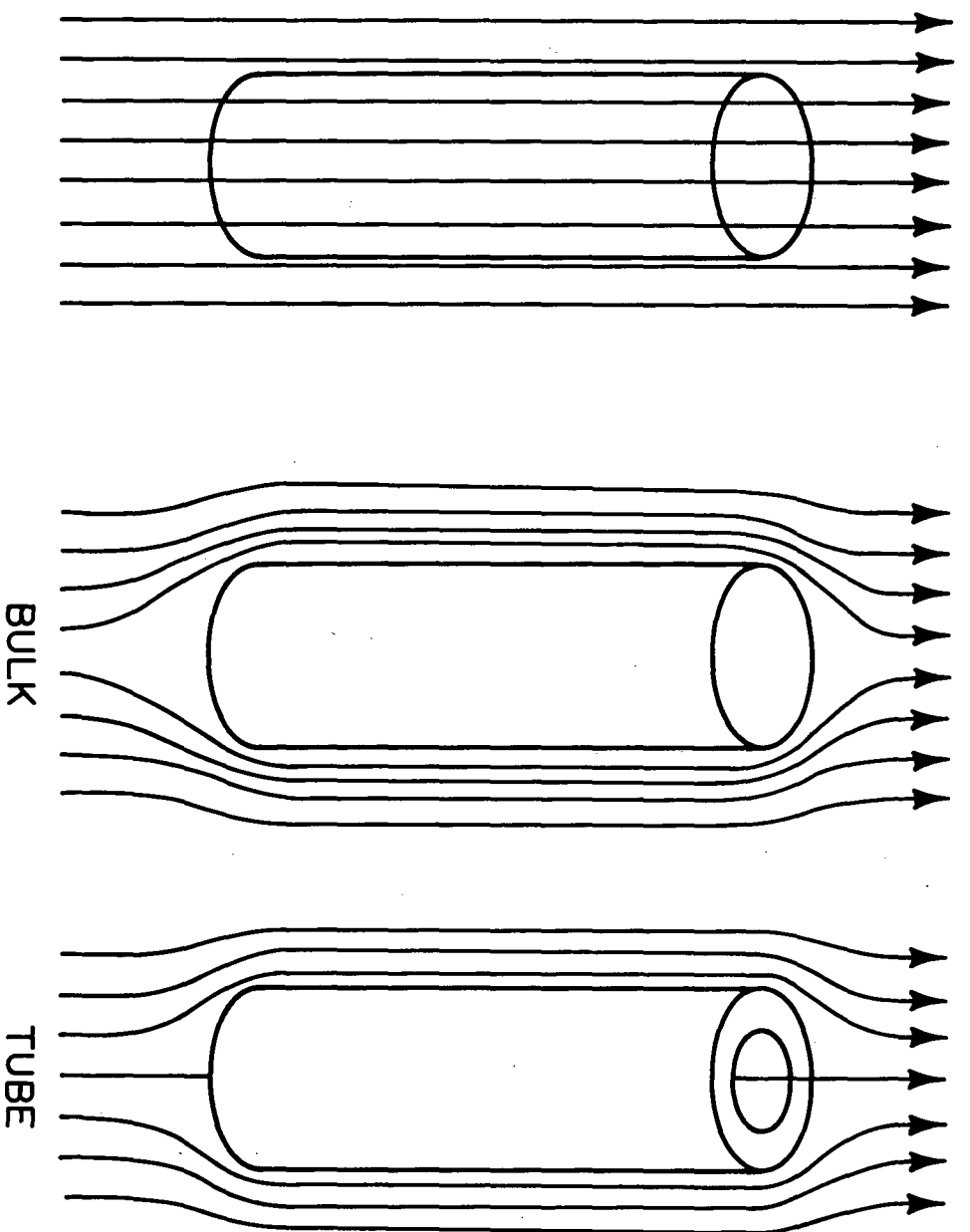
With the preceding introduction to the concept of a Josephson junction as a brief background, for simplicity we will later describe this structure in the context of a magnetic flux turnstile, which will be an adequate treatment but, for the purist, nonrigorous. For readers not familiar with quantum mechanics another representation for the magnetic field sensor will later also be given in terms of a nonlinear impedance, which may be a more satisfying representation.

MEISSNER EFFECT

Another basic property of superconductors is magnetic flux exclusion. A sample in the normal state has only a small magnetic susceptibility, and when the sample is placed in a magnetic field, the magnetic flux lines will pass through the sample essentially undistorted (sketch at the left in Fig. 3). However, if the temperature is lowered so that the sample enters the superconducting state, almost all of the magnetic flux lines will be excluded from the interior of the sample, which is called the Meissner effect;⁵ that is, the superconducting sample will act as a perfect diamagnet. Since the flux lines are excluded from the bulk of the superconducting sample, they will pile up just outside the volume of the sample (middle sketch in Fig. 3). If the sample under consideration is a tube, flux will still be excluded from the interior of the sample, but some flux lines can thread through the hole in the tube (sketch at the right in Fig. 3). Moreover the magnetic flux trapped by the cylinder cannot have any arbitrary value but must have a magnitude that is a multiple of a magnetic flux unit called the magnetic-flux quantum.⁶ The magnitude of this unit of flux is the ratio $h/2e$. The value for $h/2e$ is relatively small: 2×10^{-15} Wb. Thus, if the bore of the tube is 1 cm^2 (10^{-4} m^2) in area, the value of the trapped field will be a multiple of 2×10^{-11} T, a very small value of magnetic field in terms of present-day sensors.

MAGNETIC-FIELD SENSOR (SQUID)

A very sensitive detector of magnetic fields can be made using a superconducting loop into which a Josephson-like structure has been built.



$T > T_c$

Fig. 3 — Meissner Effect

$T < T_c$

This device is known as a SQUID (superconducting quantum interference device). The operation of such a device can be understood using the concepts of flux quantization by a superconducting loop and a Josephson junction operating as a magnetic-flux turnstile.⁷ In Fig. 4 we illustrate an otherwise totally superconducting cylinder containing a weak link, which for this example is shown as a narrow constriction or Dayem bridge.⁸ As the device is cooled through its transition temperature an integral number of flux quanta Φ_0 will be trapped in the hole interior to the tube. For simplicity let us assume that zero flux was trapped interior to the tube (top trace in Fig. 5 with $\Phi_{int} = 0$). If external flux Φ_{ext} is applied to the device, since the flux threading the cylinder is quantized and cannot change, a current will be induced to flow circumferentially in the ring to shield the interior of the ring from any change in the applied flux. Mathematically this can be written as

$$i_{sh} = (\Phi_{ext} - \Phi_{int})/L, \quad (4)$$

L is the inductance of the SQUID and i_{sh} is the induced shielding current. As the applied flux is increased, the shielding current will increase proportionally according to Eq.(4) (middle trace in Fig. 5). As the current driven through the weak link increases, according to the Josephson relation the quantum-mechanical phase difference across the weak link increase. When the shielding currents in the ring reach the critical Josephson current (I_0 in Eq.(1)) for the weak link, the quantum-mechanical phase difference across the

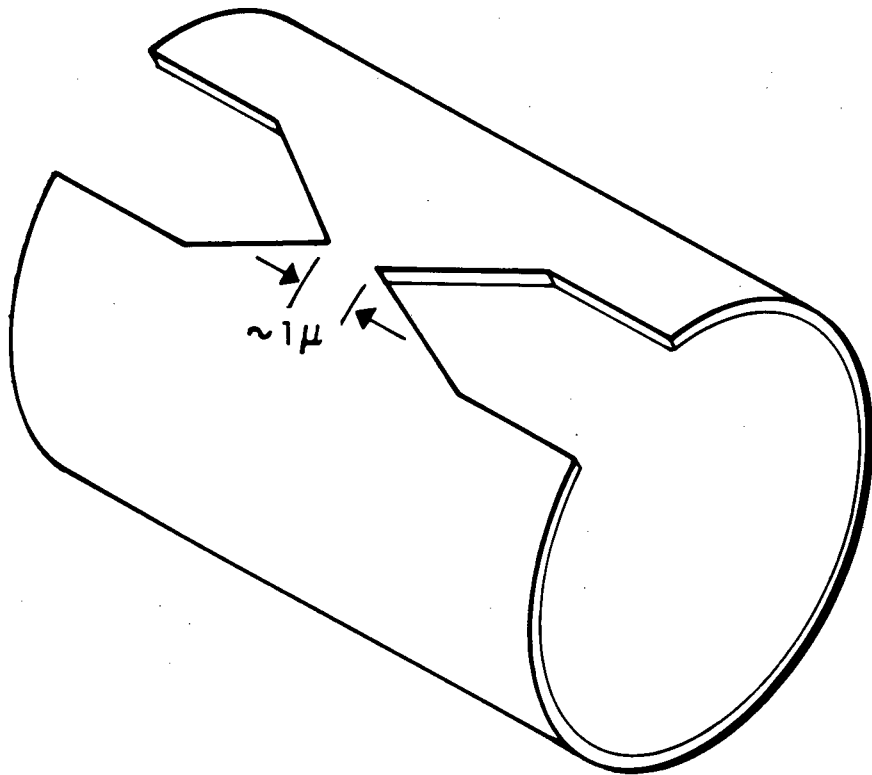


Fig. 4 — Sketch of a thin film SQUID containing a “bow-tie” Dayem bridge.

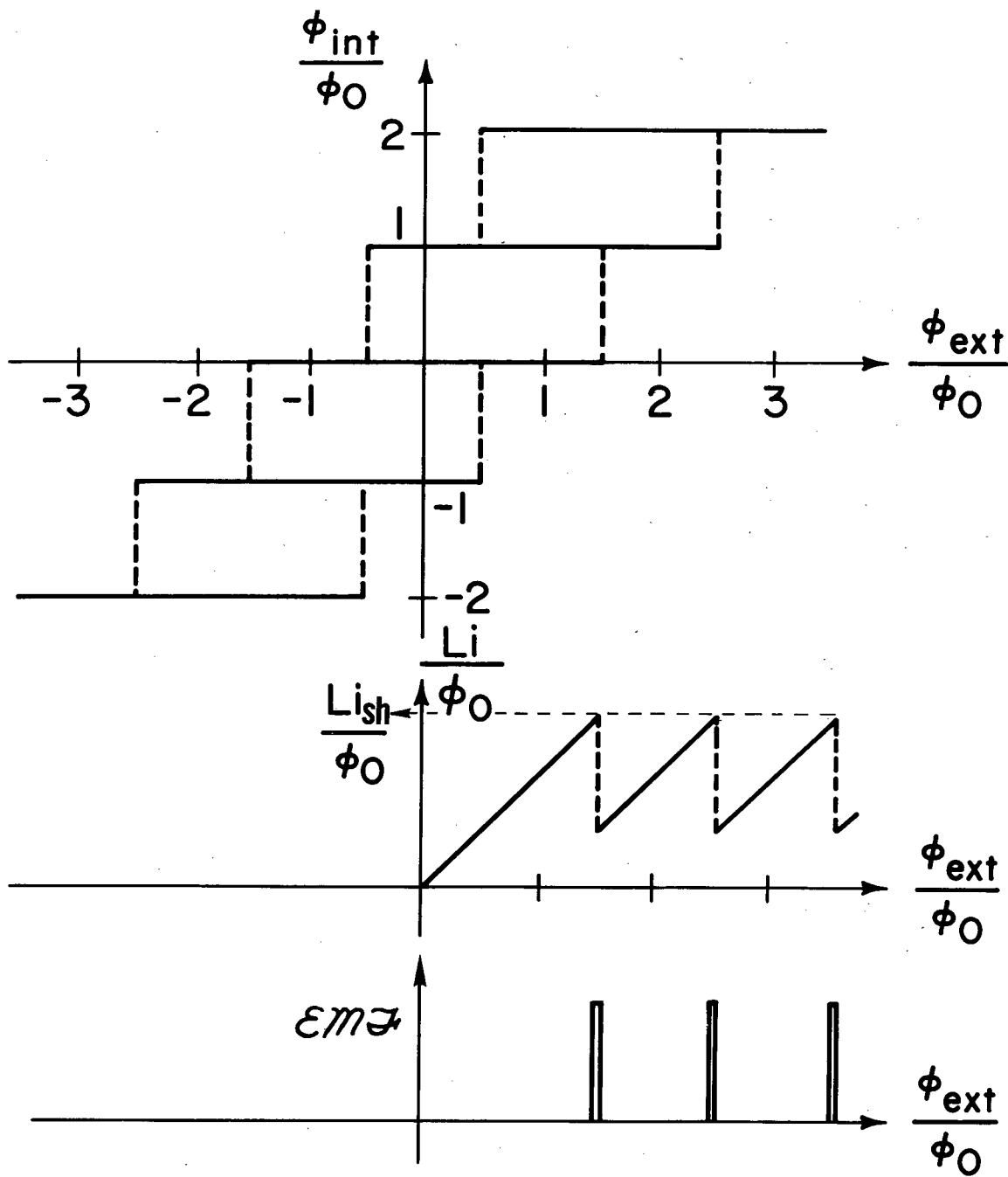
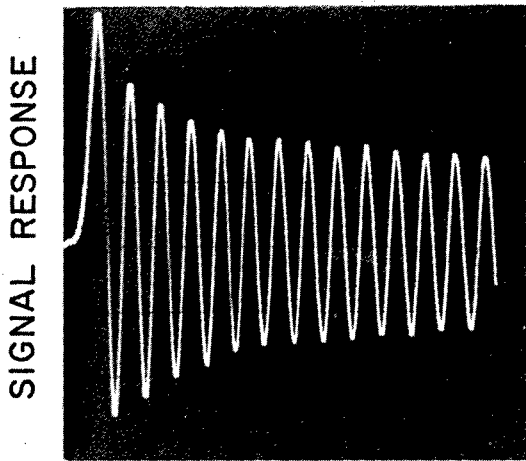


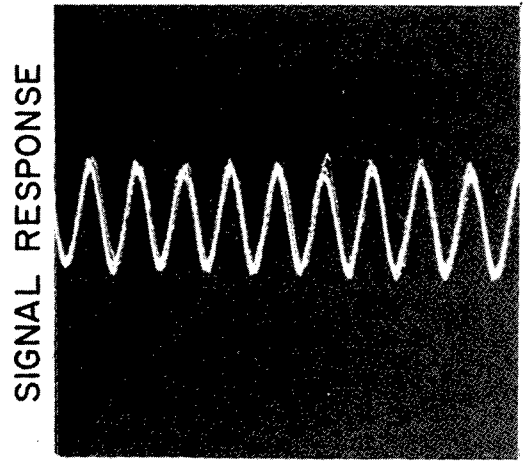
Fig. 5 — Response of SQUID to applied magnetic field.

weak link will be precisely 90 degrees and the two sides of the junction will be decoupled; the barrier can no longer support a supercurrent, and flux quantization is no longer applicable. Therefore magnetic flux can and will transit across the weak link so as to reduce the difference between the magnetic flux inside and outside the ring. In terms of quantum mechanics, once the critical current of the weak link has been reached, the system undergoes a transition from a state with n flux quanta trapped by the ring to a lower energy state with $n + 1$ quanta trapped by the ring. When the amount of flux trapped by the ring increases, the difference in flux inside and outside the ring decreases. Thus the amount of shielding current necessary to support the difference in flux is reduced from i_c to $i_c - \Phi_0/L$, and the weak link will revert back into the superconducting state. Conceptually, when the weak link is normal, any amount of flux should be able to pass across the weak link, but in practice and consistent with quantum mechanics it is most likely that only one flux quanta will transit across the weak link before the link reverts to the superconducting state.

Whenever magnetic flux enters the ring, an induced EMF $\approx d\Phi/dt$ will be induced in the ring. The relaxation time for flux entry is quite small, 10^{-12} second; thus the EMF appears as a spike or, for mathematical treatment, as a narrow square pulse (lower trace in Fig.5). Hence there will be a series of pulses induced in the ring as Φ_{ext} , the applied magnetic flux, is increased and correspondingly a sequence of opposite-polarity pulses as Φ_{ext} is decreased. The details of



RF FLUX →



AMBIENT FLUX →

Fig. 6 — Response of SQUID as function of excitation flux (left trace) and as function of ambient dc flux (right trace).

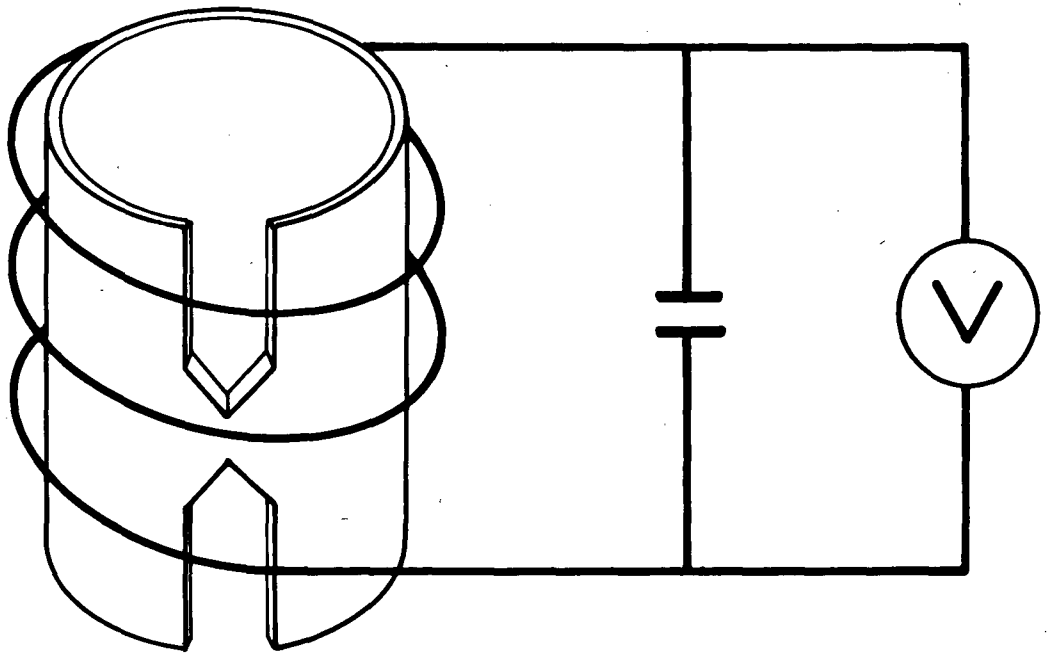


Fig. 7 — Diagram of SQUID coupled to lumped LC resonant circuit.

the time separation of these pulses can be complicated, depending on the critical current of the weak link and the time variation of the applied flux. An exact Fourier expansion for the case of a sinusoidally varying applied flux has been carried out by Silver and Zimmerman.⁷ For illustration the simpler case of an applied magnetic flux whose magnitude increases with time will be treated here.⁹ For this case there will be a series of pulses, all with the same polarity uniformly spaced in time. If Φ_{ext} has magnitude zero at time $T = 0$, the initial pulse will occur at a time which will depend on the value of the critical current of the weak link and on the magnitude and sign of any ambient dc flux that may be present. If the ambient dc flux has the same sign as the time-varying applied flux, the first pulse will occur at an earlier time, and if the two fluxes have opposite sense, the occurrence of the initial pulse will be delayed. Thus the time sequence of the pulses will be sensitive to the ambient magnetic field.

The straightforward Fourier expansion for a series of pulses with amplitude Φ_0/τ and width τ uniformly spaced in time by increments T can be written as

$$\text{EMF} = \frac{\Phi_0}{2\pi\tau} \sum_{n=1}^{\infty} \frac{(-1)^n}{n} \left(\sin \frac{2\pi n\tau}{T} \right) \cos \frac{2\pi n\Phi(t)}{\Phi_0} \quad (5)$$

where $\Phi(t)$ is the total magnetic flux acting on the SQUID. If the width of the pulses is small compared to the time between pulses ($\tau < T$), Eq. (5) reduces to

$$\text{EMF} = A \sum_{n=1}^{\infty} \cos \frac{2\pi n\Phi(t)}{\Phi_0} \quad (6)$$

For example, if the applied flux varies linearly with time, the induced EMF will have its primary frequency component at a frequency $\dot{\Phi}(t)/\Phi_0$.

Although Eq.(6) is valid only for an increasing field, we will assume that the applied flux $\Phi_{\text{rf}}(t)$ is sinusoidal and that the total flux has the form

$$\Phi(t) = \Phi_{\text{rf}} (\sin \omega_{\text{rf}} t) + \Phi_{\text{dc}} \quad (7)$$

where Φ_{dc} represents the ambient flux to which the SQUID is exposed. If this form for $\Phi(t)$ is inserted into Eq.(6) the following is obtained:

$$\text{EMF} = A' J_1 \left(\frac{2\pi\Phi_{\text{rf}}}{\Phi_0} \right) \left(\cos \frac{2\pi\Phi_{\text{dc}}}{\Phi_0} \right) \sin \omega_{\text{rf}} t + \dots \quad (8)$$

Only the term at the frequency of the applied time-varying flux is shown, since the higher order terms will be filtered out by the resonant structure to which the SQUID will be coupled in systems of interest to us. This expression indicates that the amplitude of the induced voltage varies periodically as the Bessel function $J_1(x)$ with the amplitude of the applied time-varying magnetic flux and sinusoidally with the amplitude of the dc ambient magnetic flux.

In Fig. 6 these dependences are illustrated. At the left the magnitude of the induced voltage is shown as a function of the amplitude of the excitation signal for a fixed value of dc flux for which $(\cos 2\pi\Phi_{\text{dc}}/\Phi_0) = \pm 1$. Although the behavior is not precisely Bessel in nature, it can be seen that the spacings between the zeros in the signal decrease slightly with increasing order number and that the magnitude of the signal maxima decrease monotonically with order number, although

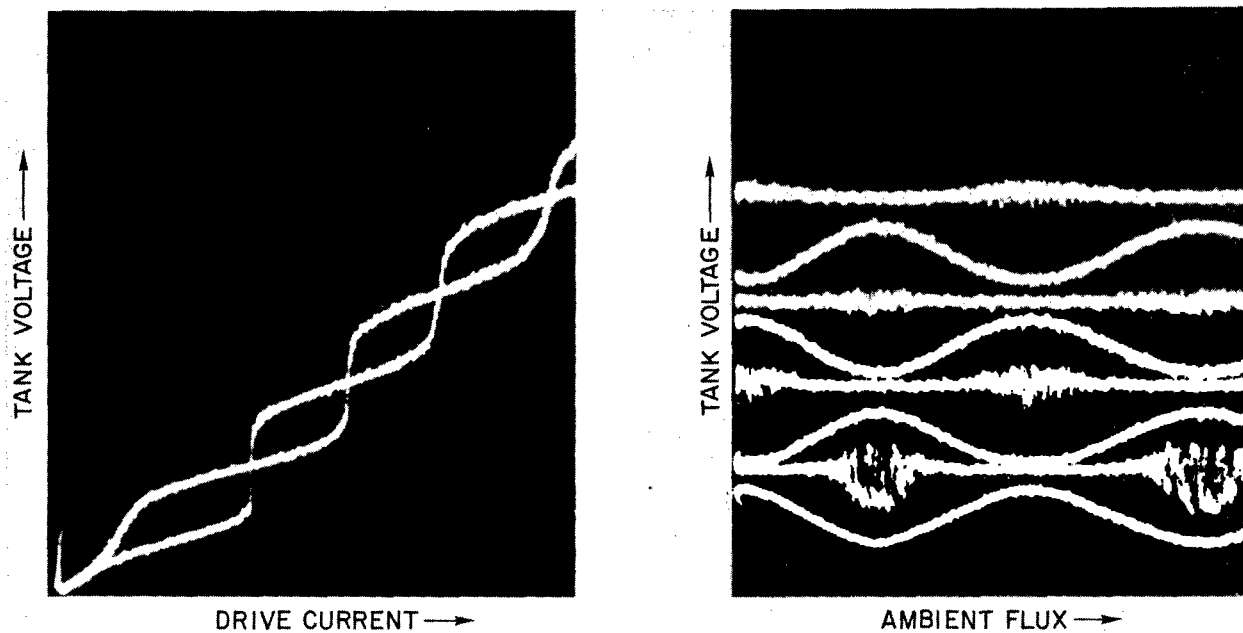


Fig. 8 — SQUID response curves. (Left Trace) rf voltage across tank to which SQUID is coupled vs. rf current imposed on tank circuit for two particular values of ambient magnetic flux. (Right Trace) rf voltage across tank circuit as function of ambient magnetic flux for certain specific values of drive current.

the falloff is not quite as fast as the $x^{-1/2}$ expected for the first order Bessel function $J_1(x)$. At the right the amplitude of Φ_{rf} was adjusted for a maximum in the Bessel dependence and the value of Φ_{dc} was slowly varied. The sinusoidal nature of the dependence of the induced EMF is obvious. The periodicity with ambient flux has been measured, and to within the precision of the measurement (0.1%) the period was $h/2e = 2 \times 10^{-15}$ Wb.

Thus to first order this simple treatment of the induced voltage pulses is a fair approximation to the true phenomena. The more detailed treatment of Silver and Zimmerman⁷ yield a better fit to the experimental data.

To observe this EMF the SQUID ought to be coupled to two coils: one that applies the time-varying magnetic flux and one that is resonant at the excitation frequency ω_{rf} to detect the induced EMF. The detection coil is resonant for two purposes: it will selectively pass only the fundamental of the induced voltage and the resonant nature of the tank circuit will provide a voltage gain of Q for the detected voltage. However, for simplicity in practice^{7,10} the same coil is used to apply the time-varying flux and to detect the induced voltage (Fig. 7). A constant drive current at the resonant frequency ω_{rf} is impressed on the resonant circuit, and the voltage across the tank circuit is measured. The impressed current produces a voltage IZ across the resonant structure, where Z is the impedance of the loaded tank circuit; superimposed on this voltage is the induced EMF from the SQUID that is transformer-coupled back into the tank. Thus the impedance of the tank to which the device is coupled will contain a

linear term, the IZ term, and, superimposed on this, the Bessel-like signal reflected from the device. If the device is strongly coupled to the tank, the signal reflected from the device will be relatively large in amplitude and the resultant voltage trace will appear to consist of a series of steps. The exact structure of these steps will depend on the value of the applied Φ_{dc} . In Fig. 8 the left half shows the voltage across the tank as a function of drive current for two values of Φ_{dc} : those values which produce the maximum excursion of the voltage for a given drive current. The step structure of the impedance curve of the loaded tank circuit is clearly seen in these two traces at the left.

From these traces it can be seen that there are certain values of impressed drive current at which the voltage experiences an excursion as the dc flux is varied. These values of current correspond to those values of magnetic flux for which the Bessel function term in Eq. (8) is a maximum. In addition for certain values of drive current the tank voltage is not modulated by the applied dc flux; these are the zeros in the Bessel dependence. The modulated portion of the tank voltage is displayed in another form in the right half of Fig. 8. The tank voltage is shown as a function of dc flux for certain values of drive current: values corresponding to the maximum modulated signal (Bessel maxima) and for those values of the drive current for which the modulated signal is zero, that is, where the voltage across the loaded tank circuit is independent of the ambient dc magnetic flux (Bessel zeros). For most of the devices examined the ambient-flux-modulated signal corresponded to one quantum of flux at all temperatures

at which the Bessel behavior was observed and was insensitive to the value of the threshold current that had to be exceeded before the onset of the modulated signal.

Details of the behavior of this device and the mode of operation just described are consequences of a quantum-mechanical treatment of the Josephson junction (or weak link) structure and of magnetic-flux quantization. However for those who do not understand or believe quantum mechanics, for circuit application, the superconducting loop containing the weak link can be treated as a device with an extremely nonlinear impedance that can be modulated by dc ambient fields. This SQUID behavior is usually monitored by coupling the device to circuits resonant in the 2 to 30 MHz frequency range.^{7,10} This frequency range was initially selected because relatively compact sources and low-noise amplifiers were readily available and relatively inexpensive. Recently in a number of experiments SQUIDS have been operated in the VHF¹¹ and microwave regions^{12,13} with reported increase in performance, that is, a better signal-to-noise ratio for the detected modulated signal.

If large field changes (large compared to the basic periodicity of the SQUID) are to be measured, it is possible to count the number of periods of the signal as the ambient field changes. However, the real usefulness of this type of device lies in the measurement of small field changes (small compared to the periodicity of the device's response). To measure small fields, the device is used in a null type of circuit.^{7,10,14} The reference point of the circuit is an extremal of the sinusoidal response of the device to ambient field changes.

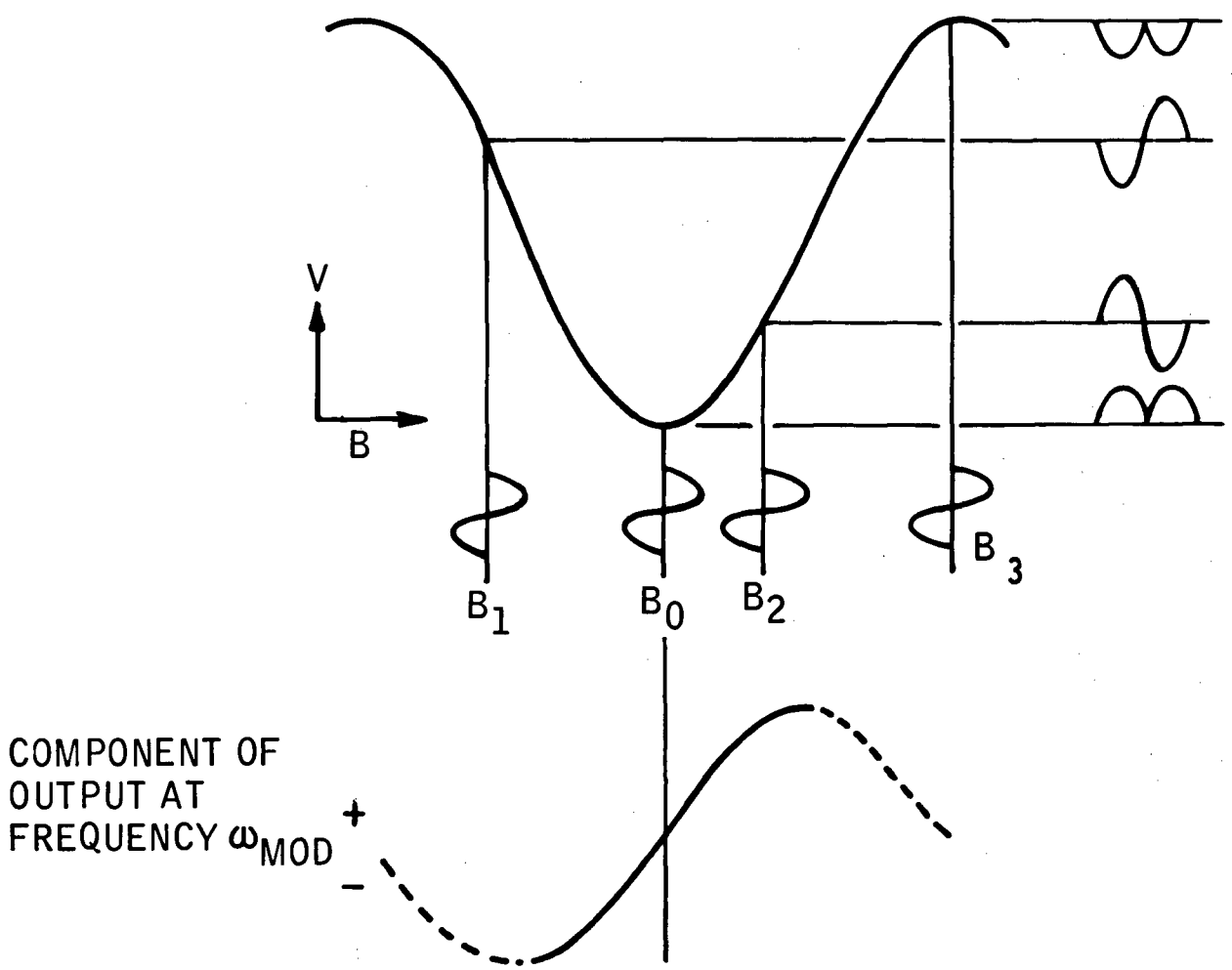


Fig. 9 — Principle of operation of feedback system used with SQUIDs.

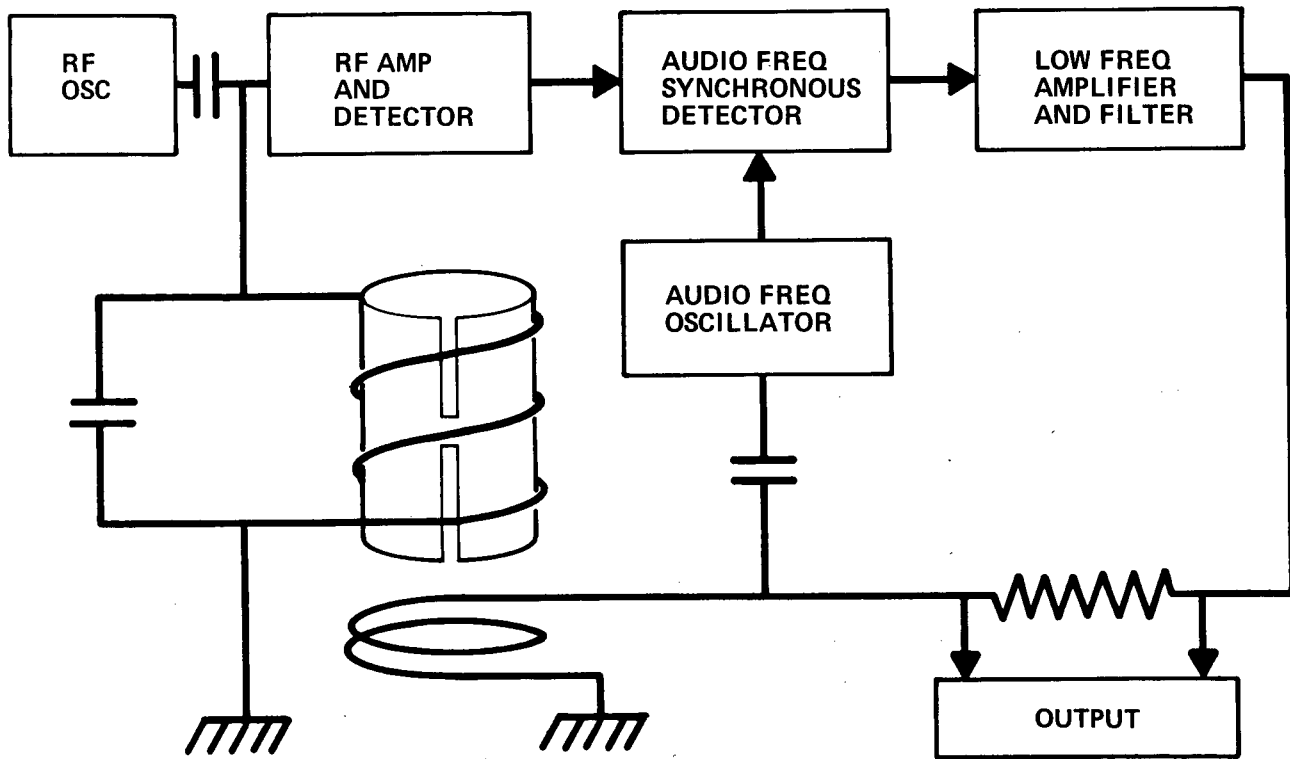


Fig. 10 — Schematic diagram of feedback circuit used with SQUIDs.

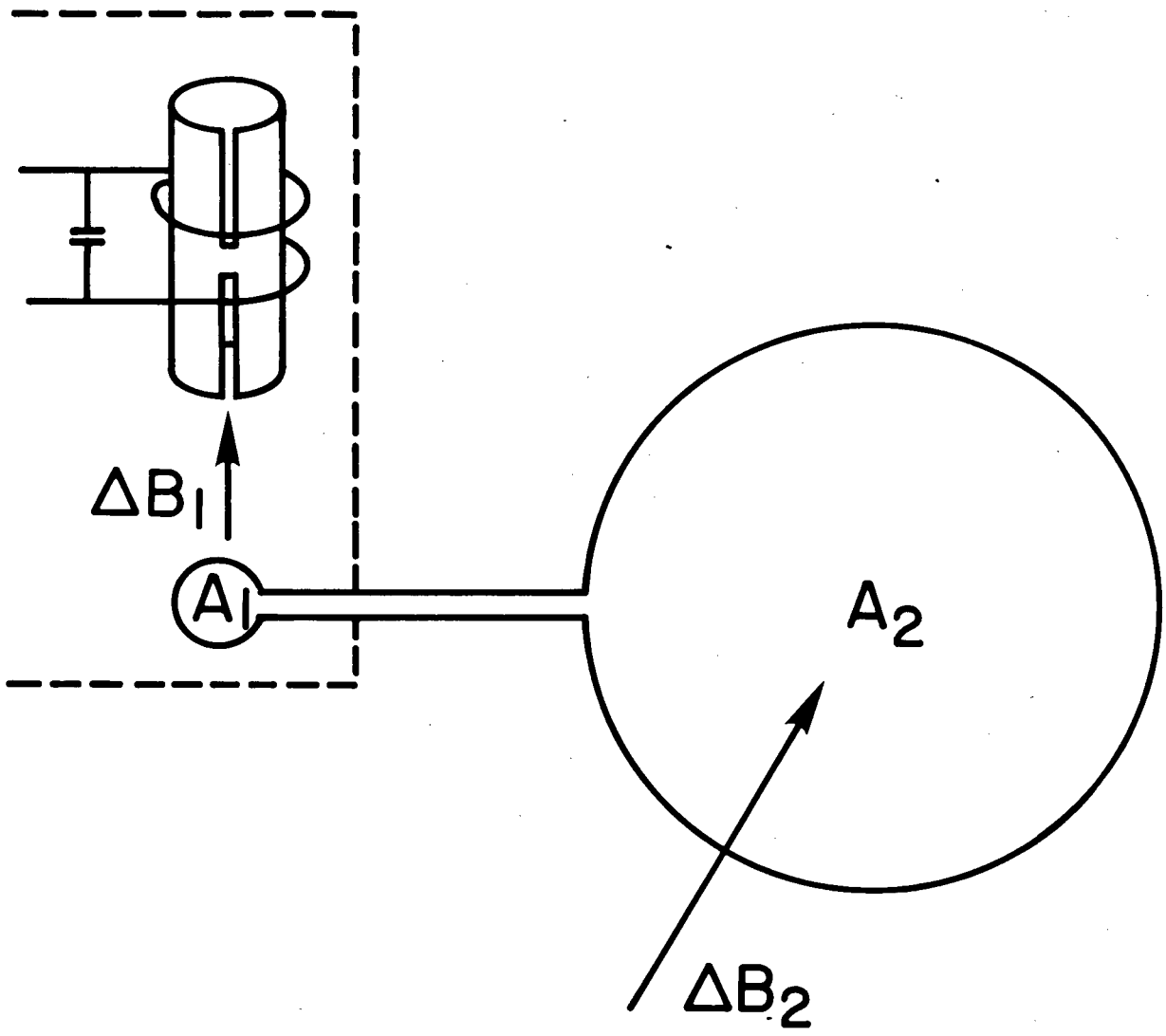


Fig. 11 — Schematic diagram of superconducting flux transformer.

For the case shown in Fig. 9, a minimum was arbitrarily chosen. In addition to the RF excitation signal, an audio-frequency flux at frequency ω_{mod} and amplitude of about $\Phi_0/4$ is applied to the device. The modulation frequency must be less than ω_{rf}/Q so that the modulation signal can pass through the tank-circuit response function; thus, for 30 MHz systems, modulation frequencies are chosen to be typically 50 kHz or less. If the ambient dc field corresponds exactly to the minimum of the response curve (B_0 in the figure), the modulation field will produce a modulation of the output signal that will look like a full-wave rectified signal at frequency ω_{mod} with a strong Fourier component at frequency $2\omega_{\text{mod}}$ but only a weak component at the fundamental ω_{mod} . However, if the ambient field corresponds to a dc field B_2 above the minimum, then the output of the device will have a strong modulation component at frequency ω_{mod} and the signal will have the same phase as the modulation field. Conversely, if the ambient field is less than B_0 , the modulation of the output at frequency ω_{mod} will have the opposite phase from the modulation field. Therefore it is possible to determine whether the ambient field has drifted above or below the field corresponding to the minimum by determining whether the phase of the component at the modulation frequency in the output signal from the device is the same or opposite to that of the modulation field. Thus, if the output of the detected signal is amplified by a synchronous detector tuned to the modulation frequency, the output of the synchronous detector will be positive, zero, or negative depending on whether the ambient field is above, coincident with, or below a minimum in the sinusoidal response curve of the device.

The output of the synchronous detector can be used to produce a correction field at the device in such manner as to bias the device back to the field value corresponding to a minimum in the response curve. A block diagram of a lock-on feedback system is shown in Fig. 10. With this type of lock-on or nulling system with 30 MHz excitation it is possible to detect small changes in the ambient field which correspond to about 10^{-3} to 10^{-4} of the basic periodicity of the device. For example, if the device is 2 mm in diameter, the basic periodicity is 6×10^{-10} T; thus with the lock-on system it is possible to detect field changes as small as 6×10^{-13} to 6×10^{-14} T/Hz^{-1/2}. This number is a measure of the basic sensitivity of a superconducting magnetometer at the present stage of development of sensor and monitoring electronics.

FLUX TRANSFORMER

The field sensitivity of a SQUID can be enhanced by employing a superconducting search coil of the type shown in Fig. 11. A small loop of superconducting wire is tightly coupled to the SQUID, and the leads are passed through a magnetic shield that surrounds the sensor and are connected (superconductively) to a large search coil which senses the field to be measured. Because of flux quantization by a closed superconducting loop, any change in flux imposed on the large search coil of area A_2 will cause an equal but opposite change in flux in the small loop around the SQUID. Since flux is the product of magnetic field B and loop area A , one can write

$$\Phi_1 - \Phi_2 = B_1 A_1 - B_2 A_2 = 0 .$$

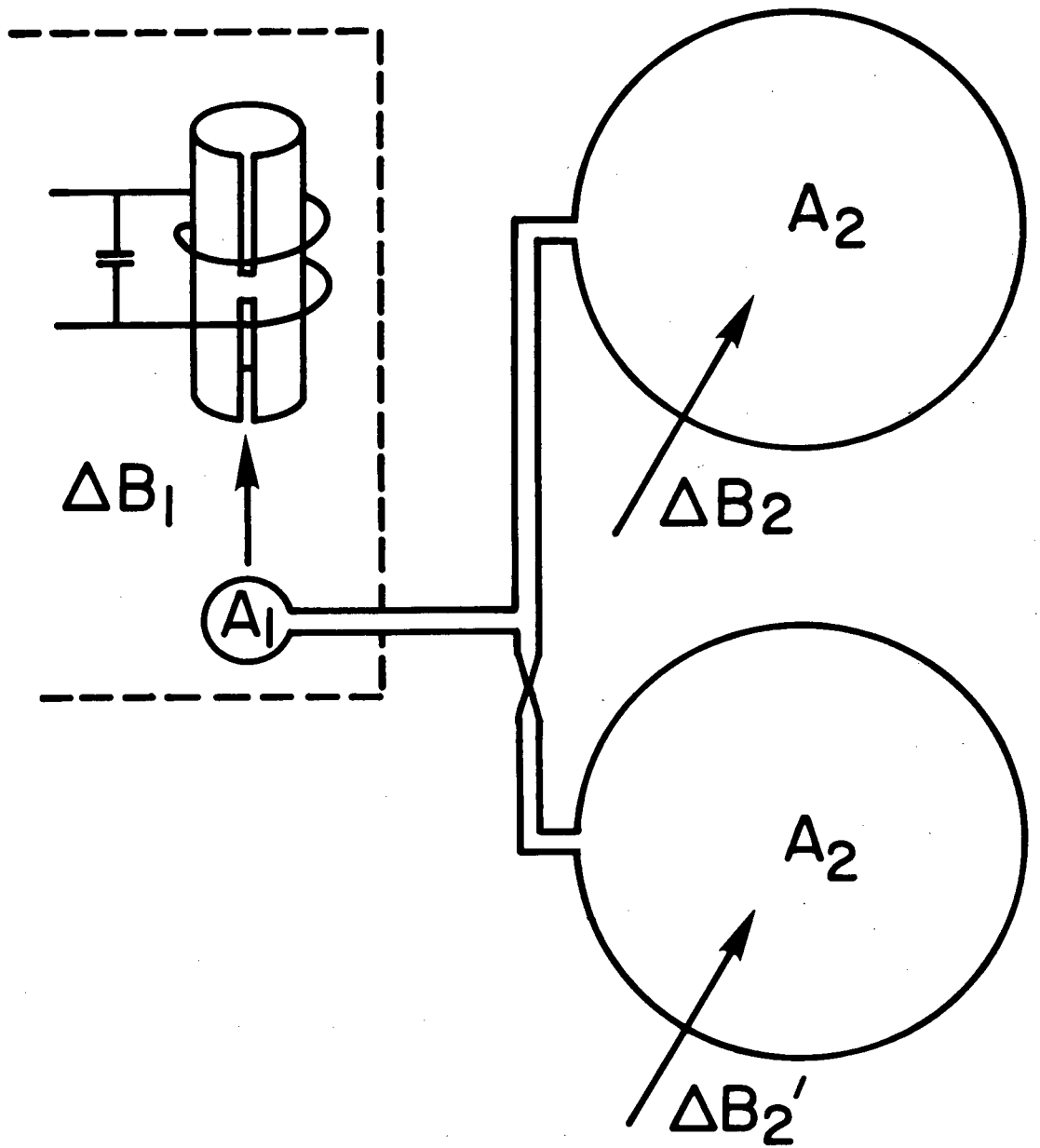


Fig. 12 — Schematic diagram of superconducting gradiometer.

Solving for the change in field B_1 produced at the SQUID, one obtains

$$B_1 = \frac{A_2}{A_1} B_2 . \quad (9)$$

Since A_2 is greater than A_1 , any change in uniform field B_2 will produce a larger change in field B_1 at the SQUID; that is, this configuration, known as a flux transformer, will provide field amplification.

This simplified treatment would suggest that an arbitrarily large field amplification can be obtained with a superconducting flux transformer. However a more detailed treatment¹⁵ shows that impedance matching is required between the primary and secondary of the flux transformer. As an example in practice, at NRL a transformer with a 6-inch-diameter search coil has been optimally coupled to a 2-mm-diameter SQUID, and a field amplification of 300 was achieved.

The flux transformer not only provides an increase in magnetic field sensitivity for a given SQUID but also allows the SQUID to be removed from the locale of the field to be measured. For example, if the magnetization of a specimen of arbitrary size is to be measured, the flux transformer makes it possible to insert the sample into the primary of the flux transformer and not have the presence of the sample disturb the fields at the SQUID.

SUPERCONDUCTING GRADIOMETER

It is sometimes desired to measure weak magnetic-field gradients, and a SQUID can be used for these types of measurements using a version

of the flux transformer known as a superconducting gradiometer¹⁵ (Fig. 12). In the gradiometer configuration, instead of the single search coil, two search coils of equal area are oriented in an opposite sense relative to the ambient field. For this case the magnetic flux in coil 1 that is tightly coupled to the SQUID is equal to the difference in the ambient magnetic flux at the two sensing coils; in mathematical form

$$\Phi_1 = \Phi_2 - \Phi_2', \quad (10a)$$

$$B_1 A_1 = B_2 A_2 - B_2' A_2 = A_2 (B_2 - B_2'). \quad (10b)$$

If a uniform magnetic field is applied, then B_2 and B_2' are equal and there will be no net signal at the SQUID. However, if the search coils are in a field with a gradient, the fields at the two coils are not equal and there will be an unbalanced signal at the SQUID. If the field amplification achieved individually by each of the coils is known and the spacing between the coils is known, the unbalanced signal can be related to the gradient of the ambient field.

The concept of a superconducting gradiometer has been proposed for use in MAD systems. Because of the great sensitivity of the SQUID and flux-transformer combination, it is possible to assemble a gradiometer with a 1-foot baseline that has a sensitivity that can be matched by conventional optically pumped vapor magnetometers only if the vapor magnetometers are separated by a baseline of 0.3 Km or more. Thus the attractiveness of using superconducting gradiometers for a MAD system, especially an airborne system is obvious!

SUMMARY AND DEVICE PERFORMANCE DATA

In this paper the principles behind the operation of a superconducting quantum interference device (SQUID) have been briefly sketched, and it has been shown that a SQUID can be represented in electrical engineering terms as a circuit element that has a nonlinear impedance and that this impedance is a periodic function of an applied magnetic field. Although this representation is not exact, it is a convenient viewpoint to take so that the operation and use of these devices are not obscured by quantum-mechanical concepts that must be used to explain the origin of the behavior of the device.

In concluding this paper, a brief summary will be presented describing the performance characteristics that can be obtained from presently available SQUIDS and SQUID electronic detection systems, and an estimate will be made of what ultimate performance ought to be achieved for SQUIDS in the near future.

These data are shown in Table I. Presently available devices are made from the soft superconducting materials and have diameters of about 2 mm. When coupled to a 30 MHz detection system, the smallest detectable signal that can be measured is of the order of $1 \times 10^{-13} \text{ T Hz}^{-1/2}$, which is within an order of magnitude of the theoretically predicted sensor noise.¹⁶ With a field enhancement of about 100 that can be obtained with a flux transformer, the present field sensitivity of the combination is of the order $10^{-15} \text{ T Hz}^{-1/2}$.

One disadvantage of the present sensors is that they are made from mechanically soft materials and thus are susceptible to destruction by mechanical abrasion and by chemical and atmospheric corrosion.

Devices made from refractory materials such as niobium would not be destroyed by abrasion and corrosion. There is an ongoing 6.1-funded research program at NRL to prepare SQUIDS from refractory materials that will be rugged, be reliable, exhibit long shelf life, and have reproducible electrical and magnetic characteristics.

The magnitude of the field-modulated signal obtained from a SQUID is proportional to the excitation frequency. Experiments carried out at NRL have demonstrated that better signal-to-noise ratios can be achieved at higher excitation frequencies. However reliable data on the field sensitivities that can be obtained by microwave-biased SQUIDS have not been as yet obtained. However the theoretical value¹⁶ for a 1-cm-diameter SQUID excited at 10 GHz is $1 \times 10^{-17} \text{T Hz}^{-1/2}$ and with good microwave electronics one should get to within about a factor of 10 of theoretical performance: sensitivities of about $10^{-16} \text{T Hz}^{-1/2}$. (This value was obtained assuming an operating temperature of 1 K. However, from the point of view of cryogenics, an operating temperature closer to 10 K would be preferred, and at this higher temperature the theoretical noise in the SQUID will be greater by a factor of $10^{2/3} \approx 5$.) With the use of a flux transformer of gain 100 and with microwave excitation, an ultimate sensitivity of about $10^{-18} \text{T Hz}^{-1/2}$ should be achieved experimentally.

ELF COMMUNICATION ANTENNAS¹⁷

The frequency range from 10 to 100 Hz is of great interest in communicating to submerged submarines.¹⁷ The existing H-field antennas are extremely long (hundreds of meters) and are limited in performance by noise associated with flexing of the long cable and from magnetostrictive noise from the ferrite used to load the cable. The

stated magnetic-field sensitivity for H-field antennas for ELF communication systems is about 10^{-14} T Hz^{-1/2} (referred to air), which is well within the operational sensitivity demonstrated by present-generation SQUIDS coupled to flux transformers with several-centimeter-diameter primaries. Thus a SQUID and its dewar system (which is of the order of 0.3 M long and several centimeters in diameter) is a possible replacement for a several-hundred-meter-long ferrite-loaded H-field antenna for ELF reception.

One problem in using a SQUID system for this communication application is that the flux transformer (and also the SQUID itself) is a vector sensor of magnetic field and any motion of the antenna in the earth's field will produce a spurious signal which might be in the frequency band of the incoming signal. Thus, to use a SQUID as an H-field antenna, a configuration must be devised which would be relatively insensitive to orientation with respect to earth's field. Since the incoming signal is coherent, that is, the phase of the incoming signal has a discrete relationship to the phase of any other portion of the signal, signal-averaging techniques can be used to extract the desired signal from background noise. Thus the SQUID configuration required for this application must provide a signal which has a relatively constant amplitude. A signal which would be invariant to rotation can be obtained by using three orthogonal SQUIDS, squaring the output signals from each SQUID, and then adding these squared outputs. If the three SQUIDS (or flux transformers which are coupled to the SQUIDS) are precisely orthogonal, then the array can rotate arbitrarily without causing any spurious signal.

However, if the orthogonality condition is not precisely satisfied then the rotation of the array must be restricted so that the variation of the output signal is within the dynamic range of the electronics used in each of the SQUID channels. Calculations indicate that the product of the degree of platform stability and search-coil orthogonality needed are within the capabilities of present-day technology. These considerations will be presented in greater detail later at this workshop.¹⁷

Thus for applications in which the received signal is coherent, a compact H-field antenna can be assembled using three orthogonal superconducting magnetometers. Such an antenna would be compact but would require a certain amount of platform stability.

MAD APPLICATIONS

In the case of a magnetic-anomaly-detection (MAD) system, the signal appears as a blip on the output display unit as the MAD aircraft flies over the anomaly. For typical aircraft speeds the signal appears in the 0.01 to 1 Hz frequency band. Present-generation MAD equipment, which detects the total field of the anomaly, is quite often limited in range due to geomagnetic background noise, which is incoherent. Thus data-processing techniques are of limited value in distinguishing between a MAD signal and background noise when the signal-to-noise ratio is less than unity. Therefore, the improvement in total-field sensitivity of the SQUID relative to optically pumped helium magnetometers is of little use in total-field MAD systems, since both types of detection system would be limited by background

noise in the frequency range of interest in MAD.

However MAD ranges can be increased by using a gradiometer mode of detection. The background noise is due to distant sources and is characterized by long wavelengths whereas the signal from the anomaly, which is a nearby source, has an appreciable gradient signature. The use of a gradiometer configuration will separate the anomaly signal from the background noise. For anomalies that have total field signatures of the order of 10^{-10} to 10^{-11} T at typical detection ranges, the associated gradient signal for the anomaly would be of the order of 10^{-14} to 10^{-15} T/m, a sensitivity readily achieved with present day SQUIDS. The gradient of geomagnetic noise in the 0 to 1 Hz band is estimated to be below 10^{-15} T/m and thus should not limit the detection range of a MAD gradiometer system.

The concept of using a stationary gradiometer for the detection of an anomaly is well established. However, if the gradiometer is mobile (for example, airborne), then any motion of an imperfectly balanced gradiometer will produce a spurious signal which probably will be within the band of interest. The magnitude of the spurious signal is proportional to the product of the unbalance of the two superconducting loops forming the gradiometer and of the amplitude of the uncertainty in the angular orientation of the platform relative to the earth's magnetic field. Thus the required platform stability is determined by how well the gradiometer can be balanced (made insensitive to the total field). Calculations indicate that the requirements on gradiometer balance and platform stability needed to

Table 1 - Squid Performance

Parameter	Present Status	Future Goals
Squid Diameter	0.2 cm	1.0 cm
Operating Temperature	4 K	1 K
Excitation Frequency	30 MHz	10 GHz
Theoretical Field Sensitivity (Rms noise)	1.2×10^{-14} T//Hz	1×10^{-17} T// Hz
Experimental Sensitivity (Rms noise)	$\sim 1 \times 10^{-13}$ T// Hz	-
Frequency Response	DC - 50 kHz	DC - 100 MHz
Field Sensitivity with Flux Transformer ($\approx 100X$)	$\approx 1 \times 10^{-15}$ T// Hz	10^{-19} T// Hz (Theory)

provide gradient detection ranges comparable to or slightly better than total-field MAD ranges can be achieved using present technology.

The application of SQUIDS in MAD systems makes use of the great sensitivity of the device which make gradient detection systems possible with the use of quite reasonable--about 0.3-m--baselines. If a gradiometer system were built using present-generation optically pumped magnetometers, baselines of the order of 300 m would be required to provide gradient sensitivities comparable to that achievable with present-generation SQUIDS.

SUMMARY OF NAVAL USES OF SQUIDS

In summary, the advantages of SQUIDS are:

- . They are small and compact systems.
- . They have great sensitivities.

The problem areas are:

- . Platform stability is required due to the vector nature of SQUIDS and superconducting transformers.
- . A cryogenic environment with operating temperatures 10 K and below is required. (This crucial problem has not been discussed in this paper.)

REFERENCES

1. H.K. Onnes, Comm. Phys. Lab. Univ. of Leiden, No. 122B, 1911.
2. J.E. Kunzler, E. Buehler, F.S.L. Hsu and J.W. Wernick, Phys. Rev. Letters 6, 89 (1961).
3. B.D. Josephson, Phys. Letters 1, 251 (1962).
4. T.F. Finnegan, A. Denenstein and D.F. Langenberg, Phys. Rev. B4, 1487 (1971).
5. W. Meissner and R. Ochsenfeld, Naturwiss 21, 787, (1933).
6. F. London, Superfluids, Vol. 1, (John Wiley and Sons, Inc. New York 1950).
7. A.H. Silver and J.E. Zimmerman, Phys. Rev. 157, 317 (1967)
8. P.W. Anderson and A.H. Dayem, Phys. Rev. Letters 13, 195 (1964).
9. J.E. Mercereau, Revue de Physique Appliquee 5, 13 (1970).
10. R.P. Gifford, R.A. Webb and J.C. Wheatley, J. Low Temp. Phys. 6, 533 (1972).
11. J.E. Zimmerman and N.V. Frederick, Appl. Phys. Letters 19, 16 (1971).
12. R.A. Kamper and M.B. Simmonds, Appl. Phys. Letters 20, 270 (1972).
13. F.J. Rachford, C.Y. Huang, S. Wolf and M. Nisenoff, Appl. Phys. Letters 24, 149 (1974).
14. M. Nisenoff, Revue de Physique Appliquee 5, 21 (1970).
15. J.E. Zimmerman, J. Appl. Phys. 42, 4483 (1971).
16. J. Kurkijarvi and W.W. Webb, Applied Superconductivity Conference, Annapolis, Md. (1972), IEEE Pub. No. 72Ch0682-5-TABSC, p. 581.
17. S.A. Wolf, J.R. Davis and M. Nisenoff. See paper later in these proceedings; also see IEEE Transaction on Communications Special Issue on ELF Communications, COM-22, 548 (1974).

Edgar A. Edelsack
Office of Naval Research
800 N. Quincy St.
Arlington, VA 22217

INTRODUCTION

There are several groups in ONR which presently support research in superconductivity. Some 80 to 85% is supported within the Physics Division and my remarks this morning will be restricted to those tasks. I will try to present a broad view of some of these efforts and highlight a few recent significant accomplishments.

Fig. 1 shows some of the naval applications of superconductivity. The list is far from complete, but I believe it includes most of the areas where significant amounts of money are now being spent by the Navy.

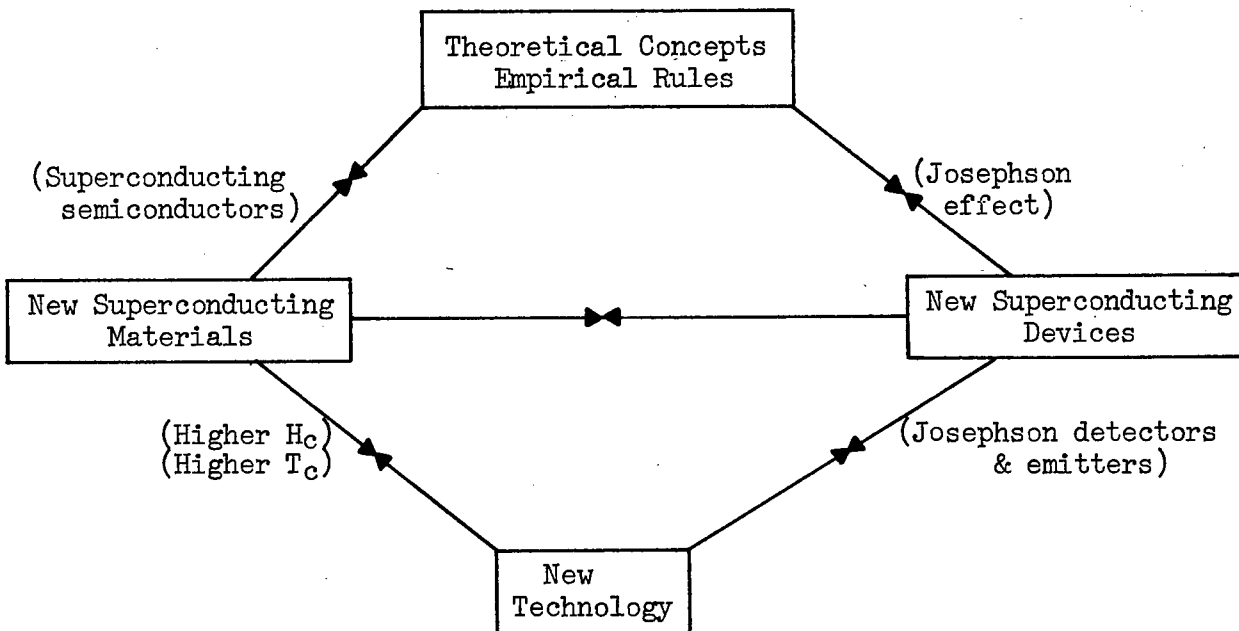
Figure 1 NAVAL APPLICATIONS OF SUPERCONDUCTIVITY

- Ship propulsion systems
- Magnetic sensors for ASW
- Electromagnetic sensors for surveillance and communication
- Electronic components for communication and surveillance systems at microwave, RF and ELF frequencies
- Magnets for mine sweeping

MATERIAL RESEARCH

Fig. 2 may be familiar to some of you. The superconducting materials research pathway unfortunately gets very little support by ONR. The major Navy effort in superconducting materials is here at NRL. What does exist in ONR in this field is supported by the Metallurgy group under Dr. Rauch. One example is Professor R. Rose at MIT who is studying the various properties of transition metal superconductors using single crystal tunneling techniques. A second is a metallurgy contract with Professor Z. Fisk at University of California, LaJolla. Fisk is experimentally investigating the normal state and superconducting properties of isostructural intermetallic compounds. I understand that these metallurgy projects will be terminated next year. It thus appears that by FY75, unless there is a major change of emphasis, there will be no superconducting materials research supported by ONR.

Figure 2
The Pathways to Payoff in Superconductivity



CONTRACT RESEARCH PROGRAM

UNCLASSIFIED

It is the superconducting devices pathway which at present receives major emphasis in ONR. Fig. 3 shows the over-all money picture. While the final FY74 numbers are not in, the total ONR CRP Program will be around \$900,000 -- a drop of some 10% from FY73. For FY75 the Superconducting Technology and Devices Programs will be combined and the projected total is some \$700,000--down 20% from FY74.

Figure 3
SUPERCONDUCTIVITY FUNDING
General Physics Subelement

<u>Contract Research Program</u>	<u>FY 1972</u>	<u>FY 1973</u>	
Superconducting Technology	\$ 745K	\$ 613K	(-18%)
Superconducting Devices	513K	471K	(-8.2%)
Subtotal	\$1,258K	\$1,084K	(-14%)
<u>In-House</u>			
NRL	211K	335K	(+59%)
TOTAL	\$1,469K	\$1,419K	(-3.4%)

SUPERCONDUCTING TECHNOLOGY PROGRAM

Now let us consider some of the details of the Superconducting Technology Program which is administered by Dr. L. Cooper. This program supports an effort at Stanford University under Professors W. Fairbank and A. Schwettman, aimed at building a large scale cryogenic facility. This facility includes a 500 foot long test bed of superfluid helium continuously cycled to a 300 watt refrigerator operating at 1.85K. The goal of this project is to build a 2 to 10 billion volt superconducting electron linear accelerator for high energy physics research. The accelerator will consist of niobium microwave cavities operating at 1300 MHz. Cavity Q's as high as 10^{11} have been achieved. This accelerator is presently under NSF management.

In a related project, this Stanford group are developing a very highly stable superconducting cavity oscillator at 8.6 GHz. The best frequency stability they have attained to date is about one part in 10^{14} . This is competitive with the best existing frequency standards.

SUPERCONDUCTING ELEMENTS PROGRAM

Now turning away from large scale applications, let us consider the Superconducting Elements Program. This program is largely concerned with microsuperconductivity -- small scale applications. This program was begun in the latter part of 1967 in an attempt to exploit the new properties of superconducting materials and devices which were discovered in the late 1960's. Fig. 4 shows the funding history of this program.

The present program is divided into three main areas: sensors, machinery and refrigeration. Fig. 5 shows the details of FY72 and FY73 picture. Who is doing the research and where it is being done is shown on Fig. 6. In all there are some 16 contractors. The program is undergoing some major changes and by the end of FY74 we plan to have terminated about five of these tasks. Let us look at some examples from various research areas.

Figure 4
SUPERCONDUCTING ELEMENTS PROGRAM EXPENDITURES

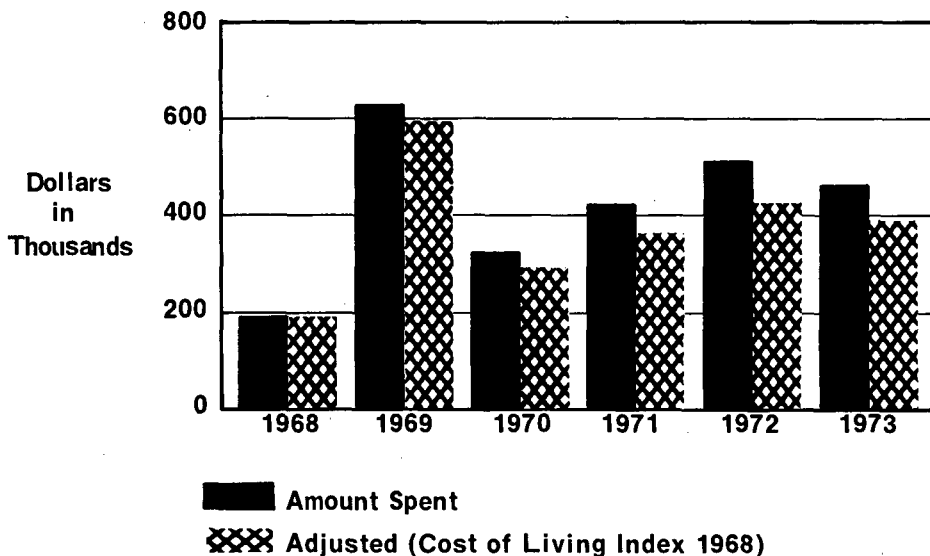


Figure 5
SC DEVICE PROGRAM

UNCLASSIFIED

<u>Research Area</u>	<u>FY 72 Funding</u>	<u>FY 73 Funding</u>
Materials	\$ 24K	\$ 0
Sensors		
Magnetic	103K	111K
Electromagnetic	89K	56K
Arrays	49K	44K
New Devices	86K	95K
Techniques	66K	35K
Subtotal	<u>\$393K</u>	<u>\$341K</u>
Machinery	75K	51K
Refrigerators	0	68K
Meetings	21K	11K
TOTAL	<u>\$513K</u>	<u>\$471K</u>

Figure 6
SUPERCONDUCTING DEVICE PROGRAM

<u>Research Area</u>	<u>Contractor</u>	<u>Investigator</u>
Magnetic Sensors	NBS	J. Zimmerman
"	Cornell	W. Webb
"	NY/SB	J. Lukens
Electromagnetic	Rochester	S. Shapiro
"	Berkeley	P. Richards
Arrays	Cornell	T. Clark
"	NBS	T. Finnegan
New Devices	Cal. Tech	J. Mercereau
"	Westinghouse	M. Janocko
"	Harvard	M. Beasley
Techniques	Virginia	B. Deaver
"	MIT	R. Meservey
Machinery	MIT	J. Smith
"	Westinghouse	M. Walker
Refrigerators	NRL	S. Collins
"	NBS	R. Radebaugh

SENSORS

From the very beginning we have tried to push superconducting magnetic sensors out of the laboratory into the realm of practical usable devices. The rationale for this was our belief in 1968 that it might be possible to achieve a factor of around a thousand greater in sensitivity over the then existing MAD gear used in the fleet. Well, after five years where are we today? One example is Dr. J. Zimmerman's group at NBS, Boulder, who have developed small reliable ultrasensitive portable superconducting magnetometers and gradiometers with sensitivities several hundred times greater than that of the ASQ-81 now used in the fleet. In addition to the sensor work, the Boulder group are developing small spun glass helium dewars with holding times of the order of several days. Presently they have some dewars with holding times of 65 hours. Most recently Zimmerman has succeeded in sputter depositing platinum and tungsten on niobium points. Josephson junctions using these point contacts have proved to be very stable and reproducible. They can be stored at room temperature and thermally cycled without deterioration and have operated at frequencies up to 10 GHz.

Professor Webb at Cornell has been investigating the intrinsic noise limits of superconducting rf-biased magnetometers. The performance of presently operating units appear to be about a 1 to 2 orders of magnitude worse than the calculated fundamental limit. However, recently, Webb believes that there may be some errors in these calculations and at the moment the question of limits of operation due to thermal fluctuation noise is still up in the air.

The contract with Professor J. Lukens at Stony Brook is a relatively new one, having begun in April of this year. He is investigating the precisely controlled characteristics of superconducting thin-film microbridges using electron-beam techniques.

Before we leave magnetic sensors, I should mention that the CNR supported work in this area has also had important payoffs in the civilian sector. It has stimulated two new areas of medical diagnosis - magnetocardiography and magnetoencephalography -- the measurements of the very minute magnetic fields due to the electrical activity of the human heart and brain.

Turning now to the area of electromagnetic sensors, Prof. P. Richards at University of California, Berkeley is studying the properties of Josephson junctions as low noise, wide bandwidth detectors of microwave and far infrared radiation. He has built thermally recyclable point contact junctions whose response to 36 GHz radiation was observed to be in quantitative agreement with theory. Richards is also investigating the use of an analog junction simulator to perform calculations which are too complicated for analytical solution. Some of these recent calculations indicate that very efficient devices can be built in the 30 - 300 GHz range. However, it is still premature to try to evaluate their performance as compared with Schottky barrier devices.

Professor S. Shapiro at the University of Rochester is also studying the properties of superconducting point contact junctions as detectors of microwave and millimeter wave radiation. He is investigating the various phenomena resulting from the coupling of a Josephson junction device to a cavity, resonant at one frequency and simultaneously driven by an external radio-frequency source at a different frequency. Simple equivalent circuit models of Josephson junctions have been confirmed by comparing the predictions of an analog computer simulator with experimental results under carefully controlled conditions.

Research on the properties of arrays made of many superconducting junctions is still in its infancy. Dr. T. Clark at Cornell has made 50 - 100 interconnected junctions and has begun to study their electrical and magnetic properties.

Dr. T. Finnegan at NBS, Gaithersburg, is studying the properties of individual and coupled arrays of Josephson junctions devices as detectors of microwave radiation. He has fabricated novel microstripline devices in which the junctions form part of a transmission line.

Now turning to the area of new devices, Professor J. Mercereau at the California Institute of Technology has for some years been studying the behavior of non-homogeneous superconducting structures in their relation to very high frequency sensors. In a recent study of proximity effect weak links of tantalum with niobium overlay, a unique very low impedance superconducting galvanometer was developed with a sensitivity of about 10^{-9} amperes for a one cycle band width.

Dr. M. Janocko at Westinghouse is studying the characteristics of superconducting electromagnetic radiation detectors of the thin film weak link geometry. These devices are being fabricated with materials having transition temperatures approaching the liquid hydrogen range -- 20K. The spectral response of these bridges covering the range from x-band (9GHz) on into the millimeter range is being investigated. In a collaborative effort with NRL, molybdenum-rhenium junctions with a transition temperature of about 12.8K will be evaluated in magnetometer configurations. They have just begun working on microbridge devices of Nb₃Ge which have a transition temperature of about 23K.

Professor M. Beasley at Harvard has been studying the properties of dc-biased superconducting thin film microbridges at temperatures well below their critical temperature. It appears that their electrical behavior is largely dominated by self-heating effects. These results may place important limitations on the temperature and voltage range over which these junctions can be expected to exhibit useful Josephson behavior.

Passing on to the techniques area, Prof. B. Deaver at the University of Virginia is studying the characteristics of weak-link type devices produced by means of ion implantation. This technique looks interesting but as yet there are no results which permit evaluation of the utility of this technique.

Professor R. Meservey at MIT is employing angular evaporating and shadowing techniques to achieve submicron resolution thin film structures. The electrical properties of these structures have been studied.

MACHINERY

Turning to the area of machinery, the two tasks shown in Fig. 6 represent cooperative efforts with NAVSHIPS. Professor J. Smith at MIT has been studying two superconducting AC machine concepts. One

involves a dual armature superconducting induction machine and the other is a thyristor-switched low-speed superconducting AC motor. Non-superconducting models of these two machines are now being built for analysis and evaluation.

Dr. M. Walker at Westinghouse is investigating the performance of sample superconducting field windings in an attempt to determine design optimization criteria for such windings. These data will be particularly useful to the group at Annapolis under Dr. J. Levedahl who are working on superconducting machinery for Naval propulsion.

REFRIGERATION

In the last category, refrigeration, Professor S. Collins at NRL is studying various means to improve the reliability and efficiency of closed cycle helium refrigerator. Since the majority of mechanical failures experienced with helium refrigerating systems have occurred in the helium compressor a part of this task is directed to the improvement of compressor design. A compressor of novel design is now under construction and should be finished shortly. Also a small closed cycle refrigerating system with special heat exchangers and expansion engines is being assembled.

The last task is that of Dr. R. Radebaugh at NBS, Boulder. This project is jointly funded by ONR and ARPA. The NBS group is investigating a prototype cryogenic refrigerator based on the electrocaloric effect in some new para-electric glasses produced by Corning. These materials exhibit large reversible temperature dependent electric susceptibilities at temperatures below 30K and therefore absorb or emit heat under the influence of electric polarization or depolarization. Radebaugh plans to build a small model and evaluate its performance from about 4 to 16 K.

Some three years ago at the conclusion of a similar talk at Panama City, I voiced the hope that there could be forged a feed back loop between these ONR supported research tasks I have just described and the efforts at the various Navy laboratories and the exploratory development interests of the various commands. Looking back over these years, the success in achieving this goal hasn't been particularly outstanding. I thus want to conclude this talk with a plea -- a plea to help us in ONR and at the same time help yourselves by highlighting the important research and engineering problems that presently plague you. By doing this you can help us in ONR direct our 6.1 research programs in superconductivity into meaningful and relevant areas and likewise help your own programs get answers to problems that urgently need solution.

HF APPLICATIONS OF SUPERCONDUCTIVITY

Nancy K. Welker
Fernand D. Bedard
National Security Agency
Fort George G. Meade, Md. 20755

There are problem areas in communications for which we believe superconductivity offers attractive and feasible solutions. In particular, we are now pursuing two uses in the high frequency region; one is concerned with the development of Josephson phenomena for a magnetometer antenna, the other exploits the zero resistance aspect of superconductivity to produce a narrow band rejection filter.

A. MAGNETOMETER:

A compact antenna using active devices is an attractive alternative to conventional antennas in some situations. The obvious advantage of size can sometimes be supplemented by others, for example instantaneous wide band width and compact array configurations. For these reasons, we undertook an effort¹ to investigate the feasibility of using a superconductive magnetometer to collect the H field of an RF wave rather than its E-field as is more conventional.

At the time we began, superconductive magnetometers were commercially available with a sensitivity of 10^{-9} Gauss and an upper frequency response of around 20 KHz. Since our interest was in the HF frequency range, 3-30 MHz, effort was needed in raising the frequency response. As regards sensitivity, 10^{-9} Gauss is impressive - until you compare it with a conventional E-field antenna and are forced to agree with the snide comment "I can do that with a wet string". However, before jumping immediately into a program to improve sensitivity, one must know how much is enough.

Figure 1 is a plot of the omnidirectional noise in a 1 Hz bandwidth experienced in England during the summer². The noise generated by world wide storm activities is seen to be orders of magnitude larger than a 300°K thermodynamic black body designated by the curve kT. Ideally, one wishes to have

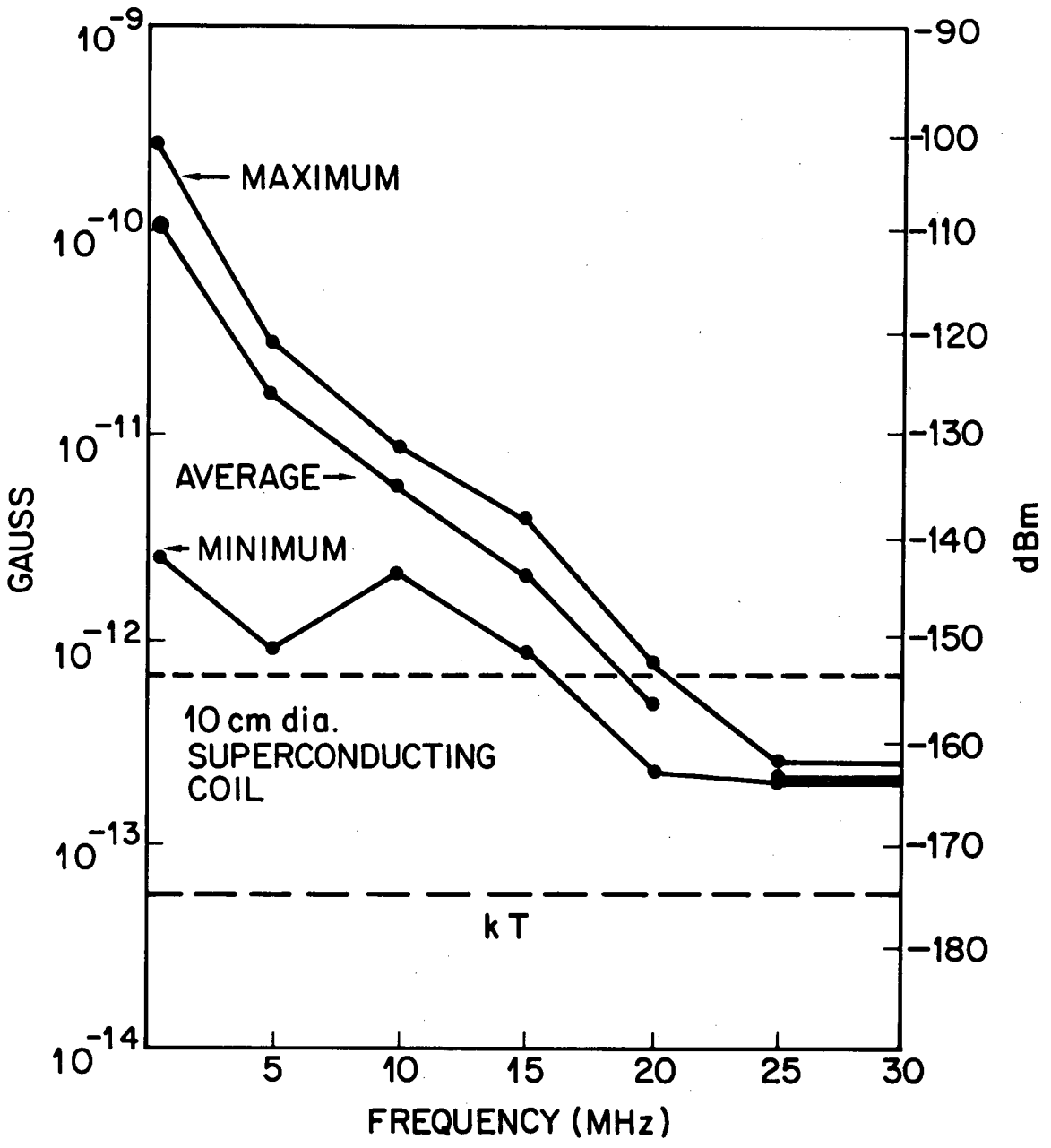


Figure 1

his system sensitivity limited by the atmospheric noise, not by the hardware; clearly a sensitivity of 10^{-9} Gauss is totally inadequate. With this in mind, we set as first step goals a sensitivity of 33×10^{-12} Gauss ($1\mu\text{V}/\text{meter}$ field strength) a dynamic range of 50db, with instantaneous bandwidth 3-30 MHz.

As background, it is useful to review the basic features of a Josephson junction as it applies to the construction of a magnetometer. (Fig. 2) If you form a sandwich of superconductor, thin insulator, superconductor (Fig. 2a) and pass a current through it while measuring the voltage across the device, you observe highly non-linear behavior. First, for a thick ($\sim 100 \text{ \AA}$) insulator, curve a is obtained (Fig. 2b). This comes about from current transport due to single electron tunneling: no current is observed until the voltage applied exceeds the energy gap in the density of states, i.e. several millivolts, whereupon an abrupt increase is seen. If the insulator is reduced in thickness, to the order of 10-20 \AA , current may now be carried by correlated pairs producing no potential drop (curve b) until the critical current value I_{max} is exceeded, and then the current transport switches rapidly to curve a. In a sense, the insulator behaves as a "weak superconductor". In the actual devices used in magnetometers the insulator is replaced by an extremely thin bridge joining the two superconductors, a so called "weak link" (Fig. 2c). Even though the I-V curve is quite different, the Josephson phenomenon appears to be the same in this geometry. This weak link is constructed by taking a superconducting thin film band which has been evaporated onto a cylinder and scribing into the band from both edges to have a very narrow bridge. One now has manufactured a very low inductance superconducting ring broken by a Josephson weak link, a SQUID. (Superconducting Quantum Interference Device). The use of this non-linear device is straight forward - but non-trivial.

Fig. 3 shows the block diagram of the system being developed. A 10 GHz microwave source, the pump, imposes an AC magnetic field upon the SQUID. At the same time, a coil, several centimeters in diameter picks up the desired signal environment (3-30 MHz) and transfers its magnetic field to the SQUID also. The superposition of these fields in the device results in a non-linear mixing of these frequencies with a parametric energy conversion. The resulting spectrum is then recombined with the 10 GHz pump to provide the desired signal frequencies. In addition, this demodulated signal is

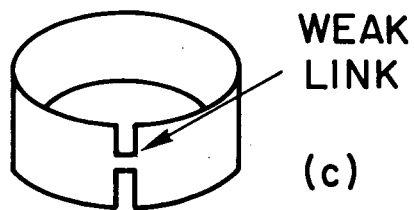
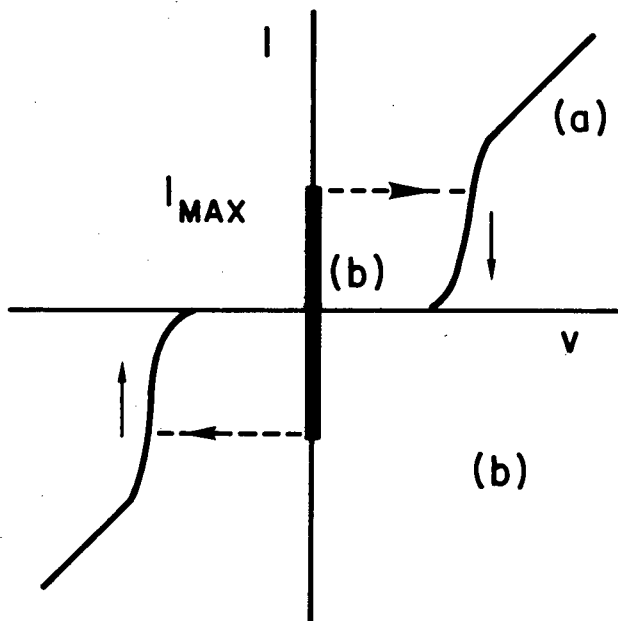
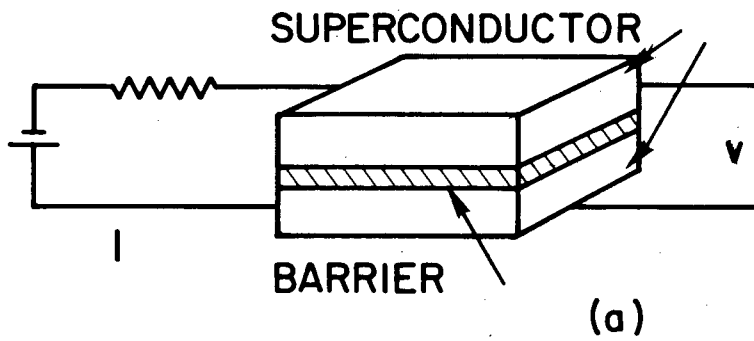


Figure 2

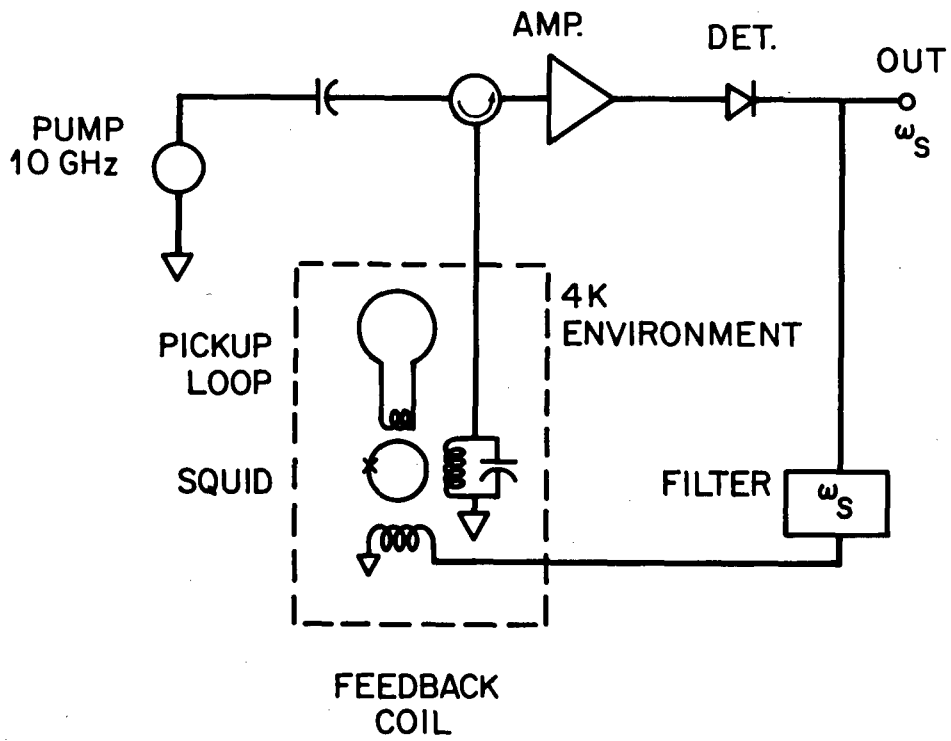


Figure 3

fed back to the SQUID to linearize the system. In fact, this linearization is essential to the feasibility of the system. To appreciate this it is necessary to inspect the appropriate part of the Josephson equation.

$$i = i_s \quad \text{Sin} \frac{2\pi}{\phi_0} \int V dt \quad \text{where, } \phi_0 = 2.07 \times 10^{-7} \text{ Gauss} \\ \text{-cm}^2$$

If we assume that the voltage picked up in the ring is experienced by the weak link, then:

$$V = \frac{-d\phi}{dt} \quad \text{and } i = i_s \quad \text{Sin} \frac{2\pi\phi}{\phi_0} \quad (1)$$

The device can now be considered to experience two fluxes, ϕ_{pump} , and ϕ_{signal} i.e., $\phi = -\phi_p \text{ Sin } \omega_p t - \phi_s \text{ Sin } \omega_s t$

Inserted into (1), this produces

$$i = i_s \text{ Sin } 2\pi \left[\frac{-\phi_p}{\phi_0} \text{ Sin } \omega_p t - \frac{\phi_s}{\phi_0} \text{ Sin } \omega_s t \right]$$

Trigonometric relations show this to be of the form $\text{Sin} [\alpha \text{ Sin } \beta]$, which produces the following product Bessel series:

$$i = i_s \sum_{m,n} J_m \left(\frac{2\pi\phi_p}{\phi_0} \right) J_n \left(\frac{2\pi\phi_s}{\phi_0} \right) \text{ Sin } (m\omega_p + n\omega_s) t$$

If we assume our system to operate at $f = 10 \text{ GHz}$, it is trivial to avoid the terms in ω_p other than $m = 1$. However, we are now caught in experiencing the harmonics of ω_s and the mixing terms when there exist other signal frequencies. To obviate this, it is necessary to feed the signal back to the SQUID and thereby reduce ϕ_s by an amount sufficient to suppress terms of $n = 2$ and higher.

At the present time, the system sensitivity is designated by the line in Figure 1. The loop has not yet been closed to allow linearity and dynamic range to be established; this is expected shortly.

Since the system really has response down to DC, if so desired, it is worth the digression to look toward that part of the spectrum and ask whether this sensitivity has any usefulness there. Fig. 4 shows the omnidirectional noise

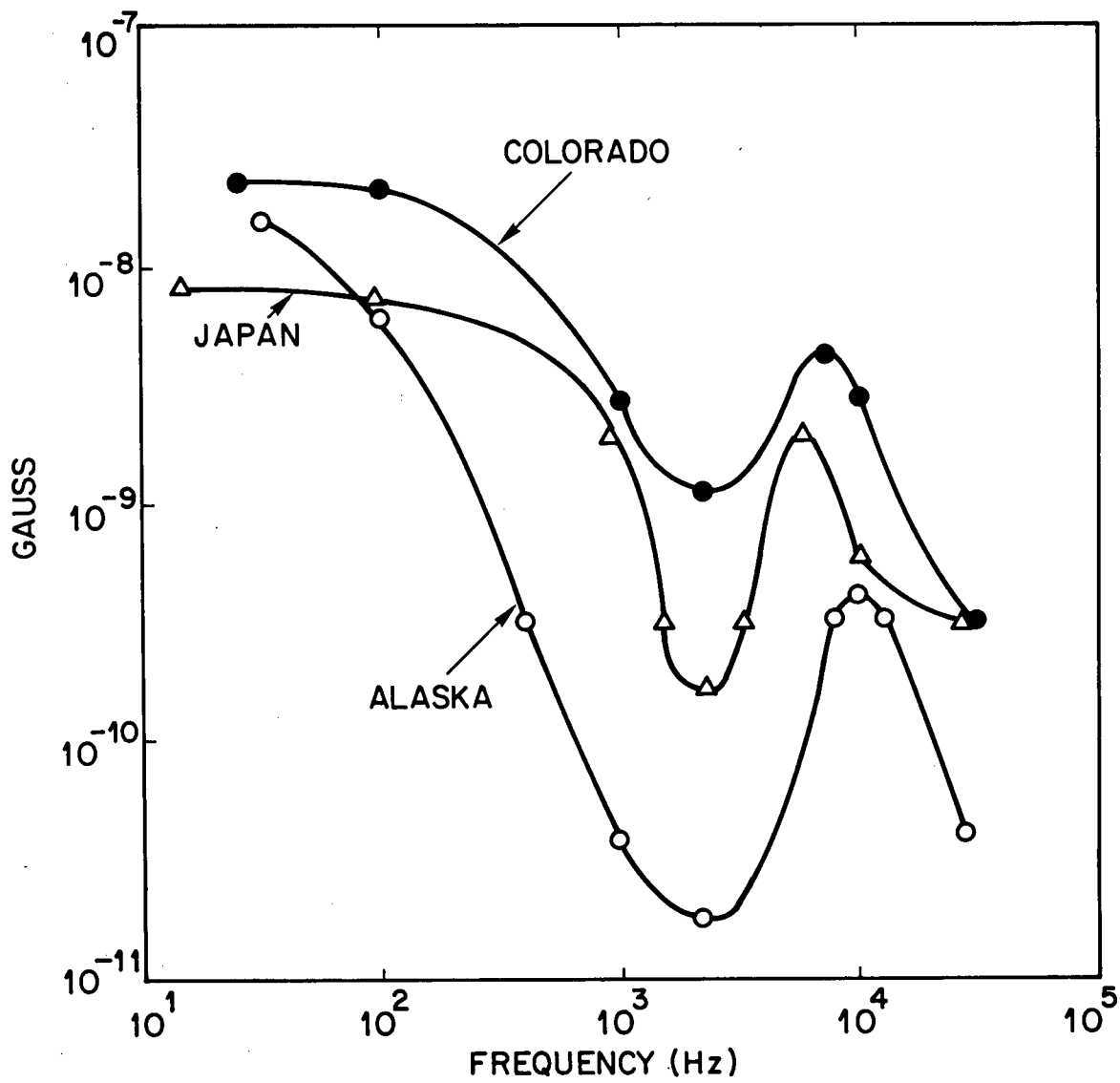


Figure 4

typical of the ELF-VLF range³. Here we note that a 10^{-11} Gauss sensitivity is excessive for earth's surface use. Fig. 5 is a graph of the attenuation vs frequency of sea water⁴. Since the noise we are contending with is atmospherically generated, it will attenuate with depth, as shown in Fig. 6 for a depth of 50 M, and 100 M. We now note that at a given depth this magnetometer sensitivity allows a higher frequency of operation at which we stay atmospherically noise limited. There exist, of course, significant other engineering problems to be surmounted to realize this sensitivity advantage.

There is another use of a small antenna for which the single element excess sensitivity is not wasted: that of compact array configurations, or so-called super-directive arrays⁵. The feasibility of such systems involves having elements sufficiently small that mutual interactions are not significant. This implies low efficiency in collecting the field energy and thus calls for devices with low internal noise. Furthermore, the elements must have very well matched responses. It appears that superconductive elements will be able to meet these conditions. Figure 7 shows a set of calculated antenna patterns obtained from several configurations of loop antennas. Curve a is that of a single loop; curve b is the result of taking three elements, equally spaced, multiplying the output of the end elements by a gain different from that of the center element, and summing the resulting signals. The result is a narrower beam pattern than that obtained from a single loop, or from three loops whose outputs are all summed equally. This improvement in directivity comes about at the expense of sensitivity, which tradeoff can be afforded if the elements are sensitive enough. Curve c is the pattern of a five element array whose overall width is the same as the three-element one. The center element, inboard pair and outboard pair contribute different, appropriate, amplitudes to be summed as the combined array output. Here again, a still narrower beam pattern is achieved at the expense of sensitivity.

The algorithm used applies a null at 90° , which already exists due to the loop characteristics; more effective rules can be established. For different frequencies, a different set of coefficients must be used. It is also possible to "steer" the maximum or a null by applying an appropriate phase shift. Finally, even though the sensitivity degrades as one lowers the frequency, this may be afforded since the background noise increases. Further, more detailed studies of these features are now in progress.

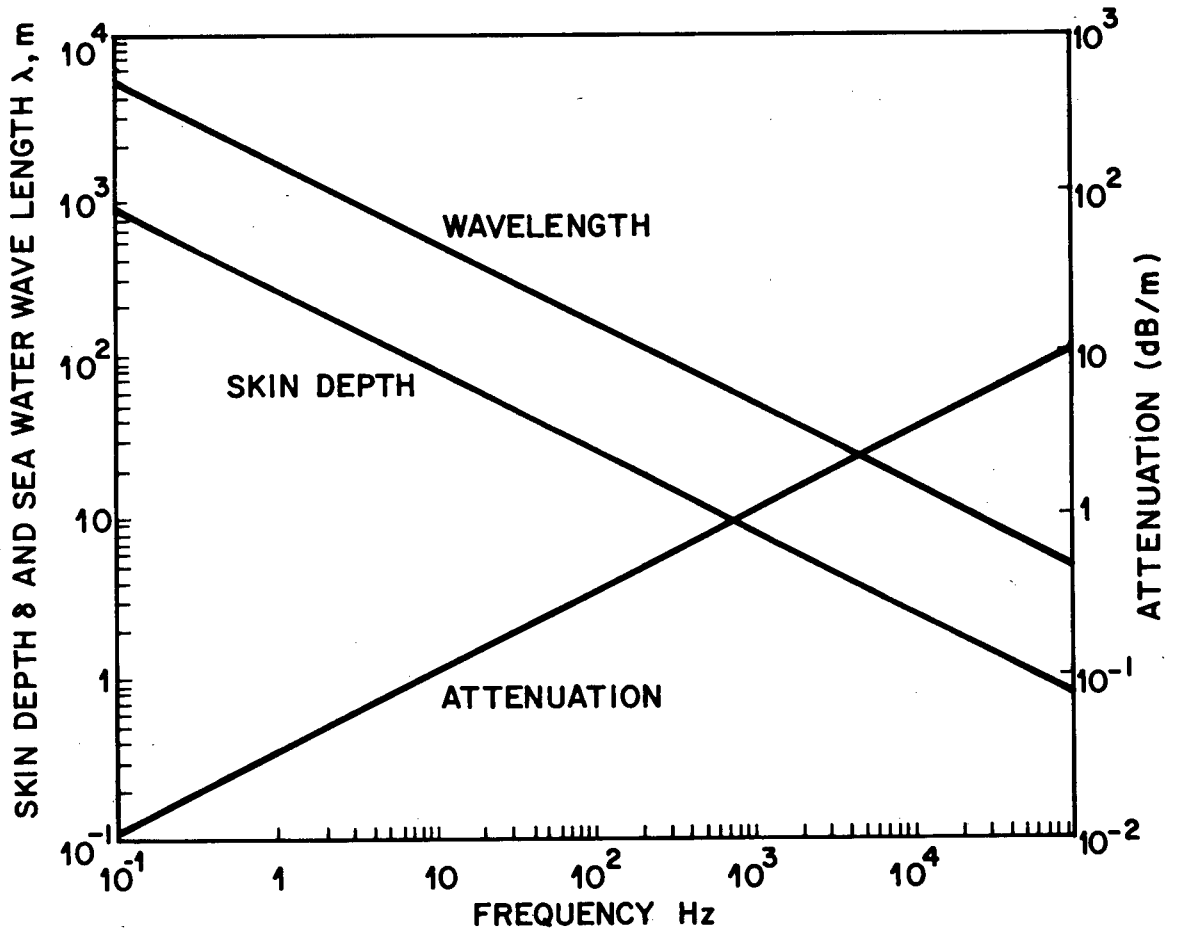


Figure 5

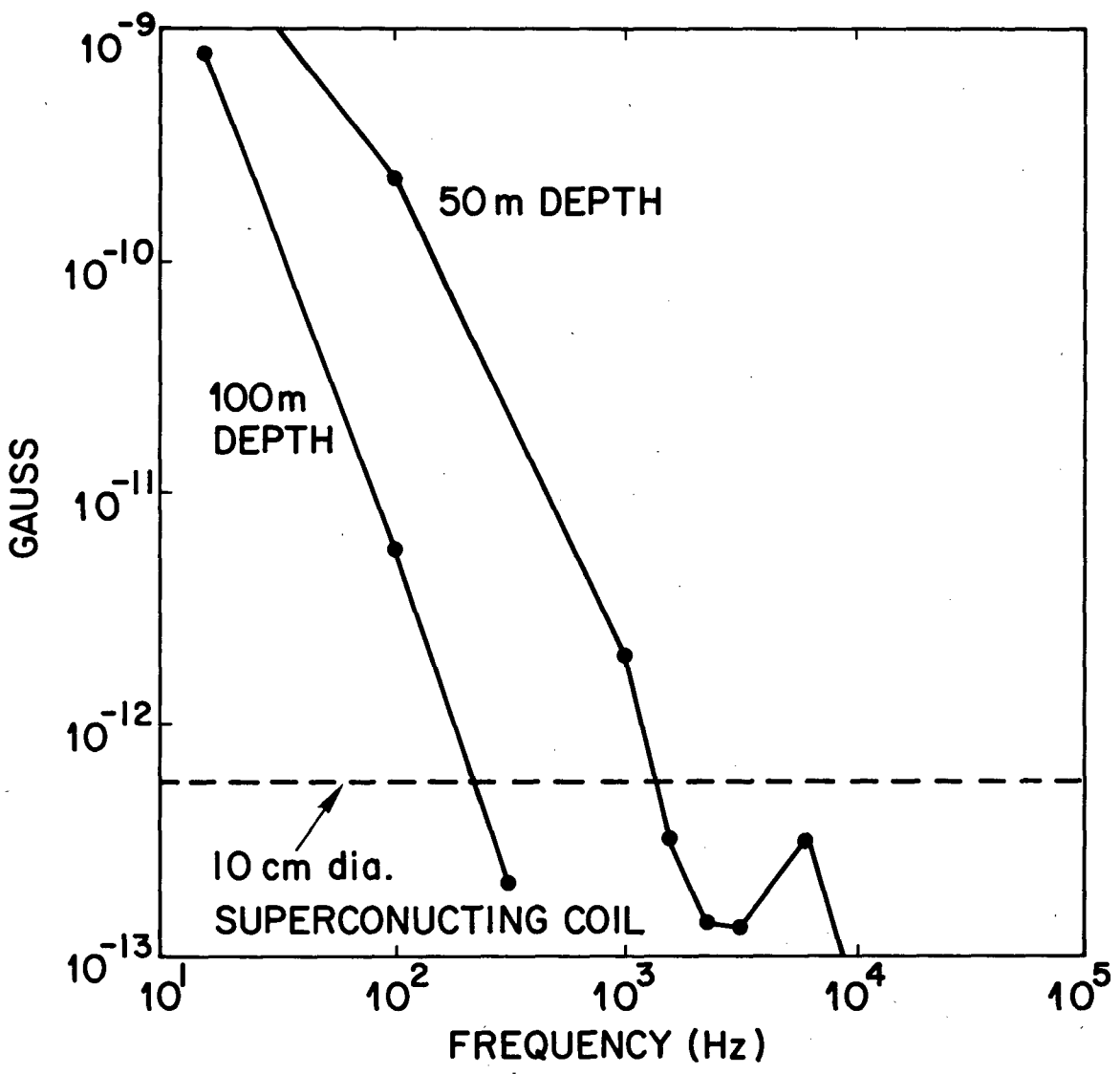


Figure 6

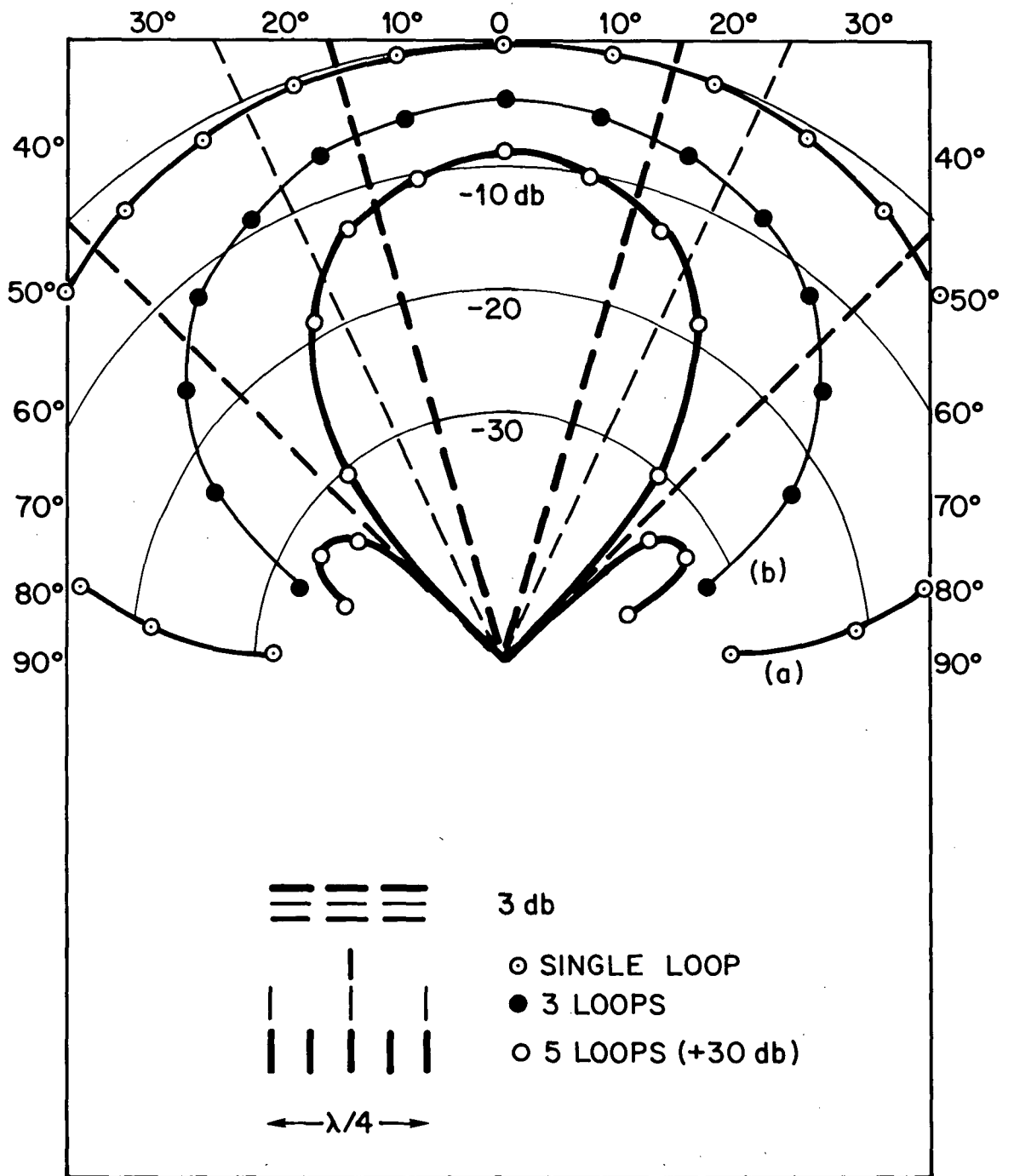


Figure 7

B. NOTCH FILTER:

In many situations, one is forced to acquire an RF signal whose frequency is very close to that of a large strength unwanted transmission. If allowed to pass into the receiver, this signal may well overload the electronics, producing spurious responses. One would like to selectively "notch out" these overloads before they reach the electronics, with negligible noise contribution and without losing the weak desired frequencies. Such a narrow band filter bank has been designed⁶ and is being built using superconducting tank circuits with Q's of 10^4 to 10^5 , each separately tunable. At the present time the elements L and C are manufactured from NbZr; it is intended to replace these with plated high temperature superconductors. The present materials allow operation with a small closed cycle refrigerator⁷. In order to make maximum use of each of the elements in the bank, we have used a conical tuning capacitor⁸ which will allow a tuning range of at least 4:1 in frequency (16:1 in capacitance). Thus the bank will have a set of 2-8 MHz filters, and a set of 8-32 MHz filters.

Since the individual filters have a very high Q, the mechanical motion of the system must be very precise and stable to make the system usable. In addition, it is important that some electrical means of changing the capacitance be implemented since the system is intended for use by field personnel, not laboratory workers. Thus, we are presently testing a motor driven differential screw assembly to perform the tuning. Preliminary tests are very promising.

In summary, we believe that there are problems in communications sciences in which superconductivity may be the most effective and even the only solution.

The antenna array calculations were initiated and carried out by Dr. John Pinkston; the work on the superconductive filter is being performed by Mr. Carl Gardner, both of National Security Agency.

REFERENCES:

1. The bulk of the work was performed under contract DAAB03-72-C-3328 with Develco, Inc., Mountain View, Calif.
2. CCIR Report 322
3. Adapted from Kraitchman; Handbook of Electromagnetic Propagation in Conducting Media; G.P.O., 1970; p. D-1.
4. Ibid; p. A-4
5. Antenna Analysis by E. A. Wolff, John Wiley & Sons, N. Y. (1966) pages 262-266 "Supergain Antennas"
6. Contracts: Airborne Instruments Lab - DA11-119-AMC-02530, dtd. Dec 66 and DAAB03-67-C-0386, dtd. Jan 69.
7. Cryomech Inc., Helium Refrigerator Model GB02
8. Analysis of Coaxial to Terminal Conical Capacitor, M. C. Selby, NBS Monograph #46, 6 Apr 62

SUPERCONDUCTING HIGH FREQUENCY RESONANT CIRCUITS

C. Hobbis
Communication Science Division

L. Weinman
Solid State Division

Naval Research Laboratory, Washington, D.C. 20375

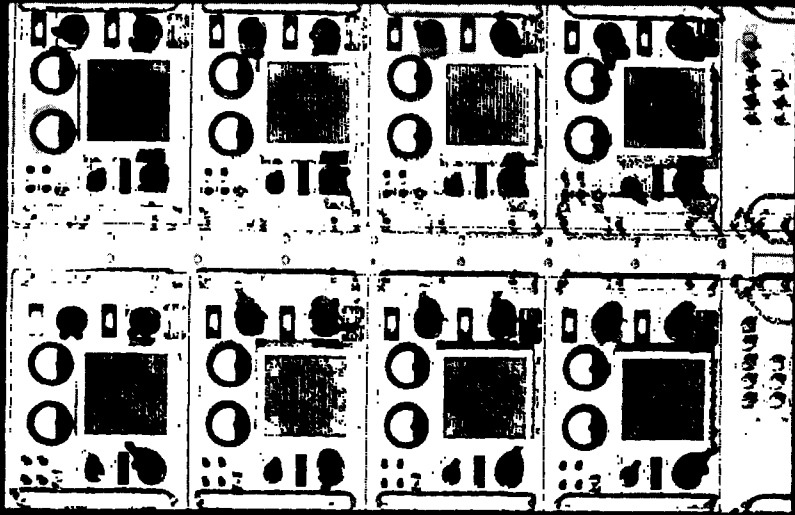
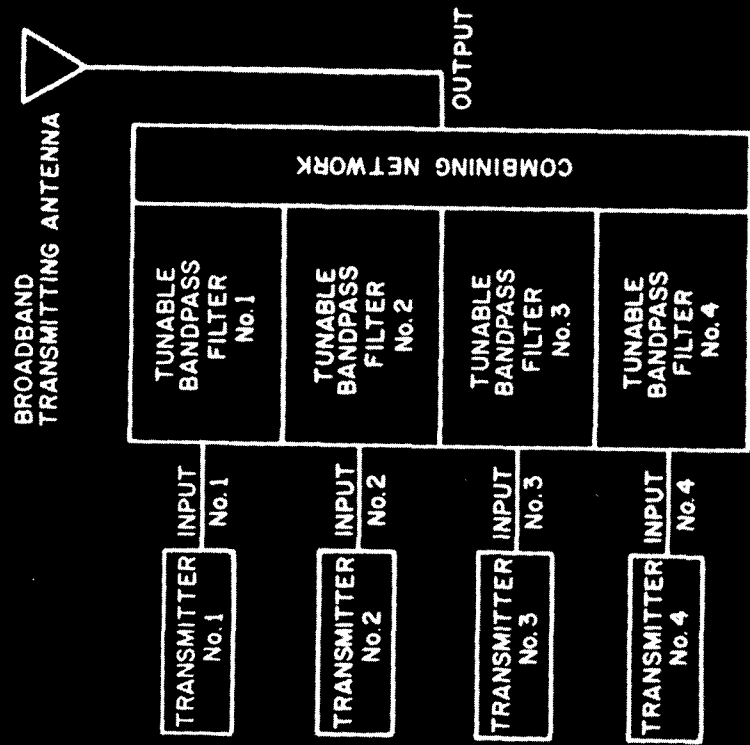
UNCLASSIFIED

The feasibility of utilizing high power high frequency superconducting resonators in Navy Communications Systems is being investigated. The application of this technology to multicoupler equipment will result in increased frequency spectrum utilization and efficiency. (A related application to antennas should relieve existing antenna siting problems.) Although the current phase of the effort is oriented to the HF (2 to 30 MHz) band, the results will be applicable to other frequency ranges as well.

Sufficient space does not exist, topside, to erect separate antennas for each shipboard transmitter or receiver. Therefore, multicoupling techniques have been developed to permit one antenna to be simultaneously coupled to, or shared by, many transmitters or receivers.

A current shipboard transmitting multicoupler, AN/SRA-56, is shown in Fig. 1. The RF path from each transmitter to the single antenna is established for each channel by a tunable filter operating into a combining network. A photograph of one of the tunable filters is shown in Fig. 2. It consists of two coupled resonators of copper construction which are tuned by variable vacuum capacitors.

GENERIC MULTICOUPLER



TYPICAL TRANSMITTING MULTICOUPLER ARRANGEMENT

Fig. 1 — AN/SRA-56 transmitter multicoupler system.

HF MULTICOUPLER

AN/SRA-56

2-6 MHz

- ISOLATE
- MATCH
- COMBINE
- FILTER

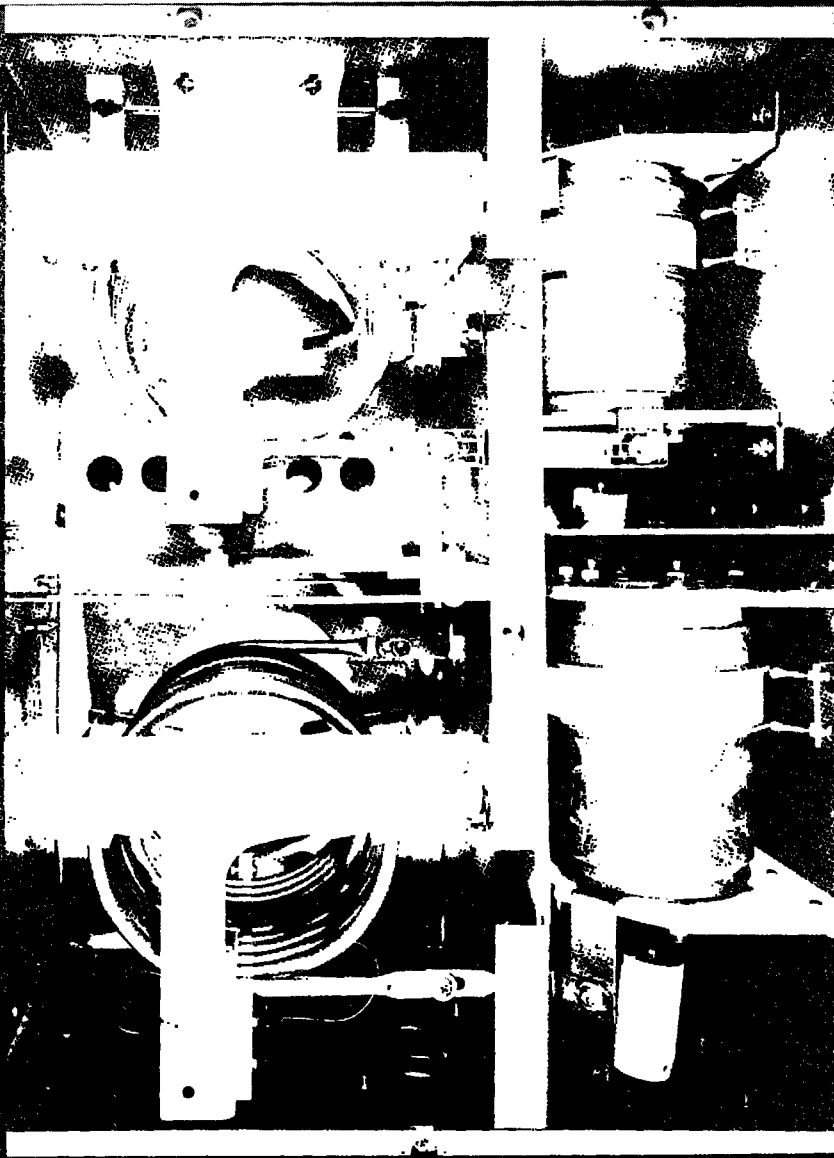


Fig. 2 — Tunable filter portion of AN/SRA-56 transmitter multicoupler system.

The response characteristics of the filter are established by the operating Q factor of the resonators. The operating Q factor, therefore, establishes the degree of isolation existing between transmitters at a given frequency separation. For the AN/SRA-56 approximately 35 db of isolation is provided for 5% frequency separation. Transfer efficiencies of existing multicouplers are approximately 65%. For the volume occupied, the performance attained by conventional multicouplers is essentially the theoretical limit.

The 5 percent frequency separation requirement imposes a severe restriction on communication systems as shown in Figs. 3a, b, and c. In Fig. 3a, a one MHz portion of the spectrum centered on 10 MHz and extending between 9.5 and 10.5 MHz is examined. If an information bandwidth of 4 kHz is assumed, there are 250 channels potentially available within the 1 MHz bandwidth. Ideally the response shape for each channel would be rectangular and of 4 kHz width. Three channels of this type have been placed within the 1 MHz bandwidth. The location of these channels has been selected based upon the performance of the conventional multicoupler.

In Fig. 3b three channels, having center frequencies of 9.5, 10.0 and 10.5 MHz, respectively, are enclosed within the response characteristics of current multicouplers. The frequency separation is 5%, which is the closest in frequency, the associated transmitters can be operated and yet be properly isolated, using current multicouplers.

The calculated performance of a multicoupler employing superconducting resonator circuitry is shown in Fig. 3c. Assuming each

INFORMATION
CHANNELS

NOMINAL BANDWIDTH =
4000 HERTZ
THEORETICAL MAX NO.
CHANNELS/MHz = 250

UNCLASSIFIED

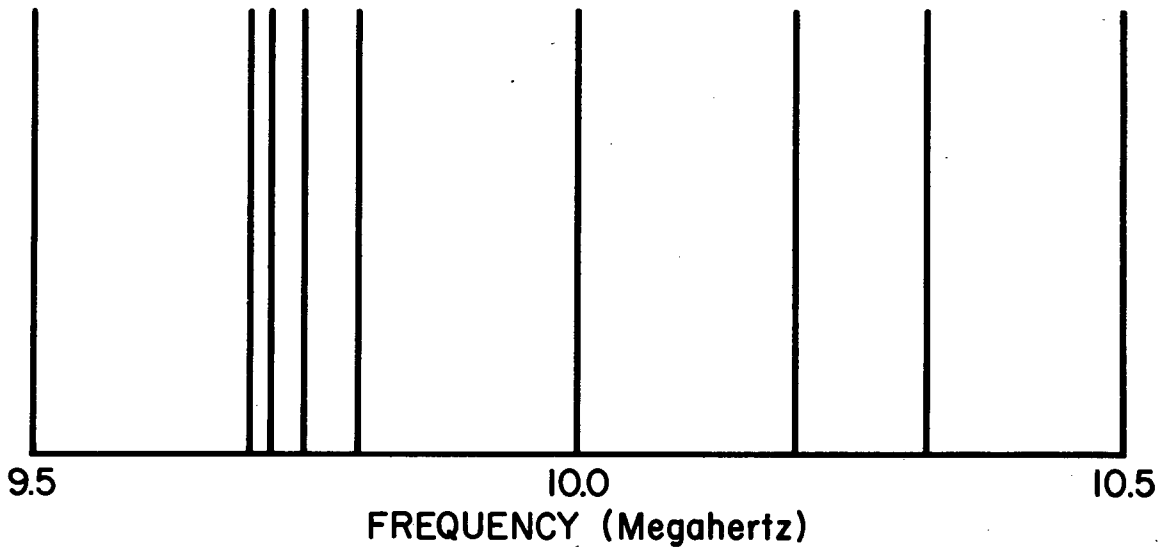


Fig. 3a — RF spectrum between 9.5 MHz and 10.5 MHz with
4 KHz information channels.

EXISTING
CAPABILITIES
MAX NO. CHANNELS
PER MHz AT 10 MHz = 3

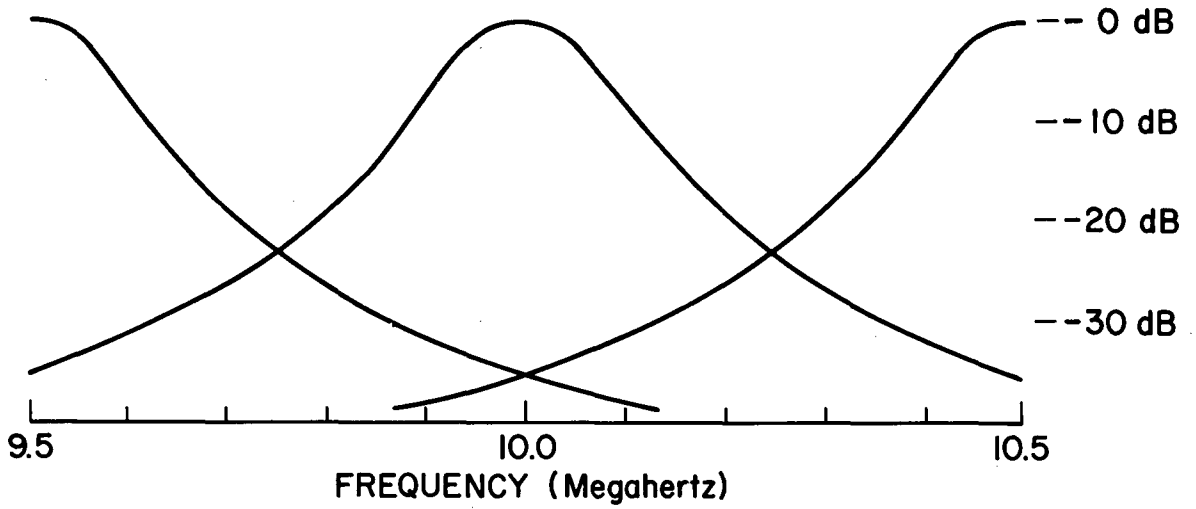


Fig. 3b — Response characteristics of AN/SRA-56 showing that between 9.5 and 10.5 MHz only three information channels can be utilized.

PROPOSED
SYSTEM
MAX NO. CHANNELS PER
MHz AT 10 MHz = 20

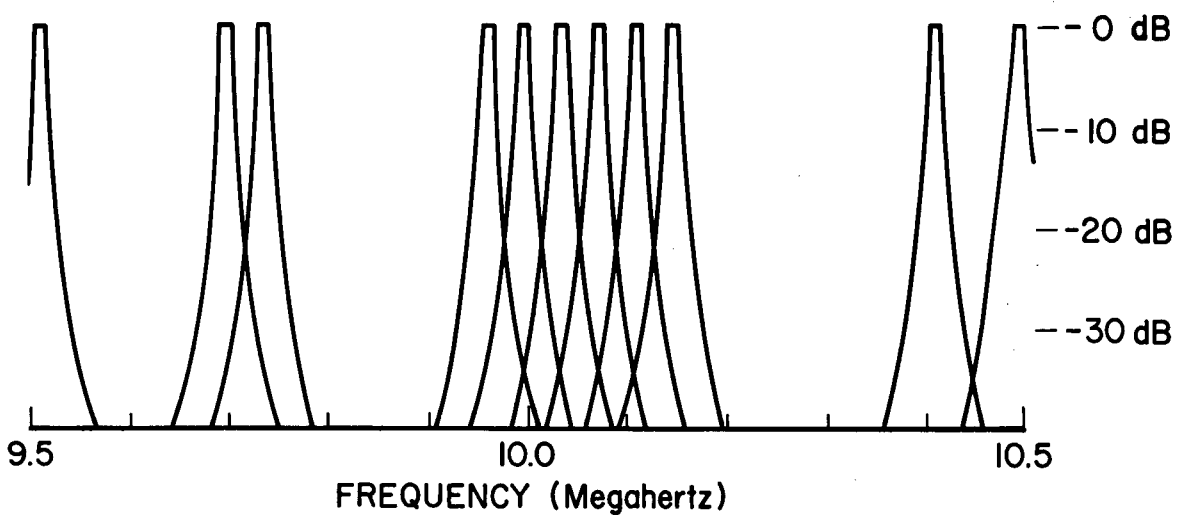


Fig. 3c — Response characteristics of proposed system showing more efficient utilization of the frequency spectrum.

filter of the multicoupler to consist of 2 resonators, connected in cascade, and having an operating Q of 1000, the same 1 MHz bandwidth could support 20 channels. A better way of describing the performance is in terms of the more efficient utilization of the available frequency spectrum. The performance of the superconducting multicoupler will permit the existing frequency separation restriction between transmitters to be reduced from 5% to .5%. The improved response characteristics will permit the use of frequencies that cannot now be utilized because of limitations in equipment performance. Several examples of the increased performance are illustrated in Fig. 3c.

There has been work on superconducting radio frequency resonators for over 20 years with some of the earliest by Hagen at NRL. This early work dealt with the loss mechanism in lead and tin cavities. In the early 60's, Hartwig, at the University of Texas, initiated a study of the residual losses in superconductors at radio frequencies. Residual loss mechanisms and the temperature dependence were studied and some understanding of losses due to "trapped" magnetic flux was gained. The major area of investigation was residual losses at relatively low powers. Residual losses which limit the unloaded Q's has become a major problem in projects involving superconducting accelerators. The losses in the RF range can be stated by the following expression:

$$R = R_{MB} + R_{residual}$$

The first part of the equation can be explained by the Mattis-Bardeen theory, which is derived from the BCS energy gap model. As will be discussed later in this text, the residual losses are the main problem in the field of microwave cavities for electron accelerators, due to the high Q's needed to make them economically feasible.

About the time Hartwig was initiating work at the University of Texas, the Army Electronics Command, Ft. Monmouth, started a program with the Airborne Instrument Laboratory of Cutler Hammer on superconducting tuned circuits. This study continued for a period of around 8 years. The devices studied were basically very low power, in the milliwatt range, for radio preselector application and a major problem area was associated with the cryogenics, and not the superconductive aspects of the system.

With the possibility of the design and construction of a superconducting electron accelerator the amount of research on the RF aspects of superconductivity took a quantum leap forward. Stanford University, Karlsruhe, and Argonne all initiated major efforts on electron and heavy ion accelerators.

In order that the construction of such an accelerator be economically feasible and to be able to gain an increase in the accelerators duty cycle, Q's of 10^{10} or greater were required corresponding to peak electric fields of 15 Mev/m and magnetic fields as high as a 1000 gauss. Research over the years has resulted in the belief that niobium is the best material for use in the construction of superconducting cavities. This is due to its high value of H_{c1} .

($H_{c1}(0)$ (T=0K) approximately 1800 gauss). As work on niobium progressed, the major problem that had to be overcome was that the critical field at the microwave frequencies was much less than the dc critical field. The answer to this problem seemed to lie in proper material preparation and surface condition. Electron beam melted niobium with as low an interstitial content as is practical is first obtained. All joints in the system must be electron beam welded and the contamination during the weld must be kept to a minimum. A major effort must then be made to obtain an ultra clean smooth surface on the niobium. The surface irregularities can cause field enhancement, field emission, hot spots, or phonon generation, all of which are possible problem areas.

At the Stanford Linear Accelerator Center a chemical polish has been utilized followed by a high temperature (1800°C) anneal in an ultra-high vacuum of 10^{-10} torr. The furnace used for this heat treatment has a hot zone of about a cubic meter in volume and costs several million dollars to build.

The Karlsruhe group has used a different approach. They first electropolish the surface. To obtain a sufficiently good polish, current oscillations must be set up in the polishing bath. Following the polishing, the surface is then anodized to provide a protective surface, (surface layer of Nb_2O_5) which also helps to smooth out irregularities. An anodized layer of approximately 1000 Å will protect the surface from environmental corrosion, i.e. water vapor on thermal cycling.

At NRL we decided that the only practical approach to the multicoupler application is the development of anodized, electro-polished resonators of niobium. The first goal was to prepare a superconducting cavity that could pass a kilowatt of power at a Q_{DL} of 1000. For efficient operation and to reduce the refrigeration requirement the unloaded Q of the structure would have to be above 10^6 . The amount of dielectric support material used had to be minimized so that this value of unloaded Q could be obtained.

Our initial resonator was an unsupported, unpolished and unanodized helical resonator structure that was resonant at approximately 16 MHz. The shield can was 8 inches long with a 4 inch inner diameter. The helix was 3 inches in diameter and consisted of 21 turns of 1/8 inch diameter wire. The characteristic impedance was approximately 400 ohms. Figure 4 shows the coil and bottom plate being prepared for electron beam welding. The electrical characteristics of this joint are critical as it is located at a point where large rf currents flow. Figure 5 shows all the components of the unsupported resonator. The shield can has been first tack welded and then given a cosmetic weld along the main joint. The flanges are electron beam welded to the shield can and an "O" ring groove for a lead "O" ring is machined. This allows the resonator to be sealed and operated with helium exchange gas. Figure 6 pictures the assembled resonator with the coupling header. Stainless steel coaxial transmission lines having a nominal impedance of 50 ohms, which are also used as vacuum connections, are shown. The resonator is assembled with titanium nuts and bolts which match the thermal expansion of niobium. A stainless

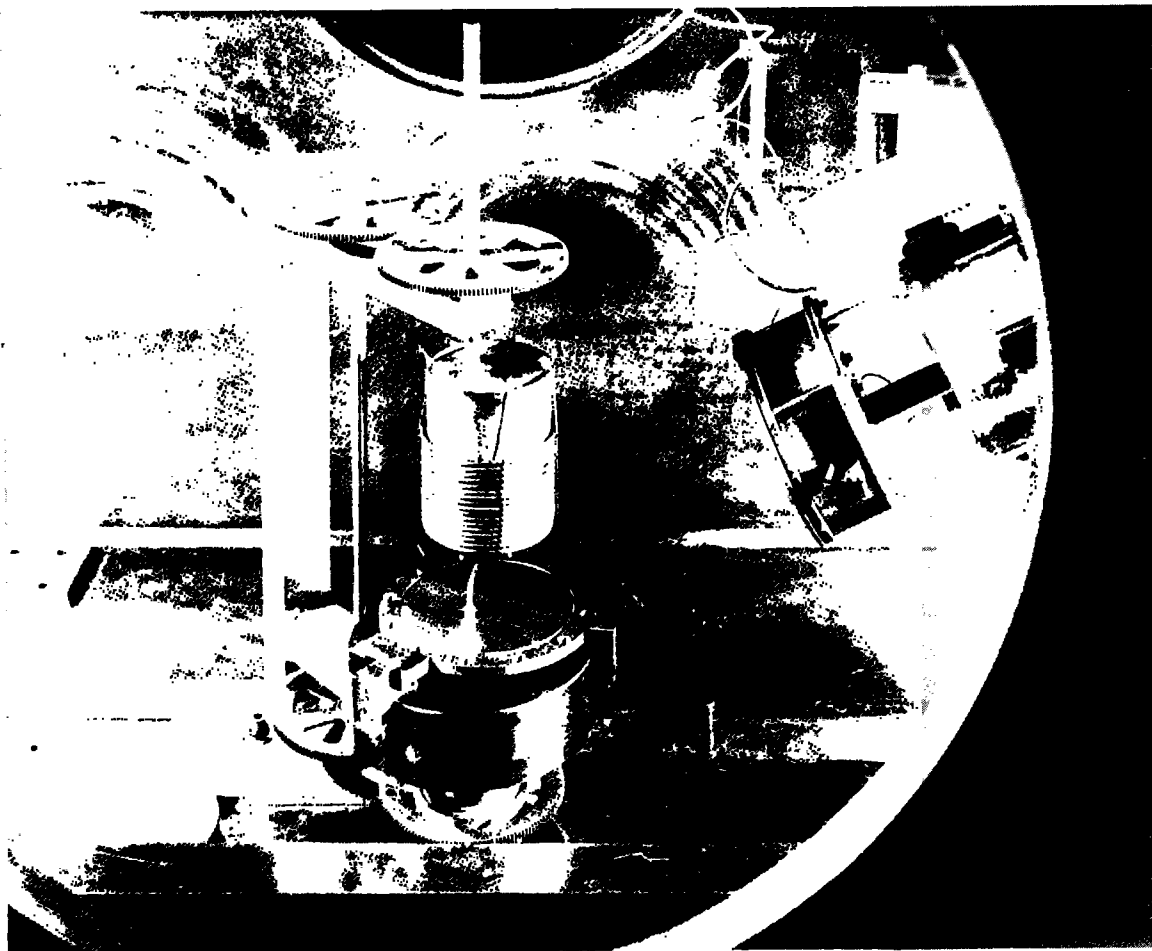


Fig. 4 — Electron beam welding of helix to bottom plate of resonator shield.

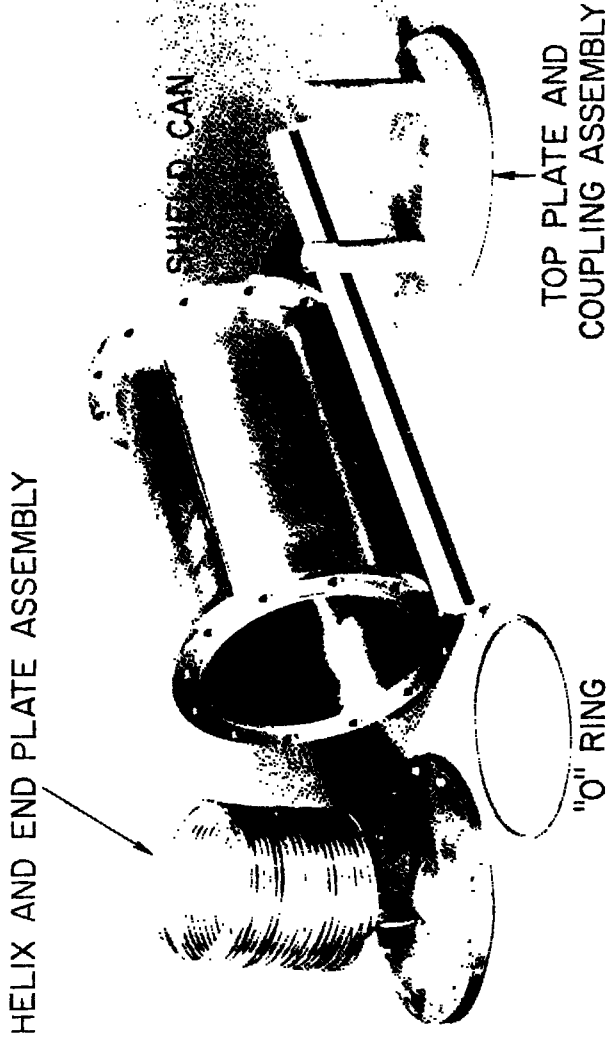
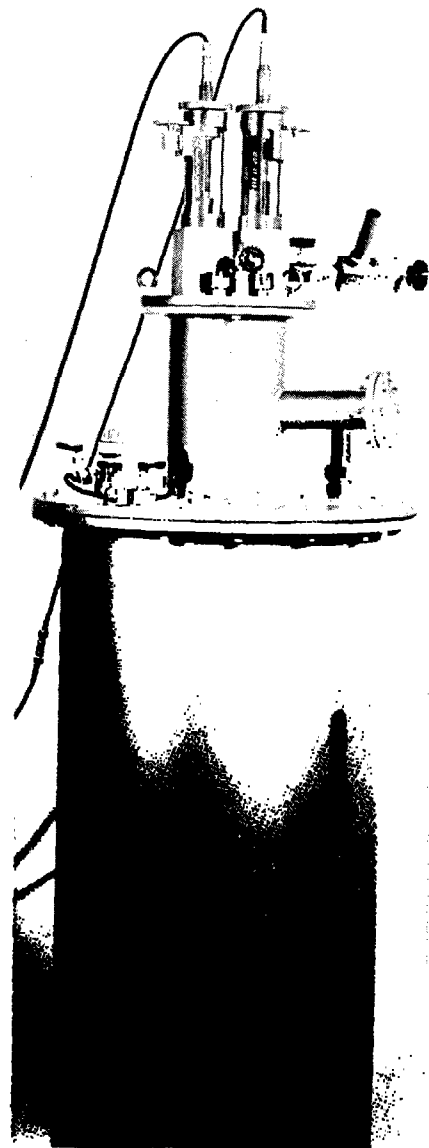


Fig. 5 -- Components of unpolished, unsupported Niobium helical resonator.



(A)



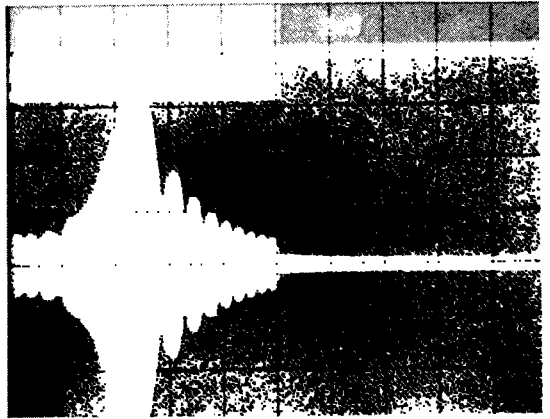
(B)

Fig. 6(a) — Assembled resonator with shield can, stainless steel
coaxial transmission lines and coupling assembly and
(b) resonator installed in Dewar.

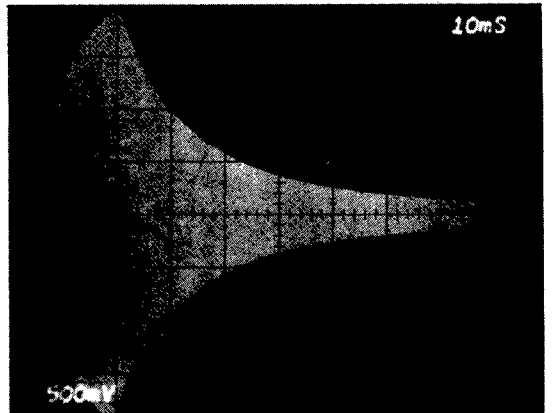
steel to niobium furnace braze connects the coupling assembly to the coaxial lines. The inner conductors of the coaxial transmission lines can be adjusted over an inch and a half of travel and the whole system is vacuum tight. A stainless steel bellows assembly and digital counters allow positioning of the probes to within three thousandths of an inch. Power is coupled to the resonator capacitively and the assembly can be loaded from a Q of 5×10^6 to 3.5×10^3 . At low power the holding time of the helium dewar is over 12 hours.

Our initial unpolished resonators were operated with helium exchange gas but this procedure was found to be **unsuitable** due to the low powers achieved before arcing or breakdown. At 10 milliwatts of power, breakdown was experienced. When it was run in the flooded condition that is, liquid helium inside the shield can, the resonator could sustain over 3 watts at a Q of about 5000 before breakdown occurred. It was observed that the resonator characteristics degraded on thermal cycling.

The initial resonator used a minimum amount of dielectric and had substantial stability problems. These problems precluded the measurement of unloaded Q factor until electronic feedback networks were designed and applied. With the electronic feedback network the test signal generator was phase locked to the natural resonant frequency of the resonator. Figure 7 shows an applied RF pulse with and without phase locking. What would appear as breakdown for the case of no phase locking is actually the inability of the generator to track the shifting frequency of the resonator.



(a)



(b)

Fig. 7 — RF response to applied pulse with and without electronic feedback.

Improved mechanical stability is required; not only to overcome the basic flimsiness of the initial resonator design but to withstand the effects of pondermotive forces that would be encountered at high power levels. Pondermotive forces are physical pressures exerted by electromagnetic fields, and always tend to reduce the resonant frequency.

Experiments have been performed on a second resonator design which incorporated improvements intended to overcome the materials degradation characteristics and poor stability of the initial resonators. All conducting surfaces are formed of anodized niobium and the helix is supported in a teflon spacer as shown in Fig. 8.

The resonator is operated flooded with liquid helium. At an operating Q (Q_{DL}) of 8000 the resonator passed over 150 watts. Arcing was observed and a picture of the arcing traces across the teflon surface is presented in Fig. 9. To reduce the field enhancement at the surface layer of the shield can the teflon support was machined down. Larger coupling probes were designed to permit lower values of Q_{DL} to be achieved. In this form the resonator has supported over 300 watts at a Q_{DL} of 3500 which extrapolates, insofar as electromagnetic stresses are concerned, to our goal of a kilowatt at a Q_{DL} of 1000. The helium is sustaining an arc at E fields of 4 Mev/m which is below the 40 Mev/m expected for DC breakdown. This may be due to several reasons among which is the condition of the niobium and teflon surfaces. If adequate mechanical clearances are maintained, bulk radio frequency resonators (that are tunable and) operating at loaded Q 's of 1000 can probably be designed which will carry a kilowatt of power.

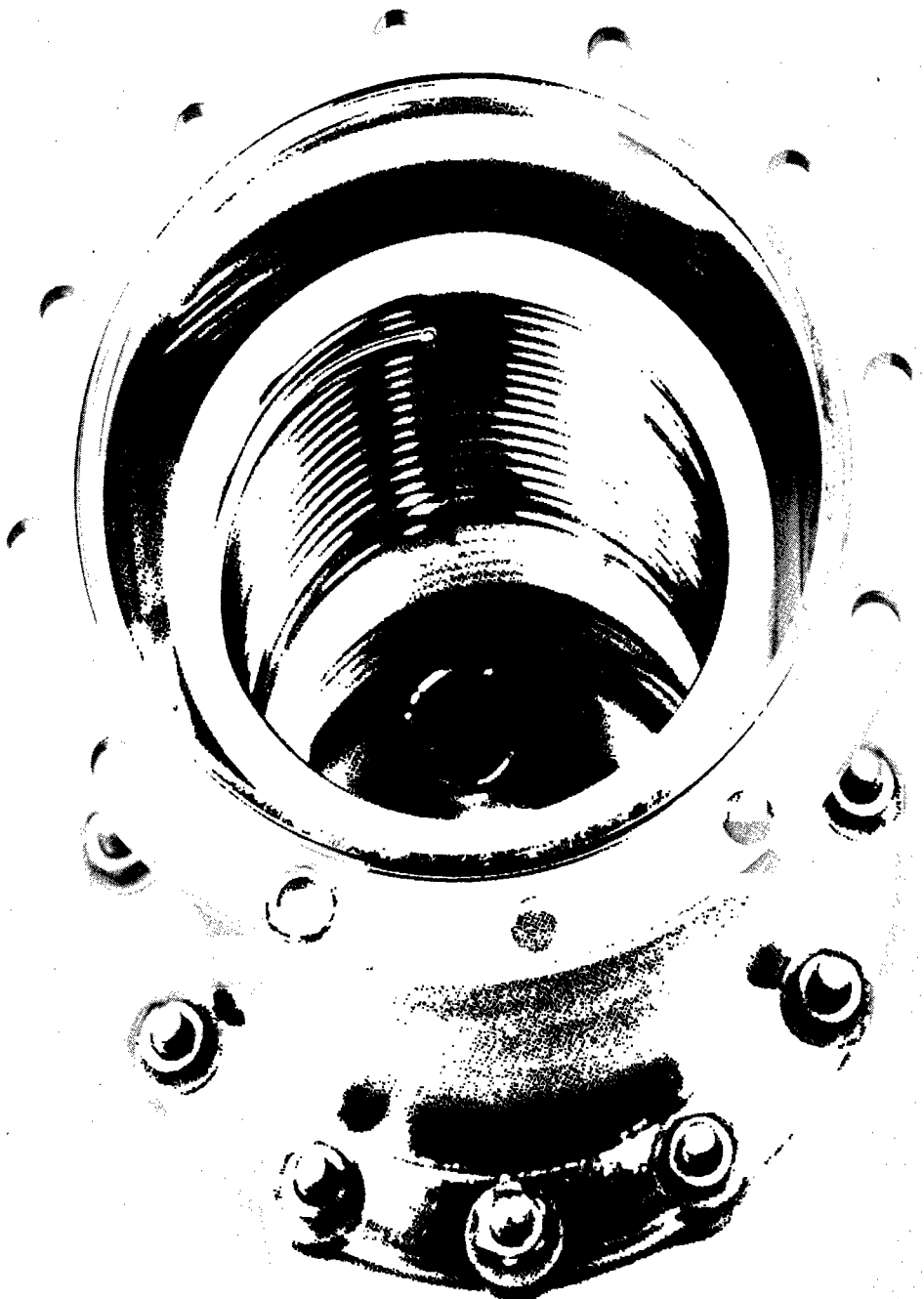


Fig. 8 — Polished, anodized Niobium resonator with teflon support.

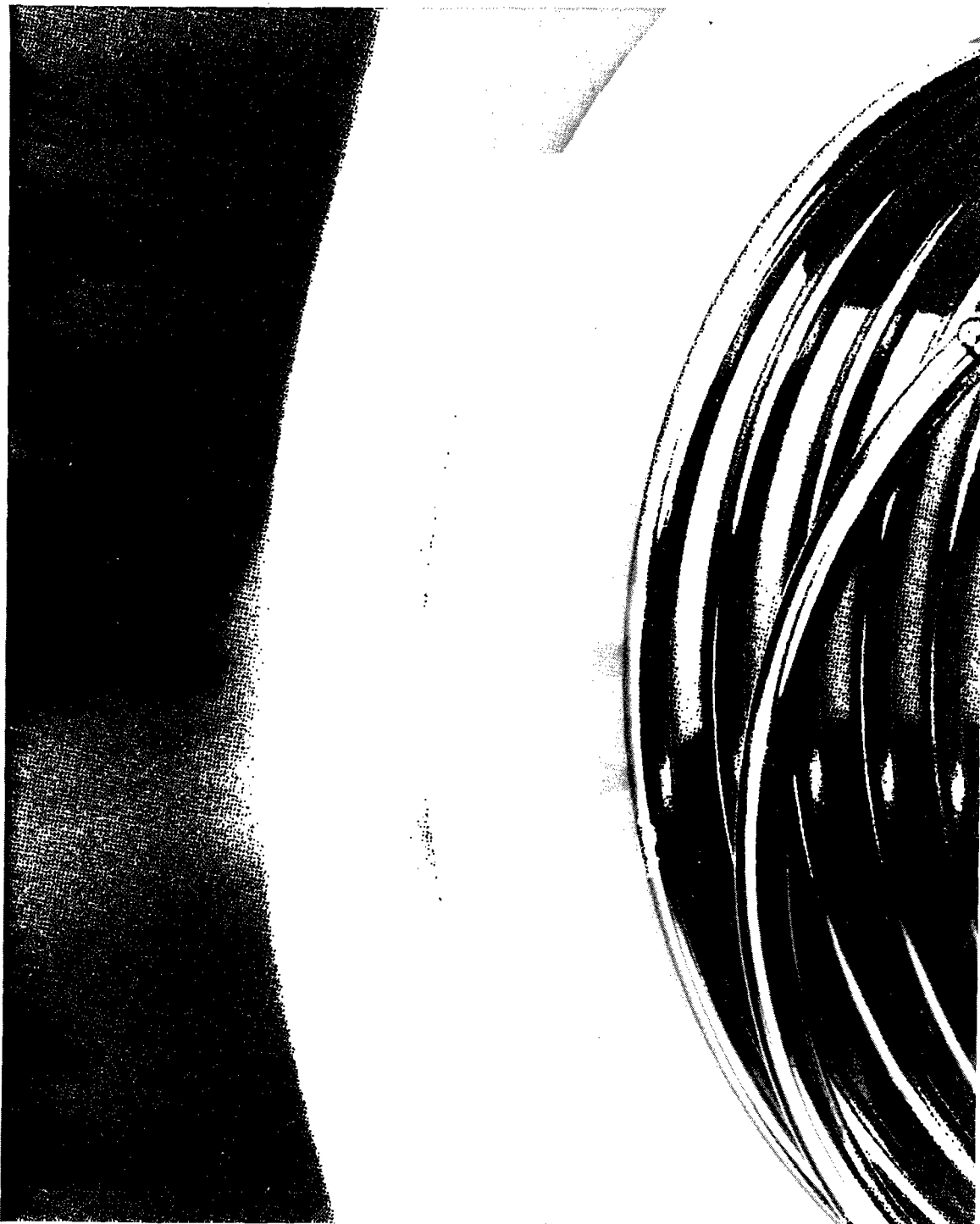


Fig. 9 — Close-up of teflon support showing "tracking" deposits where arcing has occurred.

Our efforts are presently directed toward modifying the existing resonators so that they can be loaded to a Q_{DL} of the order of 1,000 and demonstrating that, under this degree of loading, a kilowatt of power can be passed through the resonator, the latter being one of the specified design characteristics of a structure suitable for an operational multicoupler. Another design criteria is that the resonator be capable of being tuned over a frequency ratio of at least 3. A variable superconducting capacitor has been designed and will be used in conjunction with a variable inductor to provide the desired tuning range while keeping the overall size of the resonator small enough for shipboard use.

The potential payoff of applying superconducting technology to Naval communication systems lies not only in high Q circuits for multicouplers and preselectors but also includes the possibility of efficient radiators of compact size, which would ease antenna siting problems. The principal drawbacks of these applications are not associated with the superconductive aspects but appear to be solely due to the problems of providing the required cryogenic environment.

SUPERCONDUCTING ANTENNAS FOR LOW FREQUENCY COMMUNICATIONS*

UNCLASSIFIED

S.A. Wolf, J.R. Davis, and M. Nisenoff

Naval Research Laboratory
Washington, D.C. 20375

Current submarine deployment plans require greatly improved communications performance between surface or airborne transmitting terminals, and deeply submerged receivers. Improvements must be made, most particularly, to reduce restrictions upon receiver depth, speed and maneuverability. The attenuation of very low frequency (VLF) radio waves in seawater requires the receiving antenna to be relatively near the surface. Furthermore, the long trailing wire antennas and ferromagnetic-core solenoids (which may be buoy mounted) now in normal use at these frequencies hamper the submarine's operating flexibility.

The prospect that the Extremely Low Frequency (ELF) band may be employed in the near future for submarine communications provides a potential solution for some of these requirements that avoids the limitations of the VLF communication systems. Principally, ELF waves penetrate deeply enough into seawater so that sensors need no longer be towed close to the surface. However two serious problems remain.

- Trailing wire (distributed electrode) and ferromagnetic-core solenoid sensors must be long and consequently unwieldy, and hence they limit maneuverability.

- Omnidirectionality requires either an impracticable deployment of widely separated electrode pairs (one pair can be trailed, but the other pair must be deployed perpendicular to the direction of submarine motion), or development of a relatively noise free solenoid.

*This is a summary of the talk. The full text will appear as a separate NRL Report and in the IEEE Transactions on Communications, COM-22, 548 (1974).

Present solenoid sensors cannot satisfy the noise requirements for adequate performance in likely operating areas with the planned ELF transmitting capacity and the required message delivery rate. Therefore, a program for the development of a magnetic field sensor that can satisfy the performance characteristics and can, in fact, provide fully omnidirectional receiving capability without the need for an electric field sensor, will be initiated at the Naval Research Laboratory starting in FY 75.

The sensor will employ a Superconducting Quantum Interference Device (SQUID) and will permit ambient noise level performance to be achieved in the bandwidth required for ELF communications. It has been shown at the Naval Research Laboratory that SQUID sensors are capable of detecting signals at a level about 213 db below 1 volt per meter in a 1 Hertz bandwidth in the ELF band above 100 Hz. Due to inadequate shielding, measurements below 100 Hz were limited by interference from 60 Hz power lines. Therefore it is reasonable to assume that this same sensitivity is available over the entire ELF band. This sensitivity is 13 db better than that required for the proposed communication system and 43 db better than the best documented performance by a long solenoid.

The performance of the long solenoids are limited by magnetostriction and cable distortion noise caused by relative motion of the portions of the cable. These sources of noise are not present in the case of SQUID sensors. SQUID's, however, because of their vector characteristic, are subject to noise arising from motion of the (rigid) SQUID assembly in the earth's magnetic field. If the orientation of the SQUID can be adequately maintained to lower motion related noise to an acceptable level, the SQUID system could provide a self-contained omnidirectional receiving capability equal to that required for an ELF communication system for submerged submarines.

The motion related noise of the SQUID sensor can be reduced to below the ambient level by utilizing a set of three orthogonal sensors and summing their outputs continuously to form the total field vector. This permits the large earth's field component to be removable as a dc component. The problem then becomes a matter of achieving the required sensor orthogonality and dynamic range. State of the art techniques will be required to perform this task, but no breakthroughs are necessary.

Another major problem in SQUID applicability is refrigeration. The choice between an open-cycle dewar arrangement or a closed cycle refrigeration system depends on the deployment of the antenna and the reliability and noise characteristics of existing refrigerators. This aspect of the system will be studied in great detail as soon as the program gets underway.

JOSEPHSON-EFFECT DETECTORS
AT MILLIMETER AND SUBMILLIMETER WAVELENGTHS

Richard G. Brandt
Office of Naval Research
1030 E. Green St.
Pasadena, CA 91106

UNCLASSIFIED

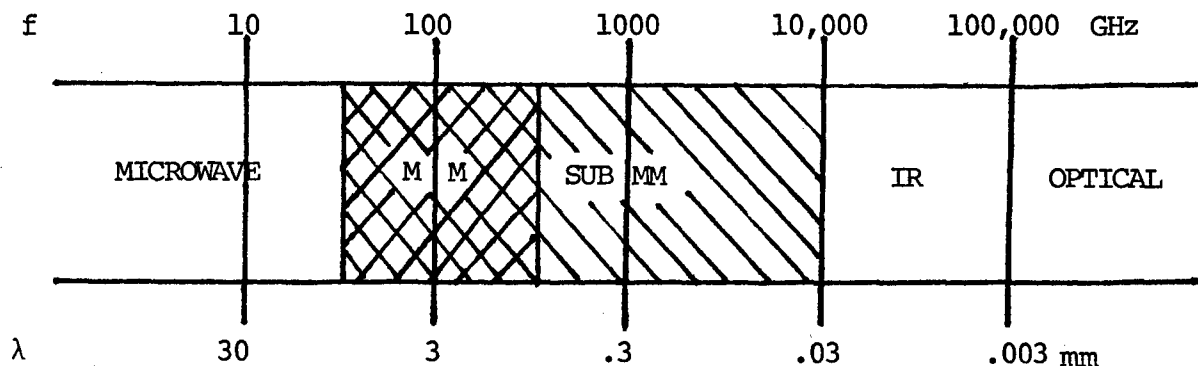
INTRODUCTION

At the first Workshop on Naval Applications of Superconductivity held in November 1970, Professor Shapiro of the University of Rochester gave a talk on this same subject. In this talk he described the various Josephson-effect detection mechanisms, and he quoted performance figures which indicated that even at that early stage of development Josephson-effect detectors compared favorably with competing devices in this wavelength region.

In this presentation I will attempt to summarize the progress which has been made in the field of Josephson-effect detectors during the past three years and will give an updated comparison of detector performance. I will also indicate the trends which can be expected in the future with regard to further improvements in such detectors. Fortunately, my job has been made easier because of a conference which was held in September 1973 on the subject of Josephson-effect detectors. In addition, I will make use of other published articles which are referenced.

POSSIBLE APPLICATIONS

The millimeter and submillimeter portions of the electromagnetic spectrum lie between the microwave region on the long wavelength side and the infrared and optical regions on the short wavelength side. The usual definition of these spectral ranges is given below.



Here we see that the microwave region has an upper frequency limit of about 30 GHz (1 cm wavelength), while the millimeter region extends from 30 to 300 GHz (that is, between 1 and 10 mm in wavelength). The submillimeter portion extends to about 10,000 GHz which corresponds to 30 μ m wavelength, beyond which lies the infrared and optical regions. Josephson-effect detectors are expected to have a competitive advantage in this intermediate spectral range from about 30 GHz to 10,000 GHz.

This region of the electromagnetic spectrum has not yet been exploited to any significant degree. One important factor is the present lack of good system components. However, this spectral region presents certain constraints to the systems designer, as well as offering definite advantages. As an example, the vertical attenuation through the atmosphere for a portion of this frequency range is shown in Fig. 1.¹ The strong atmospheric absorption in distinct frequency bands prevents long-range propagation in the atmosphere at those frequencies, but allows certain covert communication possibilities, some of which were discussed at this meeting. In the atmospheric windows where the absorption is not excessively high, scattering by aerosols and particulate matter is significantly less than at optical and infrared wavelengths, which is important in imaging through fog and haze and in collision avoidance radar.

A prime advantage of millimeter and submillimeter wavelengths is the high resolution or narrow beams which can be obtained with modest sized antennas. For example, at a wavelength of 0.1 mm one can obtain a resolution approximately the same as that of the human eye by using an antenna which has a diameter of about 10 cm. Also, the very high frequency of the radiation allows a very large information bandwidth which can be useful in high-data-rate communications. These same two advantages--narrow beam width and large information bandwidth--are present to even a greater degree in the case of optical beams from lasers, but then the precision pointing of extremely narrow beams can be very difficult, and millimeter waves may be the best compromise solution in certain cases.

In 1970 a symposium at the Polytechnic Institute of Brooklyn was devoted to the subject of submillimeter waves--their technology and

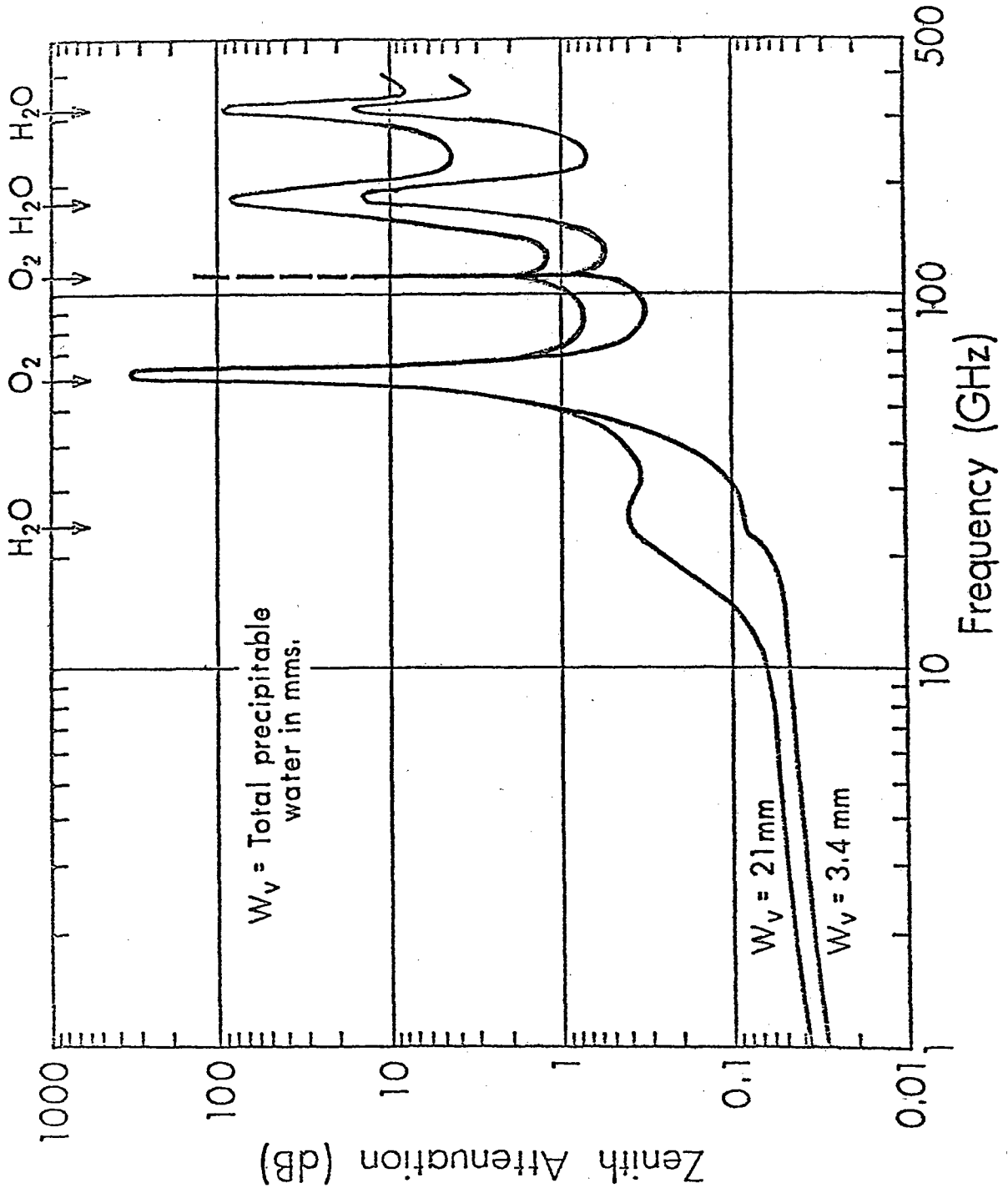


Fig. 1 — Vertical attenuation through the atmosphere.

application. At this symposium Merrill Skolnik of NRL listed 48 possible applications in the categories of radar, communications, radiometry and instrumentation.¹⁴ Selected examples from that list which are of interest to the military and which were judged at that time to have significant technical merit are given below.

REPRESENTATIVE APPLICATIONS OF MM-WAVE TECHNOLOGY

- Low Angle Tracking
- High Resolution Radar
- Secure Communications
- Wideband Communications
- Remote Sensing of the Environment
- Plasma Diagnostics

The reasons why millimeter and submillimeter wave technology can make a unique contribution for each application are probably obvious. In the case of plasma diagnostics, the application would include analysis of dense plasmas generated in laboratory experiments as well as those existing in rocket exhaust plumes.

DETECTOR CONSIDERATIONS

One of the critical components in any system of this type is the detector. There are two general classes of detectors: coherent and incoherent, depending on whether the temporal coherence of the signal is exploited or not. These two detector classes will be discussed separately below. Incoherent detectors are typically square-law or power detectors and are most appropriate for the detection of broadband radiation when the input signal-to-noise ratio is large. When the signals to be detected are weak compared to noise or relatively narrow-band, coherent or heterodyne detection may be preferable.

For many applications, such as radar and communications, one desires to detect the smallest possible signal in a frequency band which is relatively narrow compared to the known carrier frequency. For this case the customary measure of detector sensitivity is noise equivalent power or NEP, defined as the input signal power necessary to achieve a final signal-to-noise ratio of unity for a detecting interval or integration time of one second. Therefore, a more sensitive detector would have a smaller NEP. For a square-law detector or for a mixer followed by a square-law detector, the noise equivalent power is directly proportional to the square root of the postdetection bandwidth; that is, the NEP decreases as the square root of the final integration time for a wide range of values. It is customary to eliminate this dependence on postdetection bandwidth and to express NEP in units of watts per square root of postdetection bandwidth. For coherent detectors an alternative measure of sensitivity is an effective noise temperature which is related

to the noise equivalent power by the following equations:¹

$$NEP = 2k T_R \sqrt{B}$$

$$T_R = T_M + T_{IF}/\eta$$

Here T_R is the receiver noise temperature, k is Boltzmann's constant and B is the receiver bandwidth. The receiver noise temperature is the sum of the mixer noise temperature and the IF amplifier noise temperature reduced by the conversion efficiency of the mixer, designated by η .

For certain other applications it is not the noise equivalent power which is the relevant detector figure-of-merit. In particular, in radiometric applications where one wishes to determine an effective source temperature, a more pertinent figure-of-merit is the smallest detectable temperature differential, usually denoted by ΔT_{\min} . In this case the bandwidth of the source tends to be larger than the limiting bandwidth of the detector, and the ability to resolve source temperature differences improves with increasing bandwidth of the detector. Therefore, the best detector in this application has both the smallest NEP and also the largest bandwidth, and thus a meaningful figure-of-merit is the NEP divided by the limiting detector bandwidth. This ratio is directly proportional to the minimum detectable temperature differential according to the following equation¹

$$\Delta T_{\min} = \frac{NEP}{kB \sqrt{\tau}}$$

where τ is the integration time and the other quantities have been defined previously. Figure 2 illustrates how ΔT_{\min} depends on bandwidth for incoherent detectors (labeled by their NEP values) and for coherent detectors (labeled by their effective noise temperatures).^{1,15} We see that since the NEP of an incoherent detector is independent of bandwidth, the quantity ΔT_{\min} is inversely proportional to bandwidth, according to the defining equation for ΔT_{\min} . However, for coherent detectors characterized by a fixed receiver temperature the NEP has a dependence on the square root of B ; therefore ΔT_{\min} in this case is inversely proportional to the square root of bandwidth, so that the increase in sensitivity with bandwidth is slower than for incoherent detectors. Using a display of this type it is possible to select the optimum detector for achieving a desired temperature sensitivity under given bandwidth limitations. As we shall see later, the 300 K noise temperature receiver, the middle curve on the left of this figure, approximates the expected performance of the best cooled mixer detectors, while the best incoherent detectors fall between the two NEP lines shown.

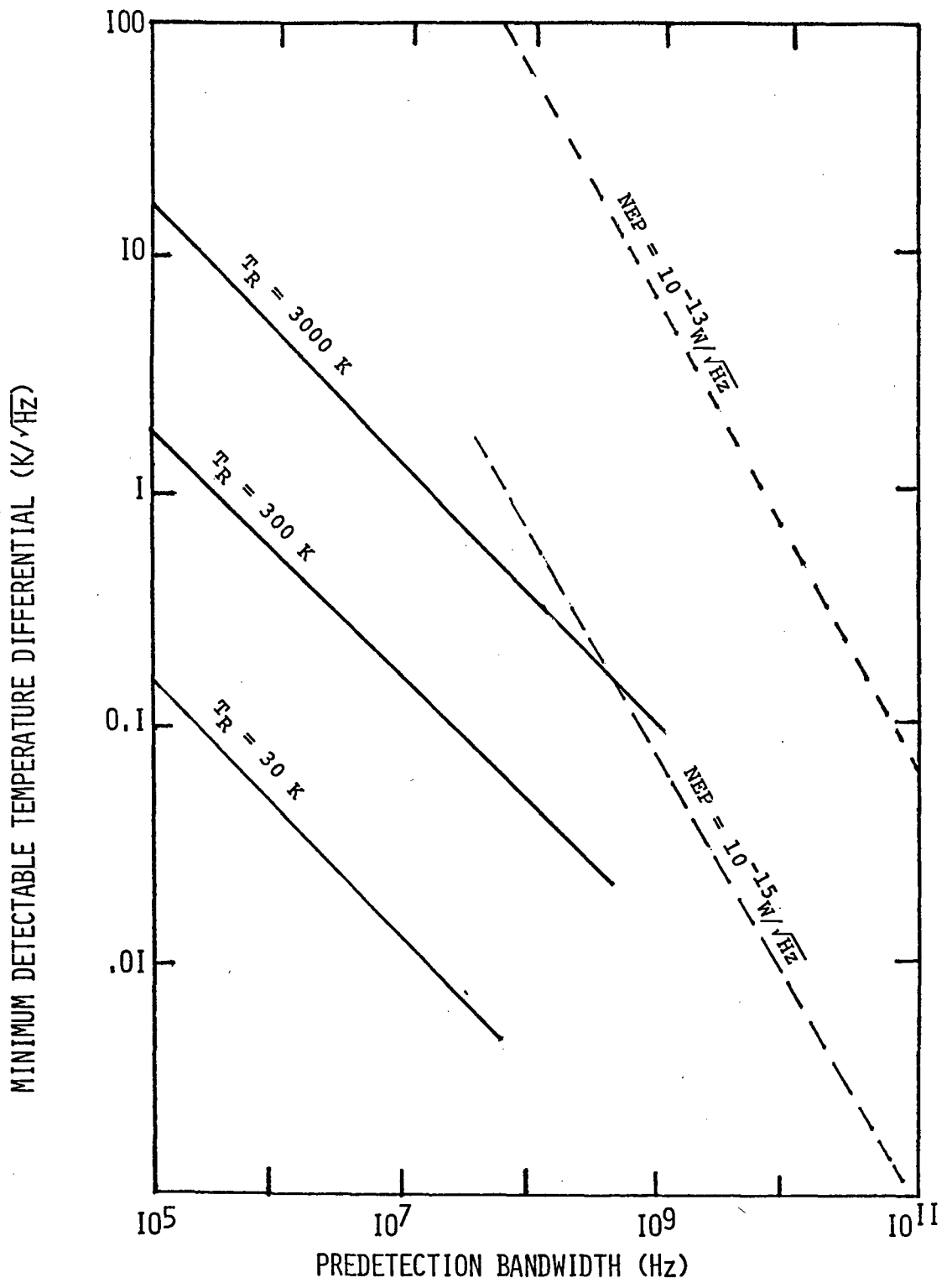


Fig. 2. Minimum detectable temperature differential as a function of pre-detection bandwidth

a. Semiconductor Bolometers

The technology associated with semiconductor bolometers is well developed, and recently three of the best devices were compared in a test performed at the National Radio Astronomy Observatory at Kitt Peak.¹ The three detectors were a Kinch-Rollin type indium antimonide bolometer, a gallium-doped germanium bolometer and a scandium-doped germanium bolometer. The measured NEPs of these devices for radiation peaked at 1 mm wavelength were 10^{-12} , 5×10^{-13} and 2×10^{-13} W/ $\sqrt{\text{Hz}}$, respectively. Therefore, an NEP of 10^{-13} W/ $\sqrt{\text{Hz}}$ is about the best that can currently be achieved with this conventional bolometric technique.

b. Superconductor Bolometers

The most sensitive superconductor bolometers employ a superconductor-normal metal-superconductor Josephson junction. The critical current through such a junction is defined as the limiting electron-pair current which can flow at zero voltage. The extreme sensitivity of such devices is based on the rapid variation of critical current with temperature. Professor Clarke and coworkers at UC Berkeley recently reported on the operation of such a device utilizing a Pb/CuAl/Pb junction deposited on a sapphire substrate.² Changes in critical current were measured with a superconductive SQUID. The measured electrical NEP was about 5×10^{-15} W/ $\sqrt{\text{Hz}}$ at 1.7 K. As is the case for semiconductor bolometers, the sensitivity should be essentially independent of signal frequency. The bandwidth of both semiconductor and superconductor bolometers is very large, probably 30 GHz or larger at a signal frequency of 300 GHz. Clarke calculates that the resultant ΔT_{min} for his superconductor bolometer may be as small as 2×10^{-4} K.² The disadvantage of all bolometers is the slow response time due to the thermal mass of the temperature-sensitive element and the loss of heat from that element to the surroundings. Typical response times are of the order of seconds for semiconductor bolometers and 10 to 100 ms for the superconductor bolometer described.

c. Josephson Video Detectors

For very small power levels radiation incident on a Josephson junction is rectified, causing the maximum current which flows at zero voltage to be decreased. This response occurs for all frequencies of radiation from dc up, hence the name "video" detector. The depression of the zero-voltage current is given approximately by

$$I_o \approx I_c \left(1 - \frac{e^2 V_s^2}{h^2 \omega_s^2} \right)$$

where I_c is the critical or limiting current and V_s and ω_s are the voltage and angular frequency of the signal, respectively. Therefore, the measured effect is proportional to input power (a square-law detector), and the magnitude of the response falls off inversely with the square of frequency in this simple approximation. Numerous Josephson video detectors have been constructed, and their performance is reasonably well optimized.¹³ At a frequency of 100 GHz (3 mm wavelength) the best measured NEP is $5 \times 10^{-15} \text{ W}/\sqrt{\text{Hz}}$, while at this same frequency theory predicts that the best performance to be expected is just an order of magnitude better, namely, $5 \times 10^{-16} \text{ W}/\sqrt{\text{Hz}}$.¹⁶ At 1 mm wavelength the theoretical maximum sensitivity is a factor of ten worse because of the dependence on inverse frequency squared, and the best measured NEP at this wavelength is approximately $10^{-14} \text{ W}/\sqrt{\text{Hz}}$ which is only twice the theoretical estimate.³ The effective input bandwidth for such detectors is usually less than for bolometers, being determined by the structures which couple the radiation to the junction. The bandwidth is of the order of 3-30 GHz for 300 GHz radiation. However, these Josephson video detectors have response times which are orders of magnitude faster than those for bolometers.

d. Josephson Regenerative Detector

Another type of Josephson-effect power detector which will be mentioned only briefly is the narrowband regenerative detector.¹³ Here the junction is coupled to a cavity, and this interaction produces steps in the I-V characteristic of the junction at those voltages where the Josephson radiation frequency is some multiple of the resonance frequency. The height of these cavity-mode steps is affected by incident radiation at those frequencies, and this is the basis of a detection mechanism. In one experiment the system bandwidth was approximately 300 MHz for a cavity resonance at 187 GHz, and the resultant NEP was $5 \times 10^{-15} \text{ W}/\sqrt{\text{Hz}}$.¹⁷ This NEP is comparable to the best achieved with other detectors just discussed, but the bandwidth is distinctly narrower. No further efforts have been made to try to achieve the improved sensitivities expected with this narrow band device.

e. Summary and Comparison

The various incoherent, square-law detectors discussed in this section are listed in Table I together with pertinent performance

Table I

INCOHERENT DETECTORS
AT 1 MM WAVELENGTH

TYPE	OPERATING TEMPERATURE	NEP	BANDWIDTH	ΔT_{\min}	RESPONSE TIME
SEMICONDUCTOR BOLONETER	77 K	$10^{-13} \text{ W}/\sqrt{\text{Hz}}$	>30 GHz	$.25 \text{ K}/\sqrt{\text{Hz}}$	1 s
SUPERCONDUCTOR* BOLONETER	1.7 K	$5 \times 10^{-15} \text{ W}/\sqrt{\text{Hz}}$	>30 GHz	$<.01 \text{ K}/\sqrt{\text{Hz}}$	$<.1 \text{ s}$
JOSEPHSON VIDEO DETECTOR	4.2 K	$10^{-14} \text{ W}/\sqrt{\text{Hz}}$	3-30 GHz	$.25 \text{ K}/\sqrt{\text{Hz}}$	$<10^{-8} \text{ s}$
JOSEPHSON REGENERATIVE DETECTOR	4.2 K	$5 \times 10^{-15} \text{ W}/\sqrt{\text{Hz}}$	300 MHz	$1 \text{ K}/\sqrt{\text{Hz}}$	$<10^{-8} \text{ s}$

*MEASURED ELECTRICAL NEP ASSUMED VALID FOR 300 GHz RADIATION.

data for operation at 300 GHz (1 mm wavelength). All measurements were made at or near 300 GHz with the exception of those for the superconductor bolometer where only an electrical NEP was determined. However, it should be possible to achieve this NEP for 300 GHz radiation. The validity of this assumption will be tested in the near future when a superconductor bolometer sensitive at these higher frequencies becomes operational.

With the exception of the Josephson regenerative detector, all devices have been made to operate close to their performance limits. The recently developed superconductor bolometer appears to be the best incoherent detector in terms of both noise equivalent power and bandwidth. Recall that these two quantities are equally important in radiometric applications, and the ratio can be used to determine a minimum resolvable temperature, ΔT_{\min} . From this figure of merit we see clearly that the superconductor bolometer is most sensitive for broadband detection. The only disadvantage of the superconductor bolometer is its somewhat slow response time. Therefore, where high sensitivity, large bandwidth and fast response time are all required, the Josephson video detector may be preferable.

COHERENT DETECTORS

a. Semiconductor Mixers

Heterodyne mixer-detectors employing semiconductor Schottky-barrier diodes have been used extensively at frequencies up to 300 GHz, although the performance of such devices generally deteriorates significantly at frequencies above 100 GHz. Some of the best work in this area is being done at the Bell Telephone Laboratories where a technique has been perfected for making small-area GaAs diodes by planar technology. Using these Schottky-barrier diodes in carefully engineered systems, a series of receivers has been constructed spanning the frequency range from about 30 - 300 GHz.¹ The IF ultra-low noise parametric amplifier used in all these systems has a bandwidth of 100 MHz. At frequencies below 100 GHz receiver noise temperatures of 700 - 750 K have been achieved. However, at frequencies approaching 300 GHz the best performance that has been achieved is a 6000 K noise temperature because of effects of finite diode capacitance, primarily. It is expected that these various noise temperatures will be reduced by a factor of approximately 3 when these receivers are cooled to liquid nitrogen temperature. The systems will also be upgraded by installing improved IF amplifiers with 500 MHz bandwidth.

At frequencies above 100 GHz a more promising semiconductor device is the hot-electron InSb mixer cooled to liquid helium temperature. Noise temperatures of approximately 500 K have been achieved recently at 1.2 and 2.5 mm wavelengths,^{1,20} and it is expected that this performance can be maintained to frequencies as high as 1000 GHz (0.3 mm wavelength). Unfortunately, the response time of the device is slow

compared to other millimeter-wave mixers, so that the IF bandwidth is limited to frequencies less than approximately 1 MHz. The device should, nonetheless, be very useful for certain narrowband applications.

b. Josephson Heterodyne Detectors

In a Josephson junction mixer there is a choice of using an external local oscillator or using the internally generated Josephson oscillation as a local oscillator. In the past both techniques have been employed in order to demonstrate feasibility. However, within the past year several theoretical studies have been published in which the relative merits of both techniques have been compared.^{16,18} It has been shown that for current-biased conditions, which is the usual situation because the low impedance of the Josephson junctions, the linewidth of the Josephson oscillation becomes broadened leading to noise broadening of the IF output, which is undesirable. Use of an external local oscillator avoids this problem and is the favored approach at present.¹³

Significant progress has been made recently in developing such detectors, principally by several groups working together at UC Berkeley. Professor Van Duzer and his coworkers have carried out an extensive set of calculations in order to explore the effects of varying various detector parameters.⁴ In performing these calculations a simple model of the Josephson junction was employed, consisting of a perfect Josephson element shunted by a constant resistance. No capacitance was included which is probably a serious omission for radiation frequencies above 100 GHz, but this model has proved to be valid below approximately 100 GHz for point-contact junctions and short weak links. Noise was included in the calculations, and this proved to have important consequences. One prediction of this model calculation is that small-signal conversion gain is possible for certain junction parameters when the IF frequency is small compared to the signal frequency. Using the results of these calculations, Professor Richards and his coworkers at Berkeley have constructed a carefully optimized heterodyne detector at 36 GHz.⁵ The efficiency of radiation coupling to the device is greater than 80 percent. They have observed conversion gains as large as 4 (6 dB) and mixer noise temperatures as low as 200 K. This noise temperature is comparable to the best performance obtainable at this frequency with cooled Schottky diode mixers which have typical conversion efficiencies of 0.5 (-3 dB) or worse. Conversion gain is desirable since it reduces both mixer and IF noise temperatures. The IF bandwidth used in the Josephson heterodyne system was 20 MHz. In terms of NEP, therefore, the best observed performance was $2 \times 10^{-17} \text{ W}/\sqrt{\text{Hz}}$.

An additional detection mode was explored by Richards et al using junctions which show negative resistance regions on their dc I-V curves.⁵ With proper biasing, conversion gains as large as 50 (17 dB)

were observed at 36 GHz with mixer noise temperatures of the order of 1000 K. This detection mode will be investigated in more detail, both experimentally and using an analog simulator which has also proved quite useful.

Preliminary experiments on harmonic mixing have also been conducted using a 9 GHz local oscillator in the 36 GHz mixer.⁵ In contrast to Schottky diode mixers, Josephson harmonic mixers perform nearly as well as fundamental mixers with the same signal frequency. The preliminary results for the harmonic mixer are a noise temperature of 400 K and a conversion loss of 7 dB. If these results apply at much higher frequencies, the problem of obtaining a suitable local oscillator will be simplified. A Josephson heterodyne detector at 144 GHz is now under construction, and performance of this device both as a fundamental and harmonic mixer will be evaluated.

The question of how well a Josephson heterodyne detector might perform at 300 GHz has not yet been answered directly. However, there are indications from the numerical calculations and the simulation studies that the conversion efficiencies observed at 36 GHz can be extrapolated without change to at least 300 GHz. For niobium junctions the prediction is that the conversion efficiency will remain constant up to 500 GHz and then fall off with inverse signal frequency squared.¹⁸ Also, the experiments at 36 GHz reveal that the dominant noise process is Johnson noise in the junction shunt resistance.⁵ Therefore, mixer noise should not vary with frequency if the simple junction model remains approximately correct at the higher frequencies. Thus, it is not unreasonable to assume that the performance obtained at 36 GHz can be extended to 300 GHz, once coupling efficiency is optimized at that higher frequency.

Other experiments have actually been conducted at frequencies much higher than 300 GHz. T. Blaney of the National Physical Laboratory in England has investigated Josephson mixing using a cw hydrogen cyanide gas laser at 891 GHz as a local oscillator and a second offset HCN laser as the signal, with IF frequencies up to several MHz.⁶ Radiation was coupled to the device via a light pipe or by direct focusing with a lens. Noise at the output was dominated by the room-temperature (450 K) IF amplifier so that a mixer noise temperature could not be determined. Because the conversion loss measured in the experiment was about 30 dB, the effective noise temperature of the IF amplifier (amplifier noise temperature divided by conversion efficiency) was approximately 450,000 K, and all we know is that the mixer temperature is much less than this value and the corresponding NEP is less than $10^{-14} \text{ W}/\sqrt{\text{Hz}}$. It seems reasonable to expect that this conversion efficiency can be improved significantly. Blaney has also demonstrated that harmonic mixing can occur at a signal frequency of 891 GHz using a microwave external oscillator, although the conversion loss in this measurement was 40 dB.

McDonald of NBS has demonstrated Josephson mixing at even higher frequencies, up to the 9 to 11 μm wavelength band.⁷ The experiments involve difference frequencies ranging from 19 MHz to 106 GHz. Although no sensitivity values have been determined at these highest frequencies, the mixing mechanism definitely appears to require the superconducting state since the IF amplitude decreases by as much as 60 dB when the temperature is raised through the transition.

c. Summary and Comparison

The performance of the various coherent detectors just discussed is compared in Table II for a signal frequency of 300 GHz (1 mm wavelength). Observe that in every case the NEP values listed here are smaller than those listed for incoherent detectors, so that this class of detector has greater sensitivity in narrowband applications. For very narrowband signals (<1 MHz) the InSb mixer would appear to be the best choice since it has the smallest NEP and has already been demonstrated in practice. However, the Josephson heterodyne detector would have the same sensitivity, based on an extrapolation of lower frequency results, and there are no fundamental bandwidth limitations for this device. Furthermore, the required local oscillator power in the Josephson junction mixer is just nanowatts instead of microwatts or more for the InSb mixer, and harmonic mixing may be acceptable with the Josephson mixer. Therefore, when the signal bandwidth is greater than a few MHz, the Josephson heterodyne detector would appear to be preferable. For detection of very broadband radiation where ΔT_{min} is the relevant figure-of-merit, we see that the Josephson heterodyne detector would be superior to most other detectors discussed, both coherent and incoherent, except for the superconductor bolometer which has an estimated ΔT_{min} of less than .01 K. One advantage of the Josephson heterodyne detector over the superconductor bolometer is its faster response time ($<10^{-6}$ sec) which may be required in some applications.

CONCLUDING DISCUSSION

The three detectors which appear to have greatest sensitivity at 300 GHz are the hot-electron InSb mixer, the superconductor bolometer and the Josephson heterodyne mixer. The proper choice of detector depends on the application. Not surprisingly, each detector, including the semiconductor device, must be cooled to liquid helium temperature for best operation. The semiconductor device has already been operated at 1.2 mm wavelength, and it is expected that the same level of performance can be maintained to 0.3 mm wavelength (1000 GHz). Although neither the superconductor bolometer nor the Josephson heterodyne detector have yet been operated at 300 GHz, arguments have been given indicating why this should be possible. For the superconductor bolometer operation at 300 GHz should be straightforward, requiring the use of known materials with appropriate absorption and conduction properties. For the Josephson heterodyne detector, in addition to optimizing the radiation coupling at the higher frequencies which is a difficult engineering task, it is also necessary to overcome junction capacitance

Table II

COHERENT DETECTORS
AT 1 MM WAVELENGTH

TYPE	OPERATING TEMPERATURE	MIXER TEMPERATURE	BANDWIDTH	NEP	ΔT_{\min}
GaAs MIXER	290 K	6000 K	100 MHz	$2 \times 10^{-15} \text{ W}/\sqrt{\text{Hz}}$	$1.4 \text{ K}/\sqrt{\text{Hz}}$
GaAs MIXER*	77 K	2000 K	500 MHz	$1 \times 10^{-15} \text{ W}/\sqrt{\text{Hz}}$	$.2 \text{ K}/\sqrt{\text{Hz}}$
InSb MIXER	4.2 K	500 K	2 MHz	$2 \times 10^{-17} \text{ W}/\sqrt{\text{Hz}}$	$.7 \text{ K}/\sqrt{\text{Hz}}$
JOSEPHSON MIXER**	4.2 K	200 K	20 MHz	$2 \times 10^{-17} \text{ W}/\sqrt{\text{Hz}}$	$.07 \text{ K}/\sqrt{\text{Hz}}$

*ESTIMATED PERFORMANCE. NOT YET MEASURED.

**MEASUREMENTS AT 36 GHz. FREQUENCY INDEPENDENT EXTRAPOLATION. COUPLING PROBLEM MORE DIFFICULT AT 300 GHz. JUNCTION CAPACITANCE MUST BE MINIMIZED, BUT POSSIBLE SOLUTIONS ARE AVAILABLE.

effects. Fortunately, a new Josephson junction fabrication technique has been developed at UC Berkeley by Ohta and coworkers which utilizes a semimetal barrier between two nonoverlapping superconductor films.⁸ The physical dimensions of the barrier region are much larger than those of typical weak links giving greater resistance to mechanical and electrical shock, and all the junction parameters, particularly the extremely low capacitance, suggest that these junctions would be ideal for high frequency applications. These junctions should be a great improvement over point contacts which are commonly used at present.

Another requirement for good detection with Josephson junctions is a relatively large value of resistance, approximately in the range from 1 - 50 ohms. Except for the new semimetal barrier junctions⁸ and also proximity effect junctions,⁹ this is not easily achieved with thin-film weak-link structures. However, the use of series arrays of junctions permits junction resistances to add. Furthermore, it has been shown that closely spaced junctions can give a coherent response to incident radiation,^{10,11} thereby increasing the sensitivity. This is an active research area at present which could have a significant payoff for millimeter-wave detectors.

Another research area which has considerable promise for millimeter-wave detection is Josephson parametric amplification. It has been experimentally demonstrated that conversion gains in excess of 10 dB can be achieved at radio and microwave frequencies in a degenerate mode situation where the Josephson pump frequency is twice the signal frequency.¹⁹ In this case the frequency of operation is limited to a narrow range. Another experiment conducted at microwave frequencies confirms the existence of another parametric amplification mode in which the signal frequency is slightly higher than the pump frequency which is generated internally via the Josephson effect.¹² The estimated input bandwidth for this mode is significantly larger than for the degenerate case, but the magnitude of the conversion gain has not yet been measured. The noise temperatures of these devices are expected to be reasonably low, in which case Josephson parametric amplifiers could be serious competition for other millimeter-wave detectors.

The response of Josephson-effect detectors will deteriorate slowly above some frequency in the submillimeter range which depends on the materials used. At this specific frequency the photon energy of the radiation is sufficient to break electron pairs and destroy superconductivity. By using superconductors with transition temperatures higher than niobium (9 K) which is extensively used at present, the electron-pair binding energy is increased and the upper frequency limit for radiation detection can be raised close to the infrared region. However, details of operation at submillimeter wavelengths are not completely understood so that quantitative predictions of performance are not yet possible, although the existence of Josephson

mixing in the submillimeter range has already been demonstrated, as has been mentioned earlier.

In summary, I have described a rapidly developing technology of Josephson-effect detectors which promises to produce competitive and possibly unique devices at millimeter and submillimeter wavelengths. This technology owes its existence to a diverse research base where new ideas are created and explored. This research effort is supported in part by the Navy through the Office of Naval Research, and important additional contributions are being made by several Navy laboratories.

REFERENCES

UNCLASSIFIED

1. A. A. Penzias, Proceedings of the International Conference on the Detection and Emission of Electromagnetic Radiation by Josephson Junctions (to be published in Revue de Physique Appliquee); A. A. Penzias and C. A. Burrus, Annual Reviews of Astronomy and Astrophysics 11, 51 (1973).
2. J. Clarke, *ibid.*
3. B. T. Ulrich, *ibid*; ———, Proceedings of the 12th International Conference on Low Temperature Physics, 867 (1970).
4. F. Auracher and T. Van Duzer, *ibid*; ———, J. Appl. 44, 848 (1973).
5. Y. Taur, J. H. Claassen and P. L. Richards, *ibid.*
6. T. G. Blaney, *ibid.*
7. D. G. McDonald, F. R. Petersen, J. D. Cupp, B. L. Danielson and E. G. Johnson, *ibid*; D. G. McDonald, A. S. Risley, J. D. Cupp, K. M. Evenson and J. R. Ashley, Appl. Phys. Lett. 20, 296 (1972).
8. H. Ohta, M. J. Feldman, P. T. Parrish and R. Y. Chiao, *ibid.*
9. J. E. Mercereau, *ibid*; H. A. Notarys and J. E. Mercereau, J. Appl. Phys. 44, 1821 (1973).
10. T. F. Finnegan, J. Wilson and J. Toots, *ibid*; T. F. Finnegan and S. Wahlsten, Appl. Phys. Lett. 21, 541 (1972).
11. T. D. Clark, *ibid*; ———, Phys. Rev. B1, 137 (1973).
12. H. Kanter, *ibid*; ———, Appl. Phys. Lett. 23, 350 (1973).
13. P. L. Richards, F. Auracher and T. Van Duzer, Proc. IEEE 61, 36 (1973).
14. M. I. Skolnik, Proceedings of the Symposium on Submillimeter Waves, 9 (1970).
15. F. R. Arams, Infrared to Millimeter Wavelength Detectors (Artech House, Inc., Dedham, Mass.), 20 (1972).
16. H. Kanter and F. L. Vernon, J. Appl. Phys. 43, 3174 (1972).
17. P. L. Richards and S. A. Sterling, Appl. Phys. Lett. 14, 394 (1969).
18. C. A. Hamilton, J. Appl. Phys. 44, 2371 (1973).

19. H. Kanter and A. H. Silver, Appl. Phys. Lett. 19, 515 (1971).

20. T. G. Phillips and K. B. Jefferts, Rev. Sci. Instr. 44, 1009 (1973).

SUPERCONDUCTING RADIATION DETECTORS - -
THEIR DEVELOPMENT AND APPLICATIONS POTENTIAL

Douglas M. Warschauer
Naval Weapons Center
China Lake, California 93555

UNCLASSIFIED

INTRODUCTION

The title of this paper is somewhat a misnomer. The purpose as originally conceived was to demonstrate the potential value of Josephson junction detectors to the Navy by citing the coherent quantum nature of the effect, which leads to exquisite sensitivity coupled with extremely broad bandwidth and other desirable properties, and to point out the response at China Lake to indications that these could be made available. A look at the titles of the other presentations at this workshop suffices to convince even the most sceptical of the ultimate importance of these devices. Further, Solymar¹ in a highly authoritative but otherwise staid monograph has characterized the Josephson junction as the most versatile single device since the invention of the p-n junction, to be "made perhaps in the billions one day". With this start and enthusiasm, there is no doubt that Josephson devices are going to become an integral part of Navy hardware. Unfortunately, the current art of fabricating superconducting junctions appears to be much the same as that of fabricating semiconductor junctions and transistors in the mid-fifties: A number of configurations, a wide range of material combinations, and several competing fabrication techniques are available, without any one method, geometry, or material proven to be clearly superior to the others. Further, there are many indications that the material characteristics and techniques which are crucial for stable, long-lasting, reproducible devices have not been sifted from those which

are superficial. In fact, there is some reason to believe that many published reports are on one-of-a-kind devices, although this is rarely admitted. Since it is our purpose at the Naval Weapons Center to develop a really field-usable radiation detector system, it is necessary to face this problem in order to ensure a ready supply of sturdy devices which can be given to development people. The facility to produce a large number of identical units which have stable characteristics is imperative to gather statistics, to follow up the potential applications of arrays and to convince engineers that the techniques are ready to move out of the laboratory stage.

TUNNEL JUNCTIONS

Tunnel junctions probably have the most reliable geometry for obtaining and understanding the Josephson effects. A sandwich of two superconductors with a non-superconducting barrier is ideally a planar configuration which fits well with formulated theory, should be relatively easy to fabricate, and be replete with material and geometric virtues for obtaining the best device parameters. For this reason, many experiments have been done using numerous combinations of superconductors in conjunction with barriers of normal metals, semiconductors, organics, and mixtures best described as "gunk". Solymar² devotes eight book pages merely to listing and referencing the various combinations and perturbations whose characteristics have been reported.

For example, Fisher and Giaever³ used Al-Al₂O₃-Al junctions; Rowell and Kopf⁴ used Al-Al₂O₃-Pb junctions. Junctions like these are best stored at liquid nitrogen rather than room temperature. Miles and Smith⁵ used plasma discharge and solid state anodization as means of stabilizing such junctions. More recently Schwidtal and Finnegan⁶ describe a Nb-NbO_x-Nb junction, made by a combination of sputtering, thermal and plasma oxidation and varnish sealing, which they find durable and capable of being stored at room temperature for several years. They also report that somewhat similar Pb-PbO_x-Pb junctions could not be stored at room temperature for more than one day. Matisoo⁷ gives a brief review of oxide barrier experiments and others, such as those of Giaever⁸ and Seto and Van Duzer⁹ using CdS and Te respectively.

Problems with tunnel junctions include differential expansion which requires thermal cycling with care; the absorption or inclusion of oxygen within an oxide layer, at voids, or dislocations which then can migrate, giving an aging effect slowed only by low temperature storage; the presence of various suboxides, particularly of tin and lead; the growth

of whiskers in tin; pinholes and non-stoichiometry in semiconductor films, necessitating heavy oxide layers for insulation in the pinhole case; interdiffusion of the superconductor metal into semiconductor barriers, reducing the effective barrier width and providing erratic geometry. Less often mentioned are the presence of certain organics such as pump oil and inorganic molecules such as water vapor, despite the bulk of junctions being made in oil-pumped vacuums of 10^{-6} Torr or less, the use of air exposure and solutions of photoresists. The value of bombardment and sputtering methods may be more a matter of cleaning than of compacted deposit. The successful early use of barium stearate blocking films^{10,11} is probably not only a testimonial to the skill of the experimenters using them but also to the stubborn persistence of an effect in showing itself once it is discovered.

MICROBRIDGES

The weak link bridge typically consists of a reduced area a few microns in each dimension connecting two relatively thin sputtered or deposited films of superconducting metals. Herein lies a triple dilemma: First, years of intensive investigation have shown that the field of thin films is in itself a special field--the exact conditions of deposition, substrate, substrate temperature, vacuum, cleanliness, etc., determine the precise structure and purity of the final film. Second, a clean surface of metal is usually a catalyst for all sorts of reactions involving the contaminants (as they must be viewed) which subsequently land on it. Conversely, a dirty film is usually not what the physicist or engineer envisions in his ideal device. Finally, third, a geometry involving the dimensions of the typical weak link is an open invitation for surface and edge effects not at all typical of the bulk. A recent paper by Laibowitz¹² describes submicron Nb Josephson microbridges fabricated by an electron beam-resist technique. The resistive transition shows that the 6 micron connecting pads become superconducting at 9.2°K while the link has its transition at 6.7°K. Josephson effects are seen only below this latter temperature. Laibowitz attempts to relate the double transition to oxygen at the surface and at grain boundaries in the bulk. He also points to other phenomena which can strongly influence the microbridge: Irregular rather than ideal link geometry, chemical impurities, grain boundary and surface scattering.

POINT CONTACTS

Little more need be said about the typical point contact geometry other than that in addition to all the phenomena discussed to this point one can add the uncertainties of rough surfaces, problems of mechanical expansion and contraction, and susceptibility to vibration. Semiconducting

point contact diodes were in production before the transistor appeared, but now they are generally used only when the frequency is so high that junction capacitance is the major problem.

PROGRAM

Dr. Dinger of the Naval Weapons Center, using a 10^{-6} Torr vacuum and oxygen obtained by distillation from the liquid, was making cross-stripe Sn-SnO_x-Sn junctions which exhibited Josephson steps, until it was noted that an oil film could be observed on the originally clean substrates and microscopic examination of the junctions using the Nomarski technique revealed the presence of various film defects plus stripes at interfaces which appeared to have a different composition from the body of the films. Everett¹³ indicated that he and Cook had to resort to a quick flash technique to get good tunneling junctions. It was then decided to build junctions by the best UHV technique possible. Figure 1 shows an apparatus in which both an electron gun and dimple boats can be used for deposition on a heatable substrate. Seven substrates can be exposed to the evaporated material through each of three masks for each, which be rotated into position and moved upward into direct contact with the substrate. The details of mask suspension are shown in Figure 2. A shutter is provided which has three positions-- one in which no substrate nor thickness monitor is exposed to evaporation, one in which only the monitor is exposed for rate and thickness determination, and one in which all substrates and monitor are exposed.

The masks are formed of .003" stainless sheet into which appropriate patterns are etched. Initially, after extensive bakeout, a cross-stripe arrangement will be used, in which the first deposition will be of gold and contact pads, and the second will be of a number of stripes of superconducting metal. The system will then, at least in the initial experiments, be brought up to the 0.2 bar pressure of the vapor above liquid O₂ held at nitrogen temperature while the substrate is heated. A final pumpdown and deposition of cross-stripes will complete the unit, without exposure to air, water vapor, or organics.

Several comments may be in order at this point. The initial experiments using a cross-stripe oxide barrier configuration are not dedicated to obtaining high frequency devices but to understanding some aspects of the problems described earlier. A cross-stripe geometry will enable a number of junctions to be deposited simultaneously on each of the substrates, allowing some ability to look at statistical variation.

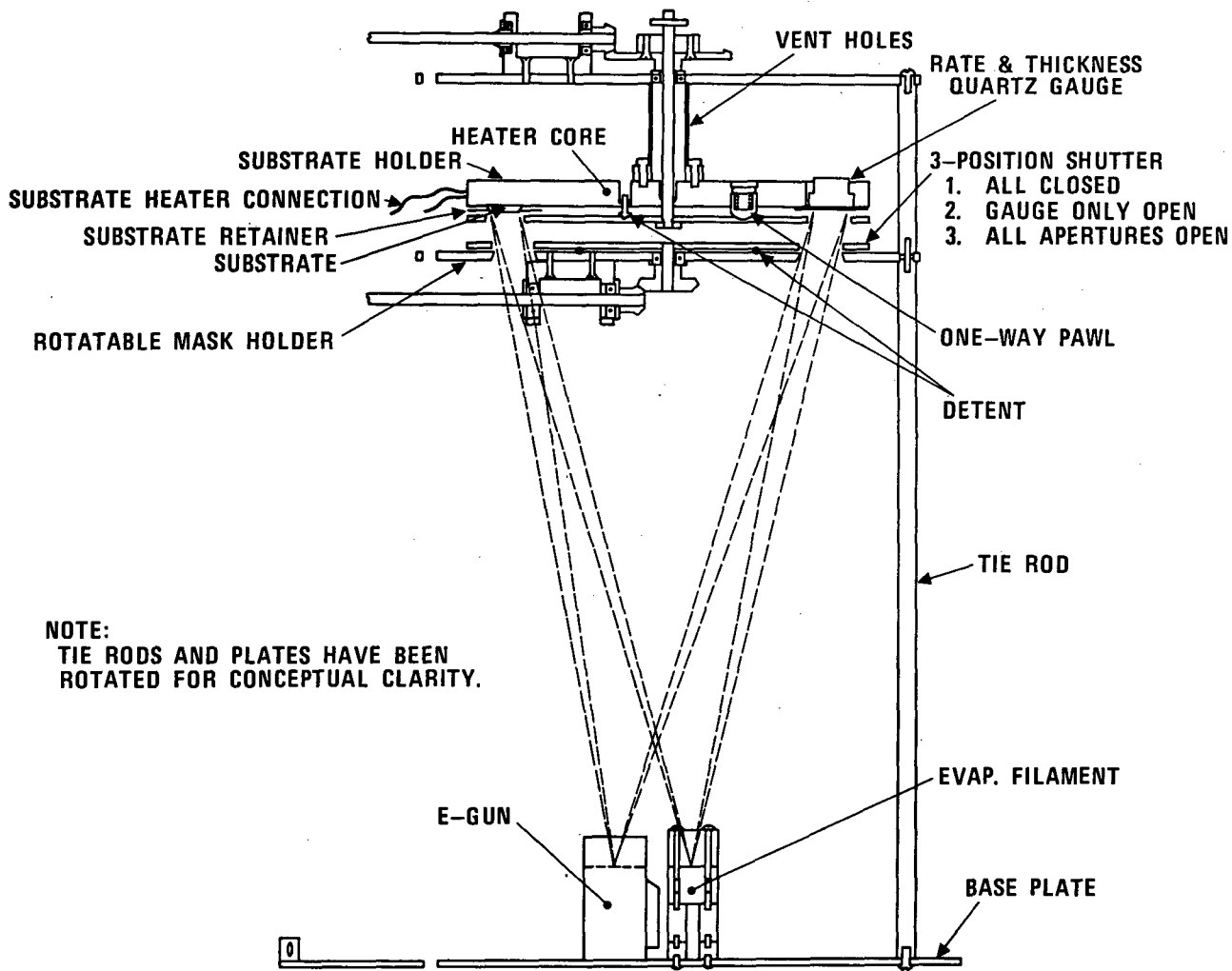


Fig. 1 — Schematic of bakeable UHV deposition system. Masks not shown in position. Seven substrates can be covered by three masks each.

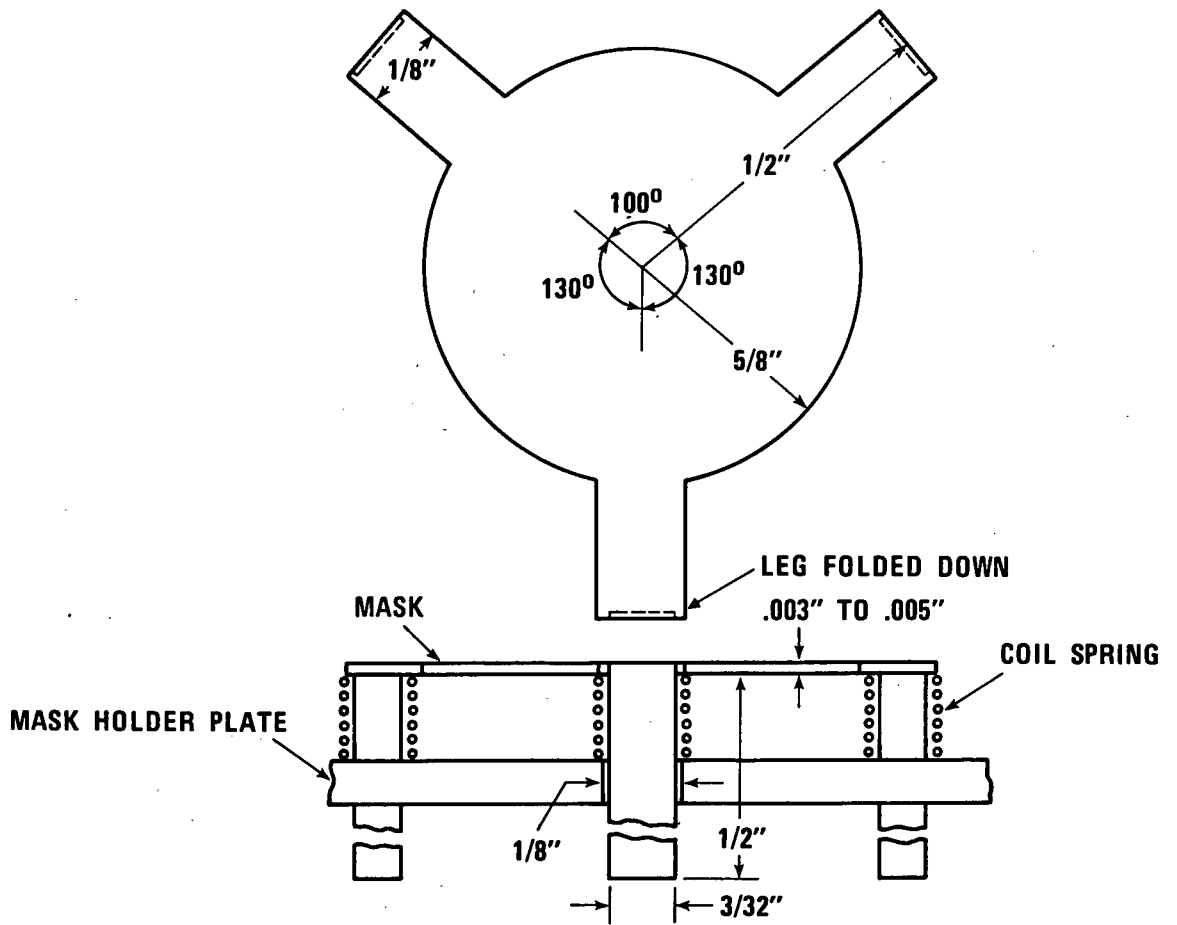


Fig. 2 — Mask outline and method of support. The deposition pattern is etched into the central part of the mask.

The system is amenable to making bridges of the Dayem or Notarys type or for local doping to achieve decoupling, as well as being useful for deposition of normal metals and semiconductors as barriers. Eventually low area geometries, such as by Buckner's¹⁴ technique, or geometries suitable for enhanced coupling to stripline or waveguide may be able to be fabricated. The system can also be used for array fabrication.

Although this paper may not be notable for the new data supplied, it is hoped that the recitation of material problems and the presentation of one small technique by which to examine them will be provoking to those who have gone further. It is felt by many that the industrial success of semiconducting devices followed more directly from improved materials and an understanding of surfaces than from exotic interactions of band structure.

References

1. L. Solymar, Superconductive Tunnelling and Applications, Wiley-Interscience, (1972). P. 144.
2. Solymar, ibid, PP. 335-342.
3. J. C. Fisher and I. Giaever, J. Appl. Phys. 32, 172 (1961).
4. J. M. Rowell and L. Kopf, Phys. Rev. 137, A907 (1965).
5. J. L. Miles and P. H. Smith, J. Electrochem. Soc. 110, 1240 (1963).
6. K. Schwidtal and R. D. Finnegan, Proc. 1972 Applied Superconductivity Conference, I.E.E.E., (1972). PP. 562-564.
7. J. Matisoo, Proc. 1972 Applied Superconductivity Conference, I.E.E.E., (1972). P. 535.
8. I. Giaever, Phys. Rev. Letters 20, 1286 (1968).
9. J. Seto and T. Van Duzer, Appl. Phys. Letters 19, 488 (1971).
10. S. Shapiro, et al, IBM J. Res. Develop. 6, 34 (1962).
11. J. L. Miles and H. O. McMahon, J. Appl. Phys. 32, 1176 (1961).
12. R. B. Laibowitz, Appl. Phys. Letters 23, 407 (1973).
13. Glenn Everett, private communication.
14. S. A. Buckner, "An Experimental Study of the Riedel Singularity and Quasiparticle Damping Effects in Very Small Josephson Tunnel Junctions", Dissertation, Physics Department, University of Pennsylvania (1972).

SUPERCONDUCTING MATERIALS RESEARCH AT NRL

R.A. Hein and R.A. Meussner

Naval Research Laboratory, Washington, D.C. 20375

UNCLASSIFIED

NRL supports materials research on basic and applications related superconductivity problems. Although this work tends to be concentrated in the Transformation and Kinetics Branch of the Metallurgy Division and the Crystal Physics Branch of the Solid State Division, research on superconductivity is not exclusively restricted to these Branches. Funding for this work originates from Navy 6.1 funds.

Basic Studies:

Work in this area is directed towards the discovery of new superconducting materials and the identification of basic interactions which play a role in determining such parameters as T_0 , the transition temperature, and H_{c1} and H_{c2} , the lower and upper critical magnetic fields respectively.

L. Alloys and Compounds

A class of superconducting materials of particular interest is the Al5 intermetallic compounds. These compounds are often designated by the formula A_3B where A is always a transition metal while B may or may not be a transition metal. From a practical point of view, the case where B is a simple metal is of interest, for such compounds have the highest T_0 's, i.e., Nb_3Ge (22.3 K), Nb_3Ga (20.3 K), Nb_3Al (18.8 K), etc. However, from the point of view of trying to isolate mechanisms which play an important role in determining T_0 , compounds with B a transition metal are of significant interest. Although an earlier collaborative program^{1,2} between NRL, NSRDC (Annapolis), NBS and Westinghouse definitely established the importance of low temperature ordering anneals

(700-800°C) in maximizing T_0 (a practice that is now widespread), recent work³ with the V-Ir, V-Rh and V-Os systems show that this result is not a universal one when B is a transition metal.

The simple correlation between increased order, i.e., increased "chain-integrity", and increased transition temperatures which is inherent to the linear-chain model cannot be universally applicable to the A15 compounds. These recent results³ emphasizes the over-simplification of the linear-chain theories, and theories will have to be developed for the case where B is a transition metal.

Work with these interesting but low T_0 compounds has been de-emphasized and priority has been given to the technologically important, higher T_0 , compounds ($T_0 > 12K$). Because of its compositionally wide phase field, and the extent of earlier work, the A15 phase of the V-Ga system was chosen for our initial studies of a high T_0 compound. Results⁴ for V_3Ga shown in Fig. 1 are in keeping with the linear-chain model. However, recent work at NRL has revealed some additional interesting features through measurements of T_0 and H_{c2} . (a) Solidification segregation, even in these small chill-cast specimens, produces a thin surface layer richer in V than the bulk composition. Measuring techniques such as ac susceptibility or dc resistivity which are sensitive to the presence of a surface layer, may lead to values of T_0 which should not be ascribed to the bulk composition of the specimen. This may account for the differences in the T_0 versus composition plots of various workers. (b) Elimination of the solidification segregation in the as-cast A15 material by diffusion is very slow. Homogenization is accelerated by heating the material to high temperatures where it transforms

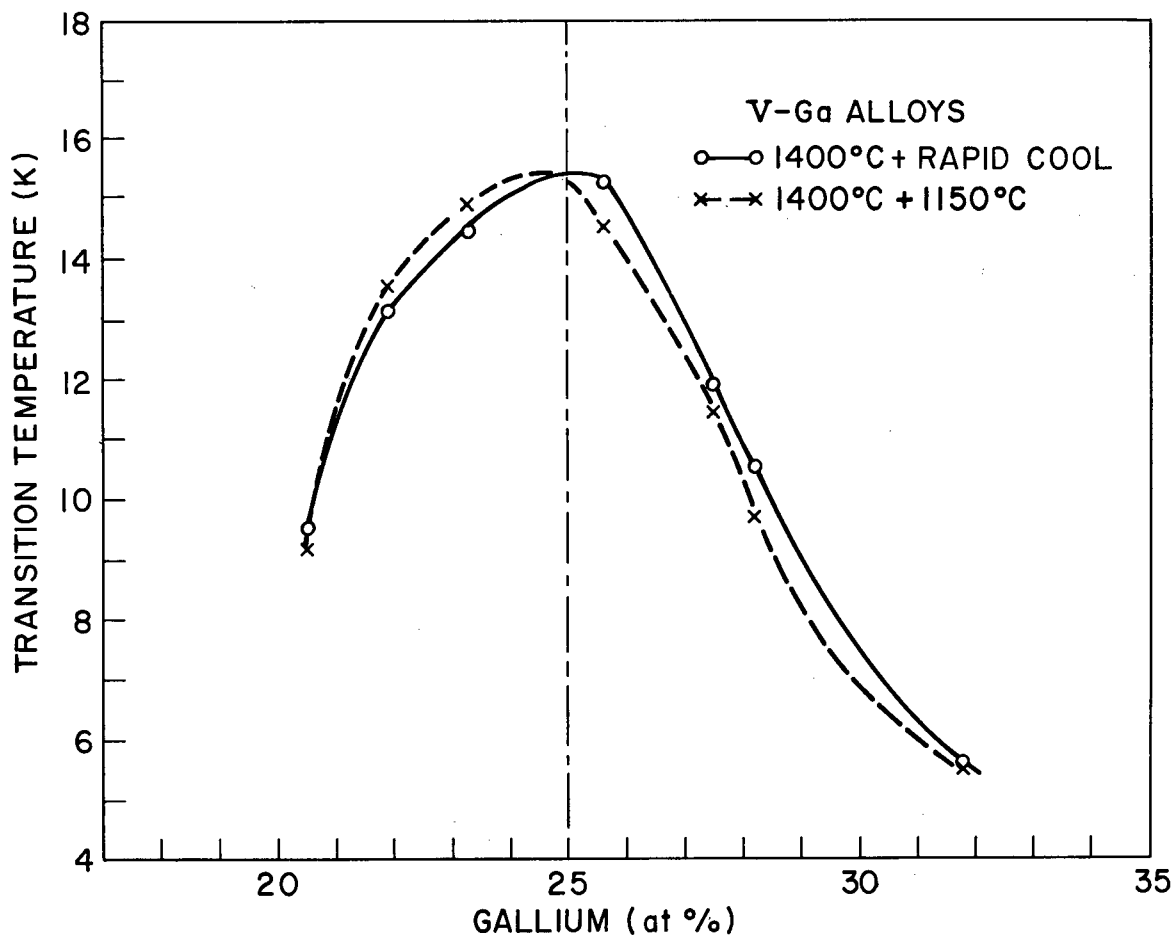
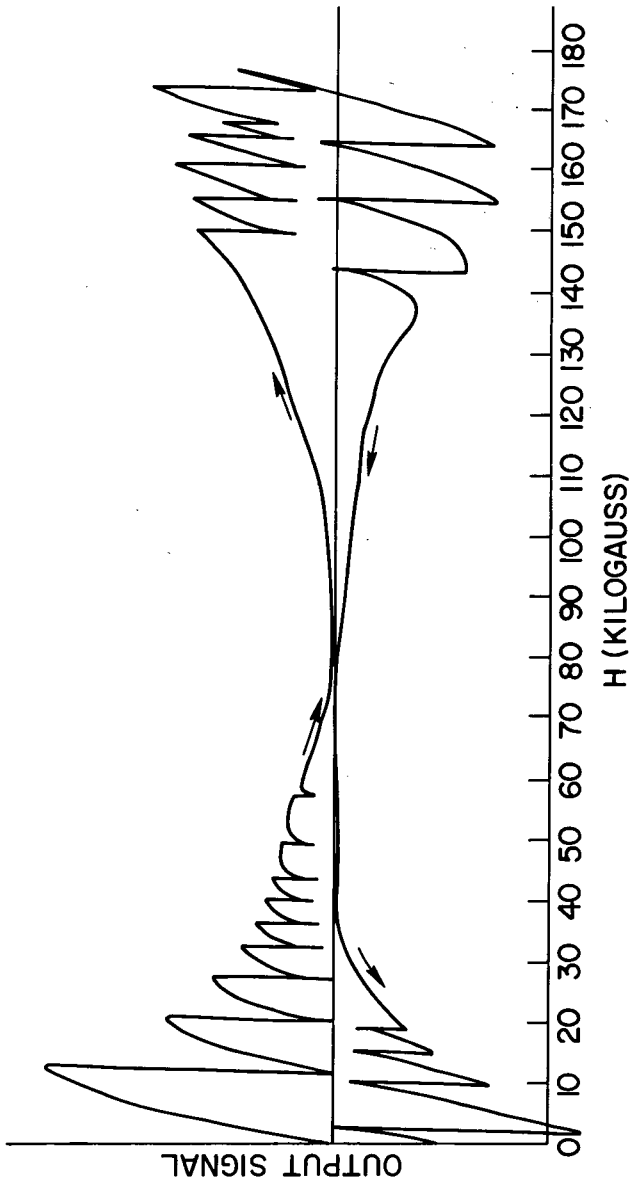


Fig. 1 — Dependence of the transition temperature of the A15 phase of the V-Ga system on composition and homogenization treatments.

to a b.c.c. structure. Fine scale segregation is inherent in the subsequent b.c.c. to A15 transformation on cooling, but this inhomogeneity, being fine-scaled, is more readily eliminated by heat-treating within the A15 stability temperature range. (c) Low temperature ordering anneals (800 to 1150°C) do not produce an increase of T_0 in the A15 phase of V-Ga, in fact a small decrease (0.8K) is often observed. In addition to measurements of T_0 versus composition, scientists at NRL have initiated studies of the high field magnetization of "V₃Ga". Fig. 2 is a plot of magnetic moment versus magnetic field. These data were obtained in our high magnetic field facility and such data are being used to study the effects of metallurgical variables on the nature of the flux jumping, appearance of the "peak effect", and measured values for J_c , H_{c1} , and H_{c2} .

Sudden decreases of the magnetic moment (flux jumps) evident in Fig. 2, release pulses of thermal energy which can lead to a premature "quench" or destruction of the superconducting state. It is for this reason that composite-conductors were developed for magnet applications. (See Section II.)

In the search for new superconducting materials - empirical rules relating the occurrence of superconductivity and high T_0 values to certain ranges of the electron per atom ratio are widely used. Previous work at NRL resulted in the discovery of 3 new superconducting elements (only 4 have been discovered in the last 12 years) and has removed any limitation on e/A as far as the occurrence of superconductivity is concerned. The rule that for high T_0 one needs e/A in the vicinity of 4.7 and 6.3 is still valid. But it also appears that an e/A of about 3.8 is conducive to high



V₃Ga MAGNETIZATION CURVE AT 4.2 KELVIN

Fig. 2 — Magnetic moment of an arc-cast V₃Ga sample as a function of magnetic field.

T_0 . Recent work⁵ at Los Alamos Scientific Laboratory employed high-pressure high-temperature techniques to prepare lanthanum-thorium sesquicarbide and yttrium-thorium sesquicarbide with T_0 in the 15-17° K range. This is a very surprising result and work is under-way at NRL to investigate the high field properties of these superconductors.

Results obtained⁵ for the sesquicarbides as well as more recent work on PdAgH compounds⁶ point out the possible existence of other higher T_0 materials which could be of technological importance. Superconductivity in the PdH system is being investigated⁷ in the Metal Physics Branch of the Metallurgy Division.

The high pressure facilities at NRL are being modified to exploit high pressures-high temperatures to attempt to synthesize metastable A15 phases in candidate systems which promise high T_0 's where the A15 phase can be formed.

Elements:

Work at ultra low temperatures (ULT) produced by either magnetic cooling or by the use of a dilution refrigerator⁸ is directed towards increasing our knowledge regarding the electronic and atomic parameters which seem to play the dominant role in superconductivity⁹. Work has also been initiated to combine ULT and high pressures to investigate the systematics of the basic electron-electron and electron-phonon interactions as they relate to the occurrence of superconductivity and to the determination of T_0 .

Superconducting Semiconductors:

The ULT facility at NRL which permits experimentation to temperatures as low as 0.015 K is employed to study a class of superconductors first discovered at NRL, i.e. superconducting semi-

conductors¹⁰. These materials are unique as a class since the T_0 is a very sensitive function of the carrier concentration, P^* , which can be varied by several orders of magnitude. (For metallic alloys and compounds one cannot do this.) Besides basic studies on the effects of composition and P^* on T_0 , work is also underway to investigate predicted "charging effects". If this prediction¹¹ is verified such materials could be utilized as unique switching devices.

II. Metallurgical Studies

For the practical utilization of superconductors in dc applications one needs "stabilized" composite conductors with reasonably high T_0 (> 8 K) so that one has reasonably high values for H_{c2} (> 50 kG) at 4.2 K. In the case of ac applications one needs similar T_0 values and high values for H_{c1} (> 10 kG). Although there are a host of materials with $T_0 > 9.2$ K all applications discussed at this conference utilize Nb (9.2 K) or Nb-Ti alloys, (9.0-9.5 K). One uses Nb in ac applications ($H_{c1} = 1.4$ kG) and Nb-Ti in dc applications ($H_{c2} = 80$ kG).

The reason why higher T_0 and H_{c2} materials are not utilized in dc applications is the need to stabilize such materials against the adverse effects of "flux-jumps". This in turn necessitates the fabrication of composites, i.e., embedding the superconductor in a matrix of high electrical and thermal conductivity.

There is no doubt about the need for higher T_0 , H_{c1} and H_{c2} composites in such areas as MHD and CTR magnets, and we can argue for the need for higher T_0 materials in other applications such as motors, generators, transmission lines, etc. It is this potential

market that gives rise to efforts to manufacture multifilament wires of the best superconducting materials. Niobium, Nb-Ti and Nb-Zr, being ductile metals and alloys, have been successfully fabricated as multifilaments embedded in a copper matrix. Very long lengths of these very delicate structures have been produced and used to build motors, magnets and the coils for applications described in this workshop. The Al5 materials, being brittle intermetallics, cannot be produced directly in these forms. During the past decade thin tapes and wires of Nb₃Sn have been produced by a variety of processes, and a large number of magnets and selenoids manufactured from these. More recent innovations by Suenaga and Sampson¹² at the Brookhaven National Laboratory and Tachikawa¹³ in Japan have produced experimental lengths of multifilament wires of V₃Ga. During this year the Japanese have marketed the first commercial multifilament superconductor containing V₃Ga.

Utilizing the technique pioneered by Suenaga and Sampson¹², we have examined the processing parameters in forming Cu-Ga/V composites, measured the growth kinetics of V₃Ga in these materials, and evaluated the structure and characteristics of the V₃Ga superconductor. The technique is derived from the fact that the Ga activity in a ductile Cu-Ga alloy can exceed that of the V₃Ga phase. Thus a ductile composite of V-rods in a Cu-Ga matrix can be reduced to fine wire by rolling, swaging, and wire drawing; and processing, similar to that used in the production of Nb and Nb-Ti multifilament wires, can be adapted for these composites. The V₃Ga superconducting phase is formed at the Cu-Ga/V interface in a final heat-treatment.

Studies have been made of the effects of the final heat-treating temperature and the alloy content of the composite on the growth rate, microstructure, and critical current capacity of V_3Ga formed in single filament wires. The High Magnetic Field Facility of NRL was used to obtain critical current (J_c) data at 4.2 K in transverse magnetic fields up to 150 kG. Samples reacted at 575°C displayed, see Fig. 3, the highest J_c values - values which remained above 10^5 amps/cm² in the 150 kG field¹⁴. The improvement in J_c with lower reaction temperature is ascribed to a finer V_3Ga grain size and to a shift in the composition of this phase toward the stoichiometric V_3Ga . The growth of this phase always displayed a parabolic time dependence and a very strong dependence on the Ga content of the Cu-Ga alloy.

Consideration of the growth mechanism and the nature of the probable phase relationships in the Cu-V-Ga system lead to a study of the effects of replacing the pure V-core with a V-Ga alloy in these reaction specimens. This substitution has yielded higher V_3Ga growth rates and significant improvements in the critical current density in this superconducting phase.¹⁵ Fig. 4 illustrates the effectiveness of these alloy changes in increasing the critical current characteristics of V_3Ga formed at 600°C in composite wires. By lowering the reaction temperature from 600 to 550°C the critical current characteristics of the V-9.0 Ga/Cu-17.5 Ga wire was further improved - this specimen sustained current densities of 10^6 amps/cm² in fields as high as 100 kG. These results demonstrate that "new" superconducting materials are being developed, and these developments will be important for many applications.

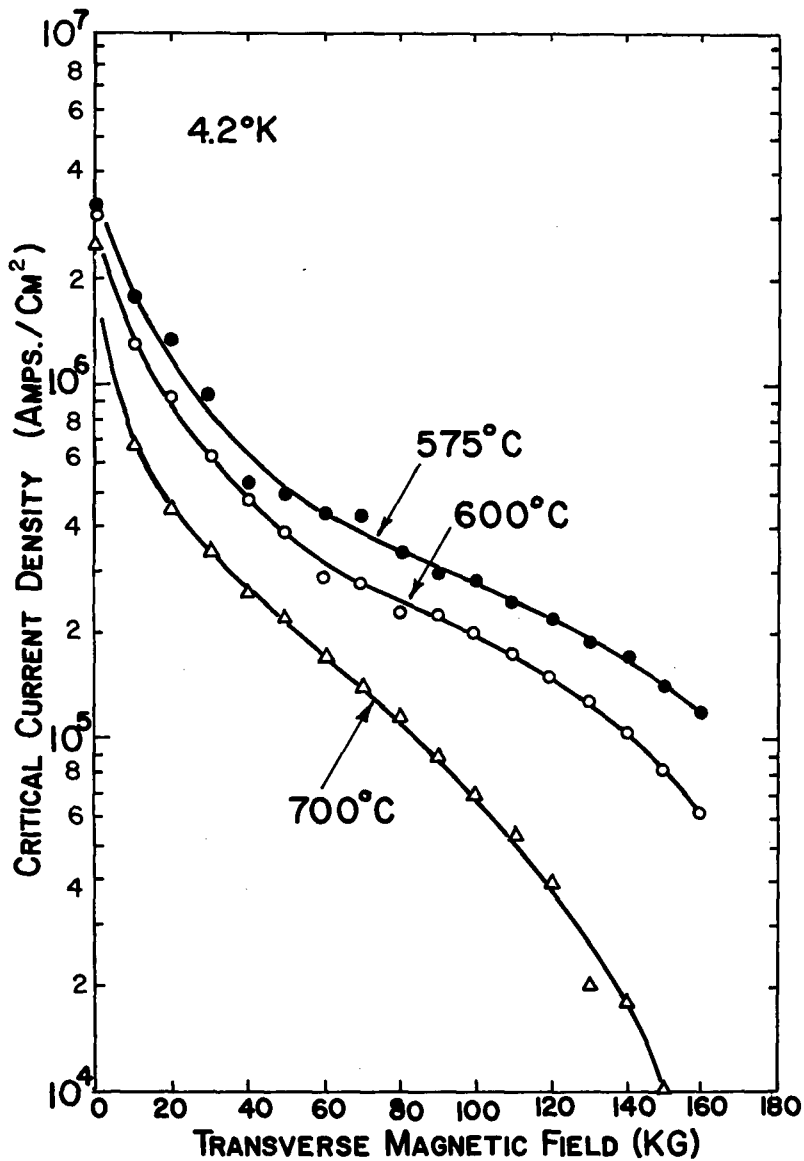


Fig. 3 — Critical current density dependence on magnetic field strength of 1.0 μ m layers of V₃Ga in 0.010 inch diameter wires for three reaction temperatures: 575, 600, and 700°C.

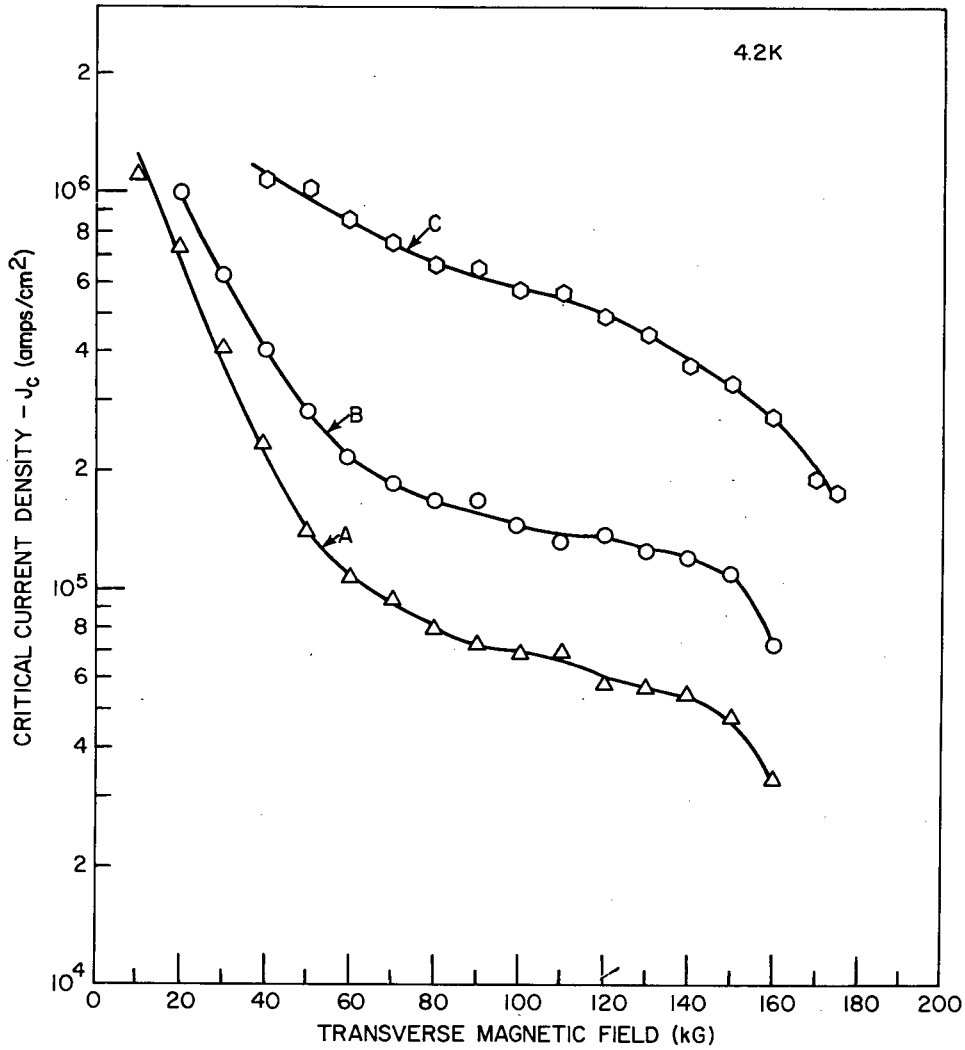


Fig. 4 — Critical current density dependence on magnetic field strength of 2.3 — 2.5 μ m layers of V₃Ga formed at 600°C in 0.032 inch diameter composite wires of these compositions: A) V/Cu-15.4 Ga, B) V-6.1 Ga/Cu-15.4 Ga, C-17.5 Ga (Ga in at. %).

REFERENCES

1. R.O. Blaugher, R. A. Hein, J. E. Cox and R. M. Waterstrat, *J. Low Temp. Phys.* 1, 539 (1969).
2. R. A. Hein, J. E. Cox, R. D. Blaugher, R. M. Waterstrat and E. C. van Reuth, *Physica* 55, 523 (1971).
3. J. E. Cox and R. M. Waterstrat, *Phys. Letts.* 46, 21 (1973).
4. B. Das, R. Huber and J. E. Cox, to be published.
5. A. L. Giorgi, E. G. Szklarz and M. C. Krupka, AIP Conf. Proc. No. 4, Ed. by D. H. Douglass, AIP, NY (1972), p. 197.
6. W. Buckel and B. Stritzker, *Phys. Letts.* 43A, 403 (1973).
7. C. A. Mackliet, D. J. Gillespie and A. I. Schindler, submitted for publication. See B. Stritzker and W. Buckel, *Z. Physik* 257, 1, (1972).
8. D. U. Gubser and L. D. Jones, NRL Reports of Progress, June 1971.
9. D. U. Gubser, *Phys. Rev.* B6, 827 (1972).
10. R. A. Hein, J. W. Gibson, R. Mazolsky, R. C. Miller and J. K. Hulm, *Phys. Rev. Letts.* 12, 320 (1964); for a comprehensive bibliography, see R. A. Hein and P. H. E. Meiser, *Phys. Rev.* 179, 497 (1969).
11. T. G. Berlincourt, *Phys. Letts.* 29A, 308 (1969).
12. M. Suenaga and W. B. Sampson, *Appl. Phys. Lett.* 18, 584 (1971).
13. K. Tachikawa, Applied Superconductivity Conf., Annapolis, Md., IEEE pub. No. 72CH0685-5-TABSC, 1972, p. 371.

14. D.G. Howe, L.S. Weinman and R.A. Meussner, Appl. Phys Lett. 23, (279) (1973).

15. D.G. Howe, L.S. Weinman and R.A. Meussner, to be published in Cryogenics.

UNCLASSIFIED

SUPERCONDUCTIVITY RESEARCH IN THE USSR WITH
COMMUNICATION APPLICATIONS

J. T. Coleman
Naval Intelligence Support Center
Suitland, Maryland 20390

Manuscript not available.

DEVELOPMENT OF THE ACYCLIC SHAPED FIELD MOTOR

M. Cannell, T. Doyle, S. Raphael
Naval Ship Research and
Development Center
Annapolis, Maryland 21402

UNCLASSIFIED

ABSTRACT

Superconductors are materials which exhibit zero electrical resistance at temperatures near absolute zero, supporting current densities in the order of 100,000 amperes per cm^{2*} in the filamentary wire form. When wound into magnets, helium cooled superconductors provide the compact, high flux source necessary for small, efficient electric machines. These advantages are illustrated in a recently completed motor built at the Naval Ship Research and Development Center (NSRDC). The laboratory machine, now under evaluation, has a unique magnet-shield configuration designed to maximize flux utilization and power density. It is 51 cm (20 inch) in diameter and is expected to demonstrate more than 5000 hp per cubic meter at propulsion motor speeds. The machine includes a stationary, niobium titanium wire, solenoidal magnet surrounded by a 1010 steel magnetic shield. Rotor and stator copper drum conductors, series connected through liquid metal brushes, operate in the magnet/shield annulus. Initial motor operation indicated that the high-efficiency, high-power density, low stray magnetic field, and small diameter requirements of full-scale naval electric ship drives can be achieved.

INTRODUCTION

A ship drive system provides the power transmission path between the prime mover, which may be a gas or steam turbine, diesel engine, or other source of rotary power, and a propeller, fan, jet pump, or other propulsor generally operating at much lower speed. When multiple prime movers or propulsors are used the drive system should also permit power-combining and cross-connection.

If the full potential of advanced hull forms now under consideration is to be realized several additional drive system features must be available.¹ Advanced gas turbine powered catamarans, hydrofoil craft, and surface effects ships are characterized by large turbine-propeller separations, constrictive machinery spaces, and demanding take off loadings. In addition to speed reduction and power distribution functions, therefore, drive machinery must be compact, easily located, reversible, and capable of variable torque ratios.

*Abbreviations used in this paper are from the GPO Style Manual, 1973, unless otherwise noted.

¹Superscripts refer to similarly numbered entries in the References at the end of the paper.

Many of the features required in advanced ship drives are inherent in electric transmissions which include motor-driven propellers powered by turbogenerators. The alignment free electric linkage provides great machinery arrangement flexibility when compared to hard-coupled mechanical drives. Control and maneuverability advantages are also evident in d-c transmissions which permit variable reduction ratios and electric reversals. These location and control benefits have seldom been available in propulsion applications because of the prohibitive size and weight of conventional motors and generators.

The advent of superconductivity, however, promises to bring these electric coupling benefits to many naval applications. Superconductors will support very high currents without resistance losses when their temperature is reduced below a critical value, typically in the liquid helium range (near 5° K). With superconducting field windings it is possible to produce very intense magnetic fields with small quantities of material and negligible electric power loss. It should now be possible to produce power with generators which are smaller than the prime movers driving them and to transmit it to motors which are smaller than the thrusters with which they are used.

The availability of practical superconducting materials in the last decade, coupled with the need for improved drive system characteristics, therefore, provided impetus for development of superconductive machinery tailored to shipboard applications.^{2,3,4,5} One product of investigations at NSRDC was the evolution of a new d-c superconducting machine concept.⁶ Termed the "shaped field machine" because of the unconventional manner in which the magnetic field geometry is established, this unique approach provides small diameter, shock resistant, magnetically shielded designs with high efficiencies and modest refrigeration requirements.

A 400 to 1000-hp motor has been designed and constructed to verify the predicted size and performance advantages of the shaped field configuration. At publication time the laboratory machine is undergoing no-load evaluation. Load testing up to the 400-hp level will be conducted with a rectifier power supply and a water-brake load. Subsequently, system performance will be determined when the rectifier is replaced by a laboratory-built, superconductive generator (of different design) powered by a 1000-hp gas turbine. Successful motor-generator operation in the laboratory will be followed by shipboard evaluation in a small test vehicle.

This paper describes the design and construction of the shaped field laboratory motor. Loss mechanisms are treated and machine performance estimated. The advantages superconductive d-c drive can provide future high performance ships are illustrated in a hypothetical 80,000-hp small water area twin hull (SWATH) ship and 40,000-hp hydrofoil (HF) craft.

SHAPED FIELD CONCEPT

UNCLASSIFIED

The size and efficiency advantages of the shaped field acyclic machine accrue directly from the unique magnet/rotor arrangement, illustrated conceptually in figure 1. The superconducting solenoidal magnet and helium vessel, or dewar, are the innermost machine elements. The intense magnetic flux generated in the bore of the solenoid is attracted by the ferromagnetic shield forcing virtually all of the magnetic flux to radially transverse the rotor twice. When current is passed through brushes and axially down the copper rotor drums the resulting Lorentz interaction provides motor action. Conventional arrangements of superconducting d-c machines include the same magnet/rotor/shield elements, but the rotor is located in the magnet bore and a lesser portion of the generated flux is utilized in the power production process.

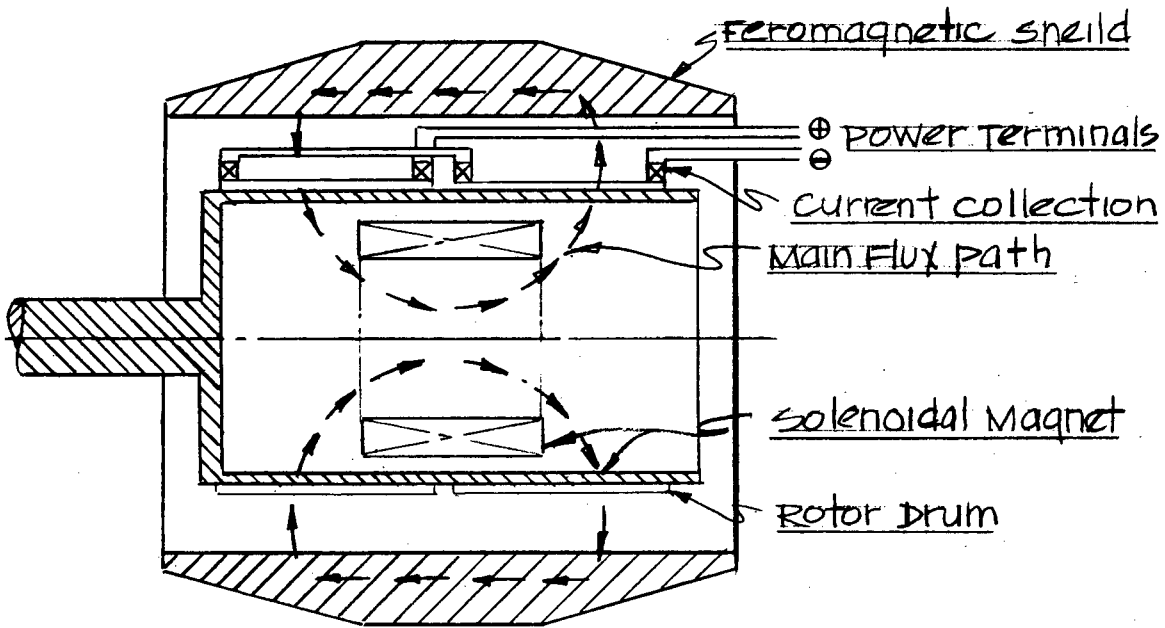


Figure 1

SHAPED FIELD MACHINE CONCEPT

Similarly, high flux utilizations are possible with internal magnet disk rotor machines which incorporate current collectors at inner and outer disk perimeters. The shield is sliced to provide narrow passages for the disk conductors which rotate when the radial current couples with the axial flux. The drum configuration is preferred, however, since it permits the reduced stray fields possible with a nonsegmented shield and is more easily adapted to high conductivity liquid metal current collectors. The improved flux utilization of an internal magnet design, coupled with the high current levels in compact liquid metal brushes, accounts for the attractive power density characteristics of the shaped field arrangement.

The capacity and maintainance benefits possible with liquid metal collectors point up a second desirable feature of the shaped field arrangement, the ability to locate brush sites in low magnetic field regions. In conventional arrangements the collector fluids, located in the magnet bore where the field is most intense, will experience severe field induced torques with correspondingly large viscous drag losses. This major source of inefficiency can be virtually eliminated in the shaped field machine and an improved efficiency characteristic results.

The opportunity to use a small, centrally located magnet-dewar assembly provides additional benefits. The cylindrical dewar, without a warm hole as in previous d-c designs, can be built with a very low heat leak, reducing refrigeration requirements and further improving efficiency. It is also protected by an almost invulnerable set of steel and copper shells and inherently rugged machine construction results.

LABORATORY MACHINE DESIGN

Major design features of the shaped field laboratory machine are shown in figures 2 and 3 in cross-sectional and isometric views. The solenoidal superconducting magnet is enclosed in the double walled, vacuum insulated, helium dewar supported by the rotor at one end through an idler bearing. At the opposite end, the dewar neck, which contains the helium inlet and exhaust lines and power leads, is rigidly attached to one bearing housing. The winding includes 13,340 turns of 0.030-inch outside diameter filamentary niobium titanium superconductor providing magnetomotive forces approaching 2 million-ampere turns.

The inline sets of four concentric drum conductors are symmetrically located about the magnet center plane and epoxy bonded to the outer surface of the stainless steel rotor shaft. The eight copper rotor drums are insulated from each other and from the shaft permitting connection in electrical series through liquid metal brushes and a similar arrangement of copper current return drums in the stator. Stator drums and terminal rods are bonded to the ferromagnetic shield.

Flux generated in the solenoid by the circumferential field current is attracted to the steel shielding. Entering the iron radially, flux

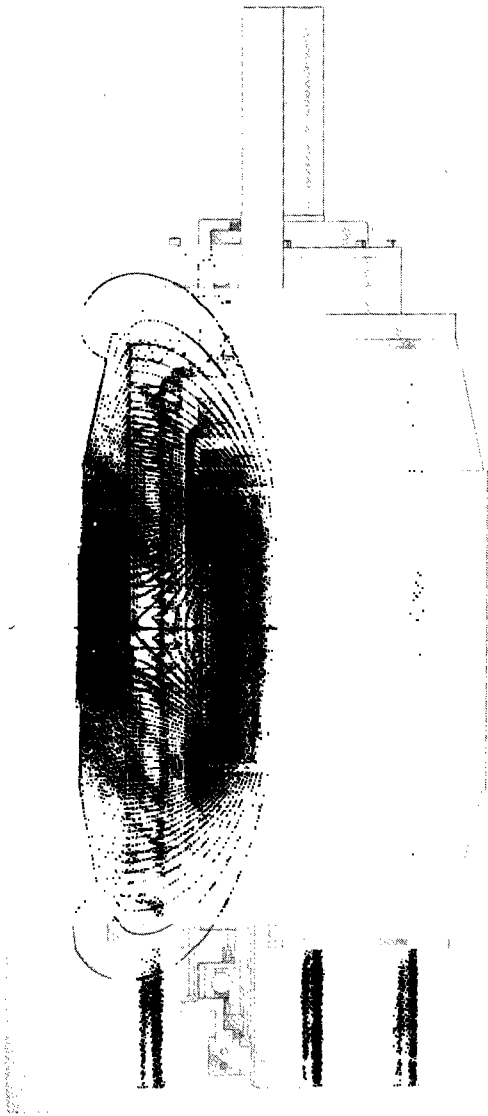


Fig. 2 — Motor cross section with flux plot.

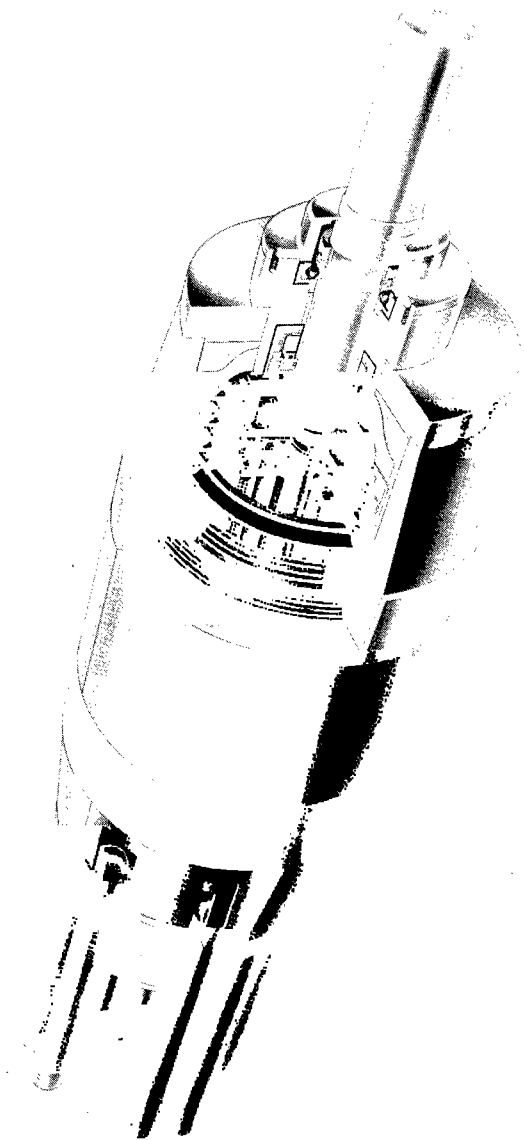


Fig. 3 — Shaped field laboratory motor isometric.

proceeds axially through the iron to the other end of the machine, returning radially to the magnet bore to complete the path. Although fields of 55,000 to 70,000 gauss exist in the magnet the superimposed flux map in figure 3 indicates extremely effective flux containment, with stray fields outside the shield limited to less than 100 gauss. Field lines are concentrated in the active drum regions and widely spaced at the collector sites, illustrating the flux utilization and loss suppression benefits of the shaped field arrangement.

When voltage is applied at the terminal rods, the resultant axial current flow in each rotor drum interacts with the adial field producing a circumferential torque. The cumulative torque developed in each drum is coupled to the output shafting through the drum-to-drum and drum-to-shaft insulated bonds. Reaction torque produced in the stator drums is transmitted through the shielding to the machine mounting points.

The brush work includes 16 copper rotor disks, two on each drum, each rotating in stator channels with the disk/channel gap bridged by liquid sodium-potassium eutectic (NaK). The collector geometry can be seen in figure 4 which illustrates machine assembly.

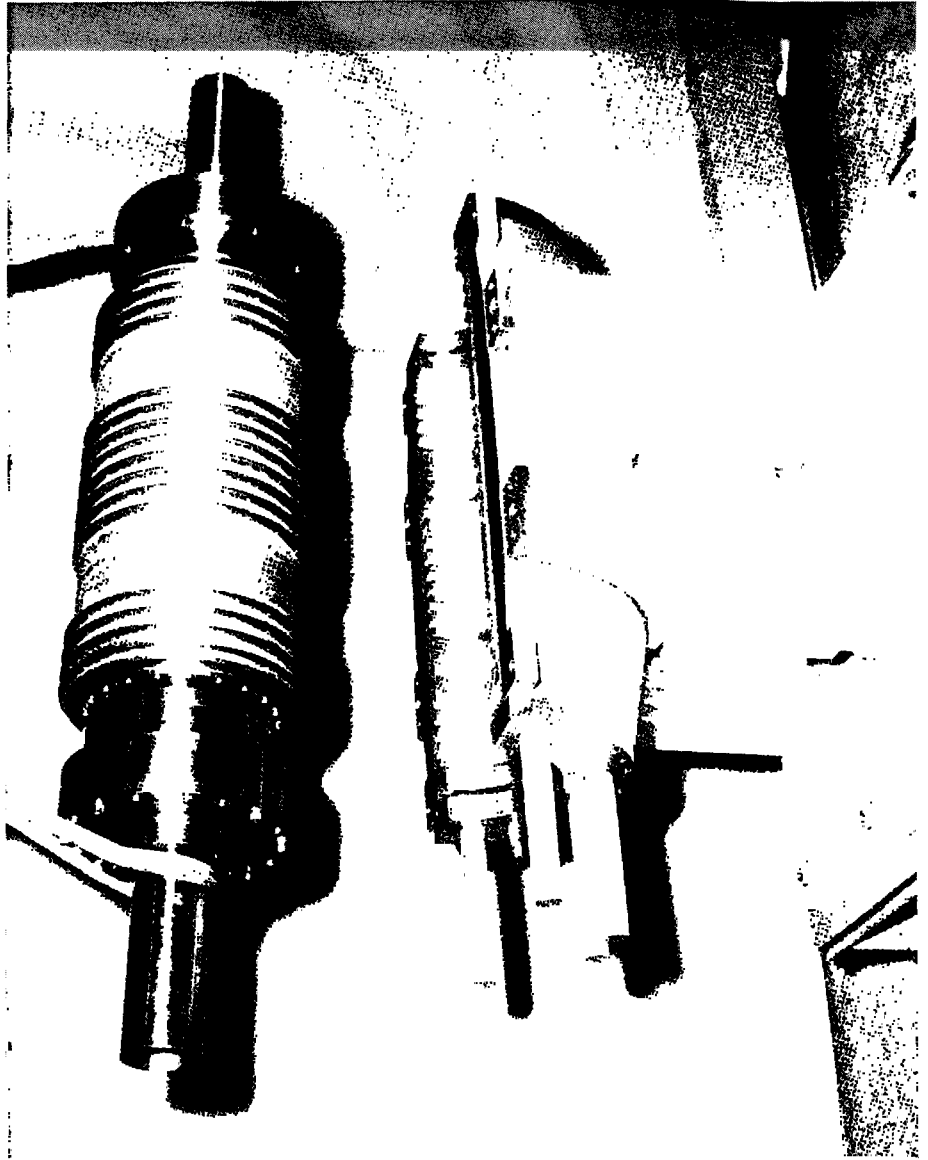


Fig. 4 — Rotor placement in bottom stator half.

The stator channels are grooves cut into copper stator rings, two annular rings electrically bonded to each stator drum. An unflooded operating mode is employed with no external NaK circulation. Small quantities of liquid metal, sufficient only to assure uniform contact around the disk/channel annulus are injected into each channel with centrifugal and magnetohydrodynamic (MHD) forces providing for NaK distribution. The fluid pools at the bottom of each channel during periods of nonoperation. A dry, oxygen-free cover gas maintains long-term NaK purity.

A nonconducting coolant fluid is circulated through parallel tubes in the stator rings to remove resistance and viscous drag generated heat. Most of the heat originating in the rotor is transferred by conduction to the stator rings across the liquid metal collectors, with a lesser portion radiated and convected to the stator drum assembly and the fluid cooled dewar surface.

The completed machine, shown in figure 5, weighs 1050 kg (2300 pounds) and displaces 0.17 cubic meter (6 cubic feet), with a (maximum) 51 cm (20 inch) diameter at the machine center plane. The shield is 76 cm (30 inches) long and the bearing housings add an additional 10 cm (4 inches) at each end of the machine. Output shafting is 10 cm (4 inches) in diameter. The conventional 25-hp drive motor provides a dramatic size comparison with the 400 to 1000 hp superconductive unit.

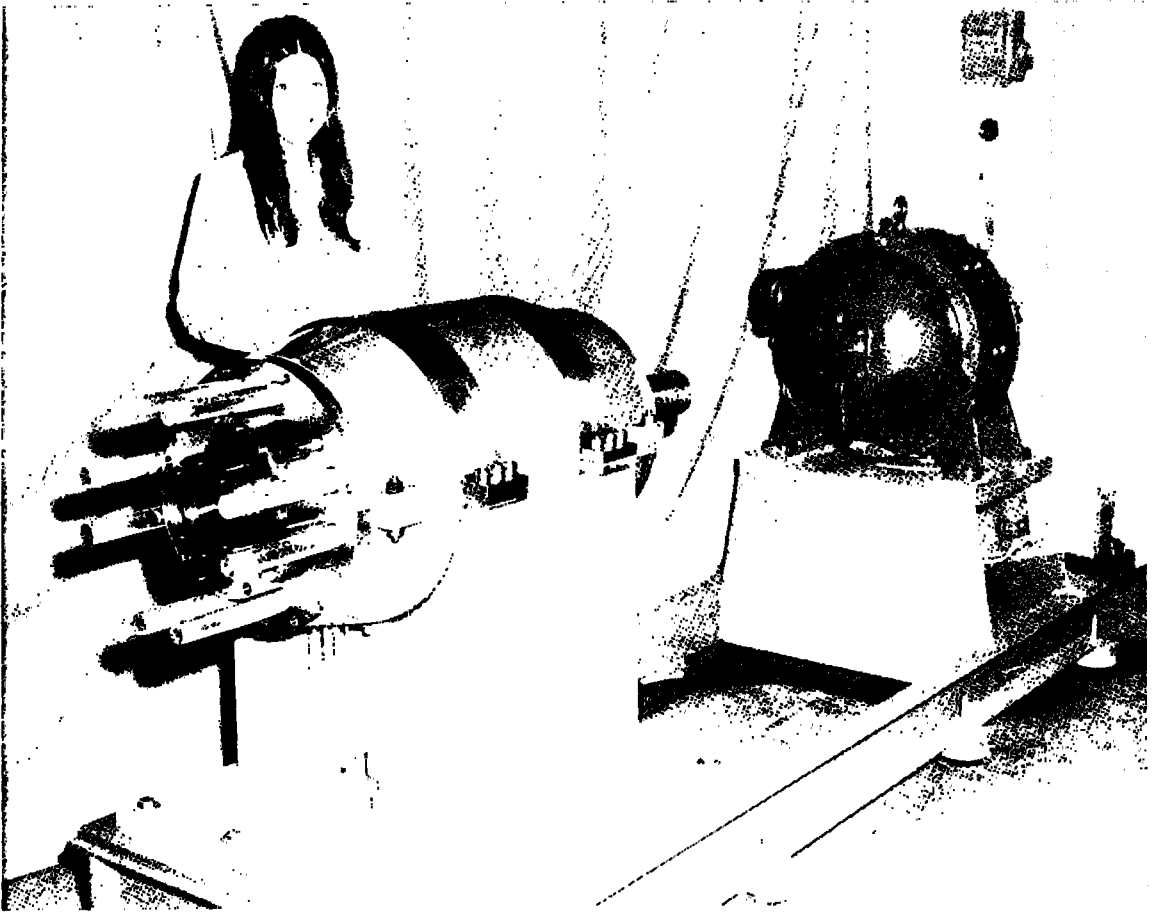


Fig. 5 — Assembled machine being readied for no load testing.

MACHINE LOSSES

Loss mechanisms in the laboratory acyclic motor can be conveniently divided into two categories: ohmic losses in the armature circuit and drag losses from collector, windage, and bearing effects reducing output torque.

Ohmic losses are proportional to circuit resistance, estimated at 30 micro-ohms in the laboratory motor. This extremely low resistance results from the use of large copper cross sections (30 to 35 cm²) and NaK collectors, whose contact drops can be rendered unmeasurable by proper surface preparation.

The preponderance of drag losses are attributable to the liquid metal collectors where three separate and distinct loss mechanisms can be identified. The normal viscous shear loss becomes a cubic function of rotor speed since the relatively narrow collector gap assures turbulent flow, these will not exceed a few kilowatts in the 1800 to 2400 r/m range appropriate to motor operation.

The two remaining losses result from the presence of axial and radial magnetic fields in the collector regions. The axial field component interacts with the radial transport current with a consequent tangential (MHD) body force experienced in the collector fluid. The resulting acceleration of the NaK provides an additional fluid shear loss proportional to the square of the local axial field. This axial field in the motor configuration, however, is in the order of 1000 gauss and the predicted losses of a few watts per site can be safely neglected. In contrast, similar collectors operating in the 40,000 to 60,000 gauss fields present in a conventionally arranged superconductive machine could generate Lorentz losses of 200 to 400 kilowatts.

The final collector loss mechanism considered results from the radial magnetic field in the collector region. The radial field component generates an axial voltage differential across the brush tip in the same manner as in the drum conductors. This collector disk voltage, however, is shorted to the stator ring through the liquid metal, and an entropy-generating current loop is established across the collector gap. In the laboratory motor the radial fields in the collectors are also quite low, in the order of 3000 gauss. With proper disk insulation these circulating current losses are limited to a few kilowatts.

OPERATING POINT PERFORMANCE

Two operating points have been selected for motor load testing, one dictated by rectifier current limits and the other consistent with turbo-generator capacity and propeller speed requirements in the test bed vehicle system. Estimates of machine performance at these two points are summarized in table 1, with significant electric and magnetic circuit parameters included. Losses, discussed above, appear quite manageable

permitting efficient operation at high-power density. The predicted motor performance over a wider range of power, speed, and efficiency conditions is included in figure 6.

TABLE 1

SHAPED FIELD MOTOR OPERATING POINT PERFORMANCE ESTIMATES

			Powered	
			Rectifier	Turbo-generator
Machine Performance	Input	: Terminal Voltage	31.74	30.11
		Load Current, A	10,000	25,000
		Power, kw	317.4	752.6
	Output	: Rotor Speed, r/m	2,400	1,800
		Torque, N-m	1,215	3,865
		Power, hp	410.2	976.5
	Power Den	: hp/m ³	2,400	5,750
hp/kg		0.39	0.93	
Magnetic Circuit Data	Efficiency	: %	96.4	96.8
	Magnet	: Field Current, A	121	150
		Generated Flux, webers	0.139	0.172
	Rotor	: Effective Flux, webers	0.098	0.120
		Flux Utilization, %	70	70
	Shield	: Maximum Field, gauss	14,400	18,000
		Stray Field at 6 inches, gauss	15	19
Electric Circuit Data	Curr Den	: Rotor Drum, A/cm ²	320	805
		Stator Drum, A/cm ²	280	695
		Terminal Drum, A/cm ²	275	685
		NaK Brush, A/cm ²	515	1,290
	Circuit	: Resistance, 10 ⁻⁶ ohms	30.3	30.3
		Back EMF, volts	31.35	29.25
Machine Losses	Elect Circ Collector	: Ohmic, kw	3.03	18.94
		: Viscous, kw	4.29	1.81
		MHD, kw	0.02	0.21
		Circ Curr, kw	3.27	2.85
	Windage	: kw	0.07	0.04
	Bearings and Seals	: kw	0.70	0.52
	TOTAL	kw	11.64	24.37

135

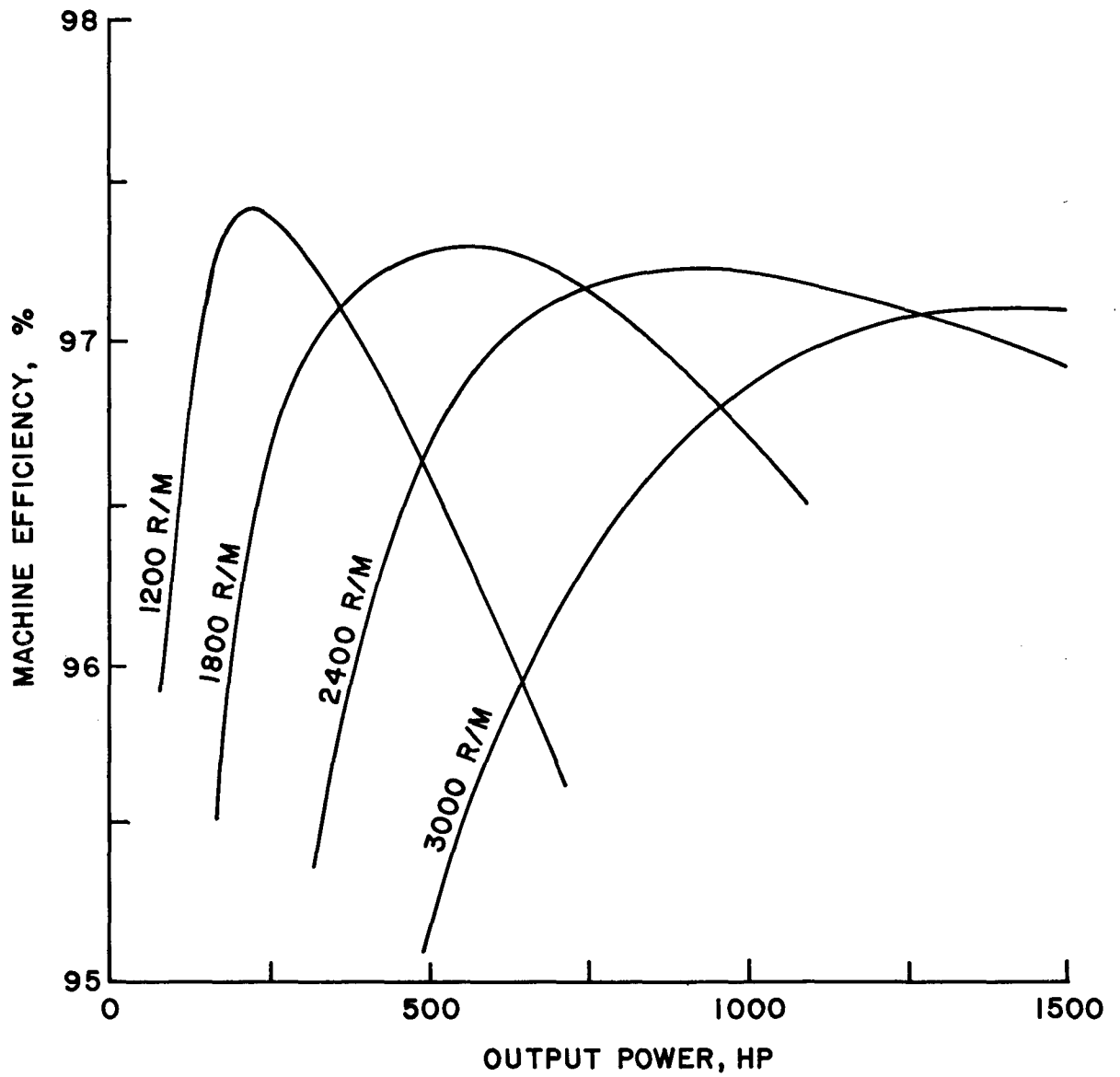


Figure 6 — Estimated Motor Performance (150-Ampere Field Current).

References

1. Levedahl, W. J., "Superconducting Naval Propulsion System," NSRDC/A, presented to Applied Superconductivity Conference (ASC), 1 May 1972
2. Appleton, A. D., "Status of Superconducting Machines at IRD," IRD Co. Ltd, England, presented to ASC, 1 May 1972
3. Fox, G. R., and B. D. Hatch, "Superconductive Ship Propulsion Systems," GE Co., presented to ASC, 1 May 1972
4. McCann, E. F., and C. J. Mole, "Superconducting Electric Propulsion Systems for Advanced Ship Concepts", Westinghouse Electric Corp., presented at the Advanced Marine Vehicles Meeting, Annapolis, Md., July 17-19, 1972
5. Levedahl, W. J., and T. J. Doyle, "Superconductive Machinery for Naval Propulsion Systems", presented at the 1972 IECEC, 5 Sep 1972
6. Doyle, T. J., "Magnetically Shielded Electric Machine with Superconductive Field Windings," US Patent No 3,657,580, 18 Apr 1972

ACYCLIC SUPERCONDUCTIVE GENERATOR DESIGN

Leroy T. Dunnington
Howard O. Stevens
Michael J. Superczynski

Naval Ship Research and Development Center
Annapolis, Maryland 21402

INTRODUCTION:

This paper will present a description of the design of a superconductive acyclic generator which is intended to supply power to the motor described in the previous paper by Mr. Doyle.¹ Included are descriptions of work done at NSRDC in the area of superconducting coil construction and liquid metal current collector technology which contributed significantly to the generator design. A brief description of the planned test program for superconducting machinery at NSRDC is also included. As this paper is intended to be a companion to those of Mr. Doyle and Dr. Levedahl², areas covered by these papers are generally avoided.

The boundary conditions for design of this generator were fixed by the output requirements dictated by the superconducting motor, and the input requirements dictated by the selected prime mover - an LM-100 marine gas turbine. These are as follows:

Output - 30 volts at 10,000 to 30,000 amps
Input - 19,500 rpm at 400 to 1000 hp

The lower power figures represent the nominal design point of the motor and the higher represent the anticipated thermal limits of the motor.

Within these boundary conditions we determined that the generator should represent the highest performance that available technology could provide with the proviso that no aspect of the design would be incompatible with the requirements of a shipboard propulsion system component. Therefore, the superconducting coil, current collectors, coolant system, and rotating elements are all called upon to perform at very high levels - but in a reliable manner. The superconducting coil is designed to provide a maximum of useable flux with a minimum weight, thus minimizing the structural heat leak to the liquid helium coolant. Non-cryogenic liquid cooling is used directly near the sources of heat, to allow a compact structure in the non-cryogenic electrical circuit. Liquid metal current collectors are used at very high surface velocities and current densities. The rotor is run at gas turbine output speed, to eliminate any gearing and provide the maximum voltage with the available flux. Numbers will be attached to these adjectives later.

GENERATOR CONCEPTUAL DESIGN:

During the initial design stage of this generator many of the available options were considered - e.g. external magnet vs internal magnet¹; disc rotor vs drum rotor; solid brushes² vs liquid metal current collectors; active³ vs passive shielding, and other less obvious choices. The particular combination of elements and their arrangement described in this section was selected on the basis of resulting in the most compact, lightweight, and efficient generator design.

An overall view of the general arrangement of the generator is shown in conceptual form in figure 1. Major features of this design are as follows.

The rotor structure is internal with respect to the magnet winding. This arrangement is dictated by the desire to run the generator at gas turbine speed (19,500 rpm), and the consequent high rotor stresses, which grow larger with increasing rotor radius. Location of the rotor outside the magnet would make these stresses intolerable due to the large radius required, and the fact that good conducting materials with relatively low mechanical strength must be used in rotor construction.

A quadripole magnet configuration was selected to maximize the flux produced through the rotor and minimize the number of current collectors. Since a single rotor element can intercept the flux produced by two solenoids, the number of current collectors required to generate a given voltage is one half the number associated with a single solenoid field magnet configuration, to first approximation. The quadripole magnet has the additional advantage of producing an external magnetic signature which decreases more rapidly with distance than solenoid field.

Liquid metal current collectors consisting of a disc attached to the rotor, meshing with a channel attached to the stator, with the gap between them filled with liquid sodium-potassium eutectic, were selected for this generator. The high current densities (3 to 10 thousand amps/sq. in.) and high surface speeds required of these current collectors, excluded the use of any known solid brush material, for reasons of efficiency and size of the current collectors.

A ferromagnetic iron shield is used to confine the magnet flux to the generator envelope. Although the shield represents more than two-thirds to the machine weight, the compactness and slight enhancement of the flux distribution, compared to that obtained with active shielding makes this an acceptable trade off. Although necessary for naval applications generator shielding could be eliminated in applications where very high local fields near the generator could be tolerated.

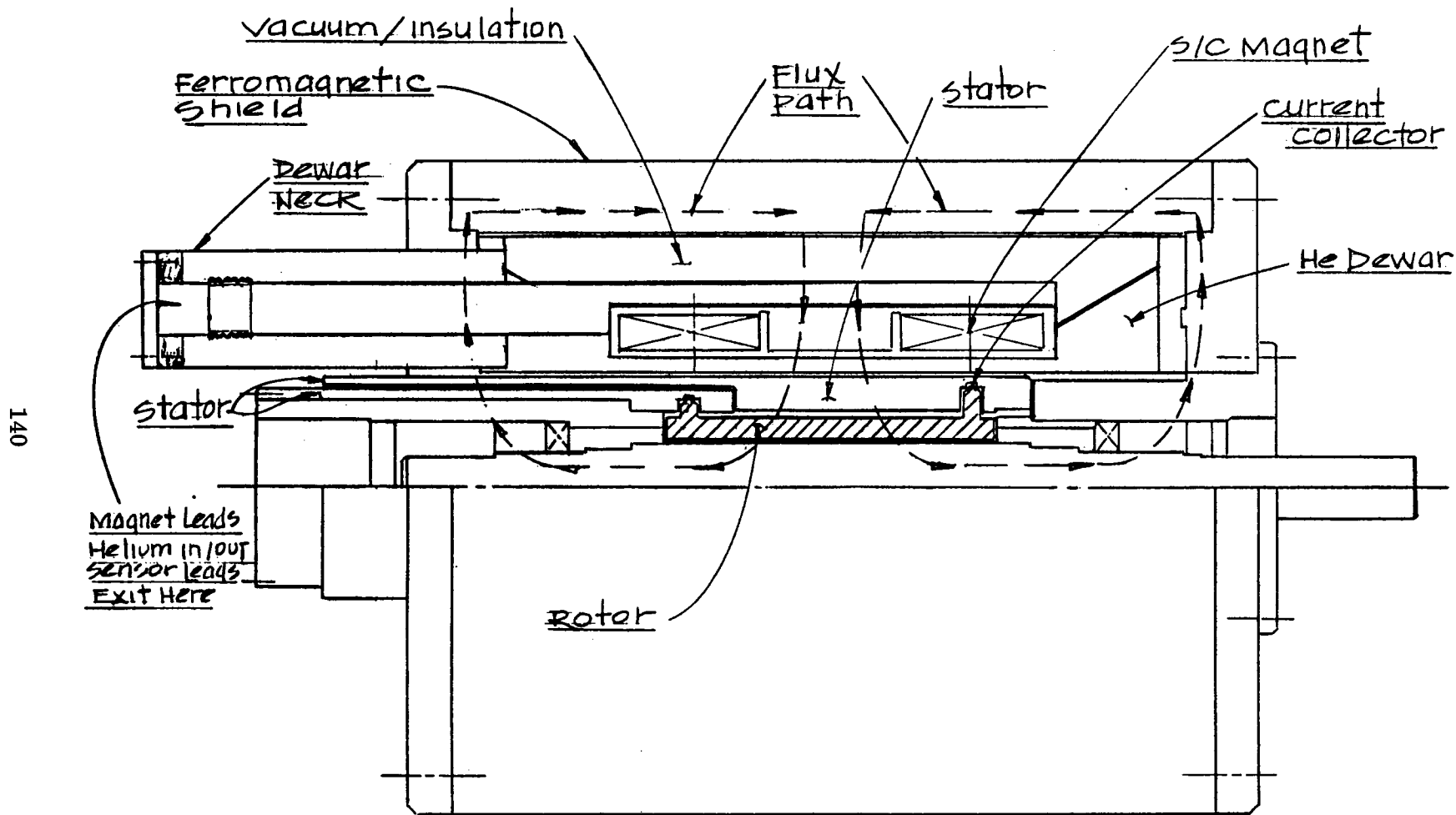


Fig. 1 — Superconducting Acyclic Generator' Conceptual Arrangement

The rotor - stator current path through the generator is arranged in an approximation to a coaxial transmission line. This geometry should effectively negate the magnetic field generated by the load current, at the magnet location, and prevent any interference with the magnet operation due to transient loads.

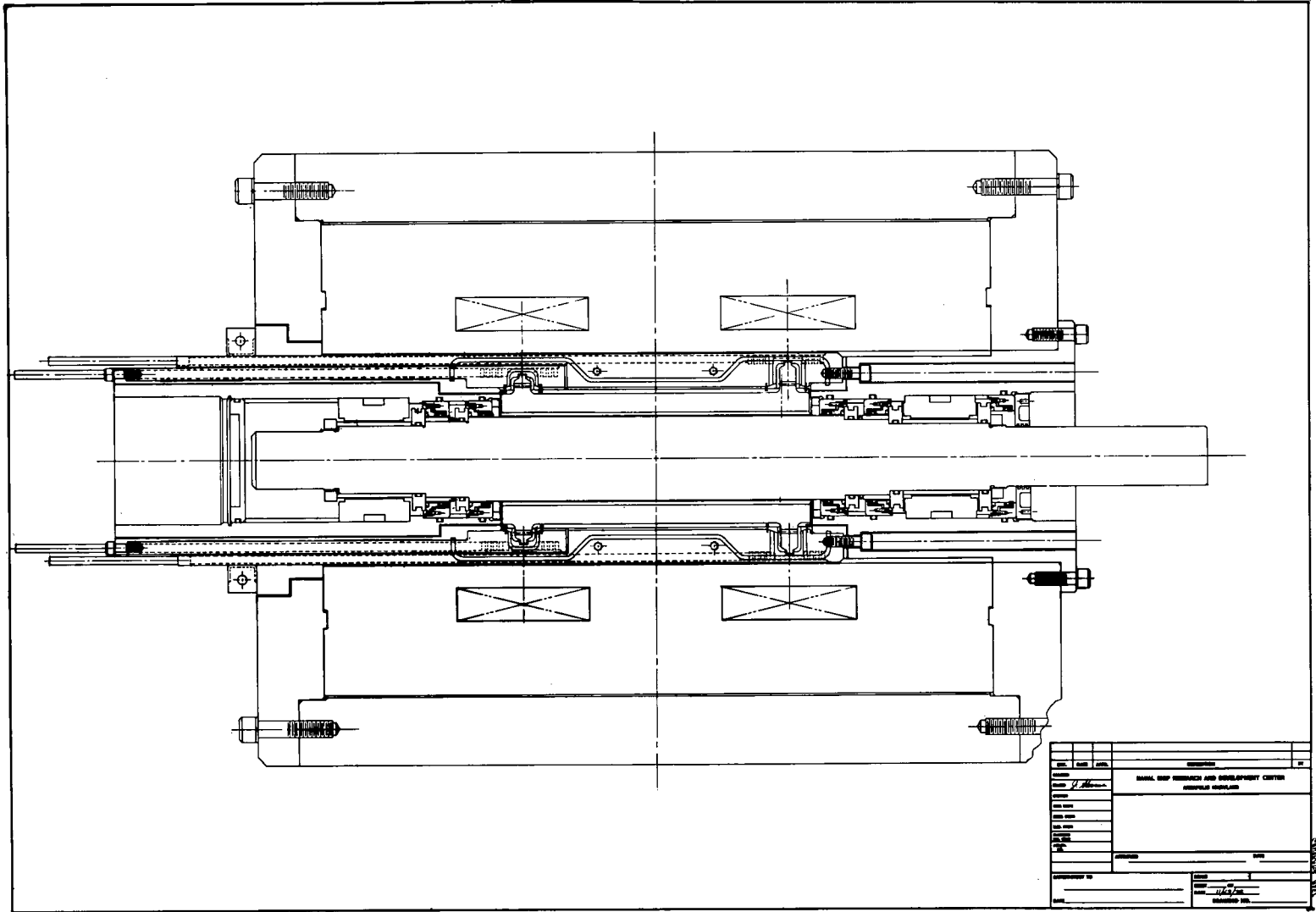
DESIGN DETAILS:

Figure 2 is a detailed assembly drawing of the superconducting generator. The dashed lines in this figure represent the path of the non-cryogenic liquid coolant. Coolant will enter via tubes extending axially from the stator, flow through channels to the collector regions, and traverse circular channels which run parallel to the collector channels. Since most of the heat generated in the generator comes from the current collectors, it is necessary to maintain very close proximity of the coolant to this source of heat to prevent large thermal gradients between the two. With reference to figure 1, the major generator parts in figure 2 may be identified.

The rotor and stator electrical circuit is formed by the two concentric stator pieces which contact each end of the rotor through liquid metal current collectors. A copper cross section of approximately 6.6 square inches is maintained through the electrical circuit, except in the current collector region where the cross section for current flow is 3 square inches. Zirconium copper was selected as the rotor and stator material due to its high strength and electrical conductivity.

The shield and shaft are made of magnetic 1010 steel and serve to reduce the reluctance of the flux path and magnetically shield the machine. The shield is also the basic structural element of the generator. Bearing housings located at each end of the rotor/stator structure serve to transfer torque to the shield from the stator, maintain shaft alignment and house the bearing and shaft seals. The bearing housings are constructed of non-magnetic material to eliminate any large forces on them due to the magnetic field. Electrically insulated mechanical joints are incorporated at various points in the structure to isolate the electrical portions of the generator from the structural parts, and to eliminate eddy currents through the bearings and seals. Although not indicated in figure 2, angular contact high precision ball bearings will be used, with oil mist as the lubricating agent.

The use of liquid NaK as the current collection material requires that the interior of the generator be kept under an inert atmosphere, and that contaminants such as oil, water vapor, etc., be prevented from entering the collector region. To accomplish this a double seal system is used at each end of the shaft. The inboard seal is a hydrodynamic face seal which confines the cover gas with extremely low leakage. The outboard seal is a special labyrinth which prevents migration of the bearing lubricant to the face seal. The space between the two seals will be purged with dry air. A positive pressure gradient will be maintained across each seal with the inboard pressure being highest.



DATE	1/14/78	REV	1
BY	J. H. ...	CHKD	J. H. ...
APP'D	J. H. ...	DATE	1/14/78
GENERAL ENGINEERING			
DARPA, ONR RESEARCH AND DEVELOPMENT CENTER			
DURHAM, NORTH CAROLINA			
PROJECT NO. ...			
DRAWING NO. ...			
SCALE ...			
MATERIAL ...			
TOLERANCES ...			
SURFACE FINISH ...			
WELDING ...			
PAINT ...			
ASSEMBLY ...			
REVISIONS ...			
REVISION NO. ...			
REVISION DATE ...			
REVISION DESCRIPTION ...			

Figure 2
Acyclic Superconductive Generator Assembly Drawing

The liquid metal current collectors were designed using a combination of experience gained in the NSRDC experimental program to be described later and the theoretical models developed by Rhodinizer⁴. The present collector configuration is shown in cross section in figure 3.

The magnetic circuit design for the generator was accomplished with the aid of computerized flux/field calculations, the results of which are shown in the flux plot in figure 4. This flux plot represents the field distribution in one quadrant of the generator, and includes the effects of iron saturation. The superconducting magnet design is again the product of the in-house experimental program at NSRDC. The magnet consists of two identical solenoids mounted on a common form with opposing magnetic moments. Each solenoid consists of 5640 turns of .022" X .028" stranded, twisted, NbTi superconducting wire with a 1.8/1.0 copper to superconductor ratio. The coil was designed for a nominal operating current of 135 amps, which will produce more than sufficient flux for generator design point operation. The entire magnet winding is potted in epoxy to prevent wire motion. Additional magnet data is given in a following section of this paper.

The dewar for the superconducting generator is designed to minimize the refrigeration requirements while providing sufficient mechanical support for the superconducting coil to sustain a 15 g shock load and avoid the presence of critical vibration frequencies over the speed range of the generator. The dewar is in the form of a thick walled hollow cylinder with the dewar neck extending between the inner and outer radii as shown in figure 1. A stainless steel shell welded directly to the coil form creates the helium reservoir. Super-insulation and two vapor cooled shields are included in the vacuum space to reduce heat leak. The magnet leads are also vapor cooled with the helium boil-off gas. The magnet is supported within the dewar structure by eight .0125" diameter X 4" long titanium alloy rods, four at each end, extended from the coil form to the end walls of the dewar. Each support rod is thermally shorted to the vapor cooled shields and is externally adjustable to allow the magnet to be located precisely within the shield to eliminate any unbalanced magnetic forces. The calculated heat leak into the dewar is equivalent to 0.7 liters of liquid helium per hour, including 0.4 liters/hour for the current leads to the magnet.

Table 2 is a summary of the physical and predicted performance parameters of the generator design.

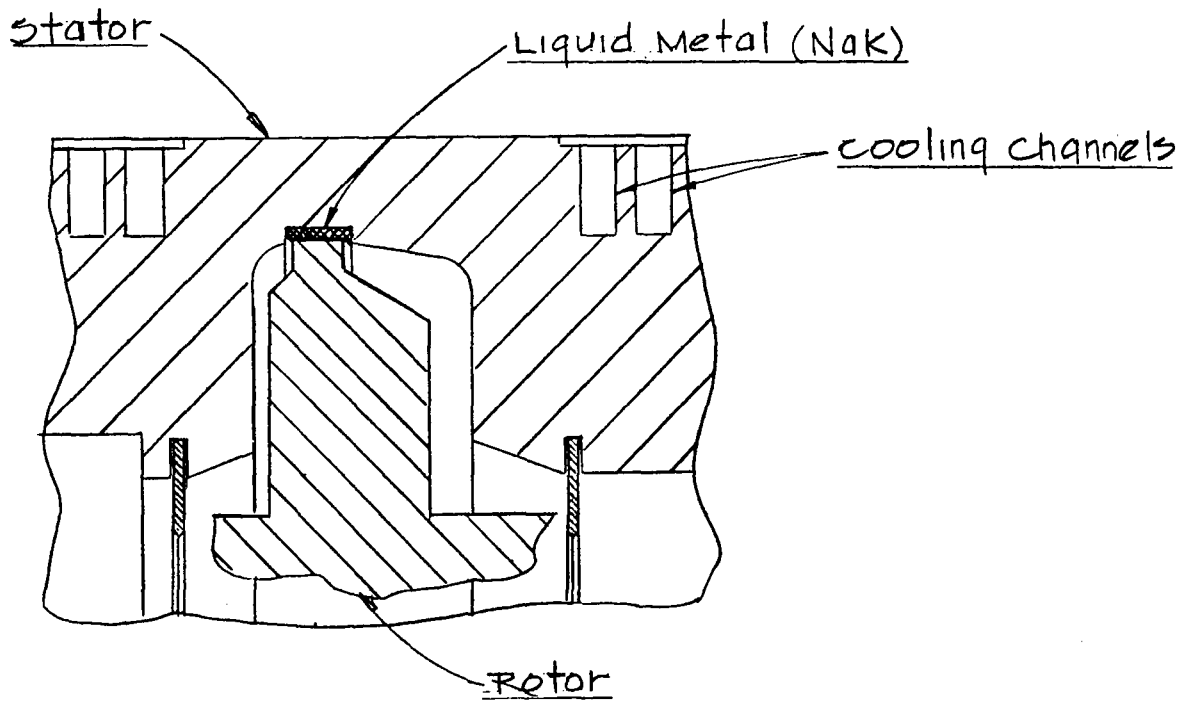


Fig. 3 — Liquid Metal Current Collector For Super
Conducting Acyclic Generator

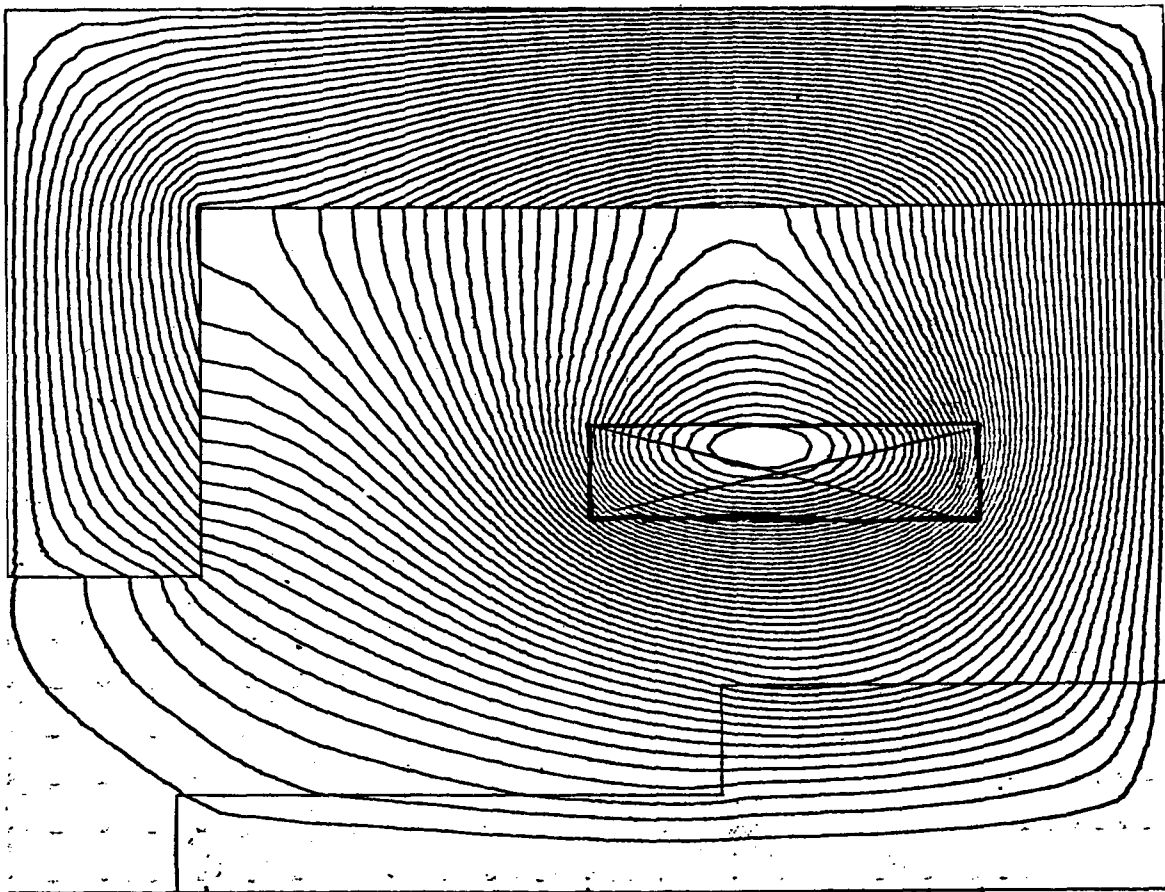


Figure 4

Magnetic Flux Plot for one Quadrant
of Acyclic Superconducting Generator

TABLE 2
GENERATOR PARAMETERS

Input:	400 to 1200 hp @ 19,500 rpm
Output:	300 to 900 kw @ 30 volts
Estimated efficiency:	97-98%
Dimensions:	18" dia. X 26" long
Weight:	1200 lb
Magnet:	2 coils, each 7.6" ID X 9.6" OD X 4"L
Design current:	135 amps
Quench current:	160 amps (calculated)
Operating current	@ 30 volts generator output - 94 amps
Maximum field	@ 135 amps 56 kilogauss
No. turns	5640 each coil
Current density (overall)	29,000 a/cm ² @ 135 amps
Total Inductance	11.9 Henrys
Dewar Heat Leak	0.7 liters/hr liquid He
Internal Machine Resistance	5 micro-ohms
Current Collector Material	Nak - 78 eutectic
Current density in conductors	1500 to 4500 a/in ²
Current Collector surface velocity	480 ft/sec @ 19,500 rpm
Coolant/Flow rate	"Coolanol" silicone oil-7000 lb/hr
Maximum hot spot temperature	rotor centerline 270°F

SUPERCONDUCTING MAGNET DEVELOPMENT

This section is devoted to a brief description of work being done at NSRDC to improve the performance potential of superconducting magnets for motors and generators. The generator magnet described briefly in the previous section is one product of this effort. The principal thrust of this effort has been to develop methods for winding and potting superconducting magnets to increase the mechanical integrity of the structure and prevent wire motion under the tremendous forces existing in high current density magnets. Figures 5 thru 14 show the various stage of coil winding. These figures show the generator coil form in the winding machine with the lead-in wire epoxied into place. The coil form is machined from a single 316 stainless steel forging and designed to withstand the 45,000 lb repulsive force between coils. Figure 6 shows the coil with a half-completed layer of wire over the 3 mil fiber glass cloth which is inserted between layers of the winding. The wire is insulated with .8 mils of formvar coating. Figure 7 indicates the methods for application of a voltage tap in the windings. This tap is also used to attach shunts across the coil to absorb energy during a quench. Figure 8 shows a completed winding/note the configuration of the current lead into the winding. Figure 9 shows the finished coil before potting. The external fiberglass wrap supplies additional strength to resist hoop forces. Figure 10 shows the application of a thin steel band around the coil. After potting, this band is removed and a smooth even surface is obtained on the outside of the coil. The banding also

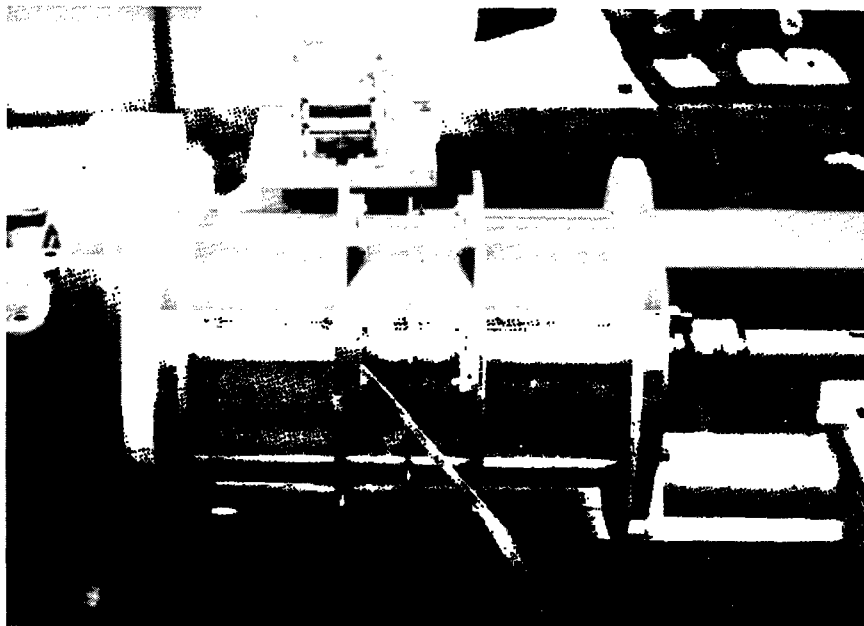


Fig. 5 — Superconducting Magnet Coil Form



Fig. 6 — Superconducting Coil in Winding Process



Fig. 7 — Attachment of Voltage Tap
to Superconducting Wire

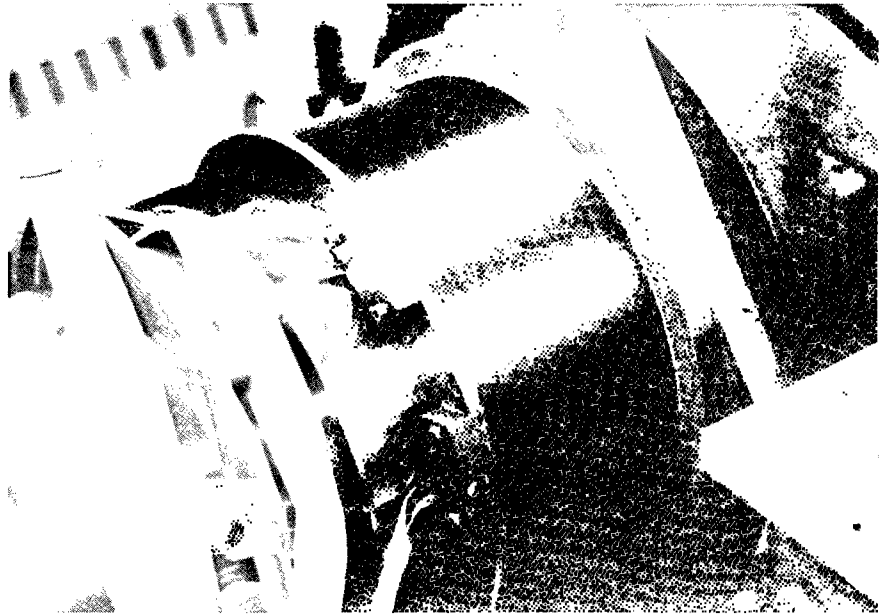


Fig. 8 — Completed Superconducting Coil Winding

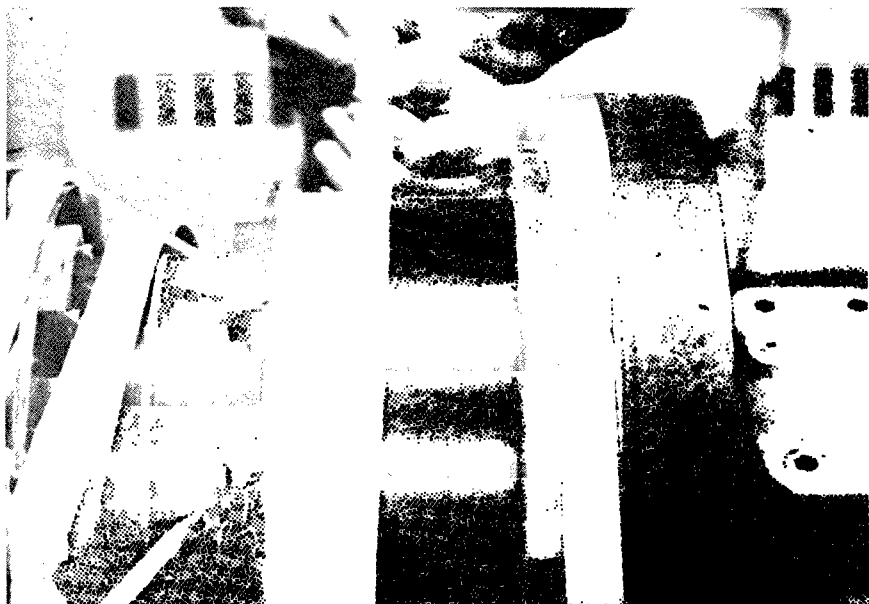


Fig. 9 — External Fiberglass Wrap Being Applied to Finished Superconducting Coil Winding

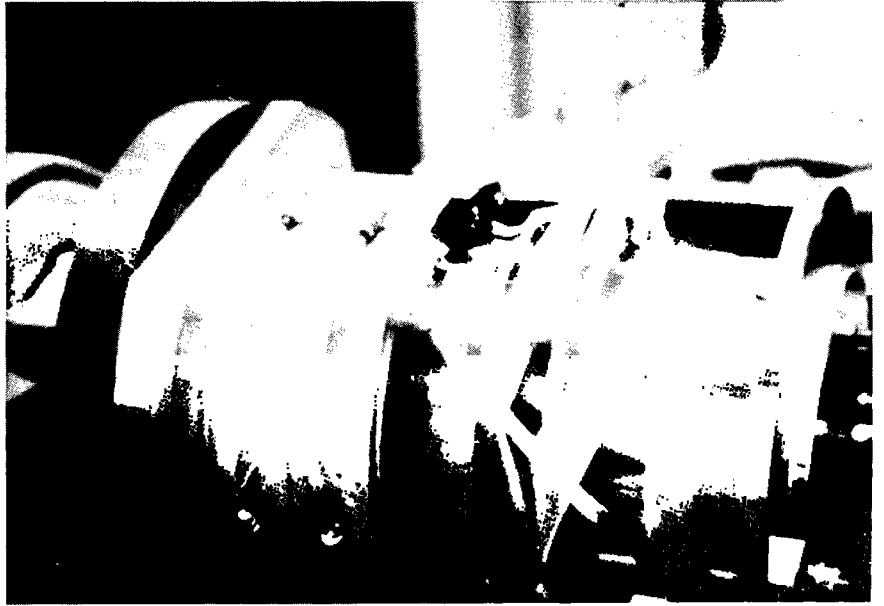


Fig. 10 — Temporary Steel Banding Applied to Superconducting Coil Prior to Potting

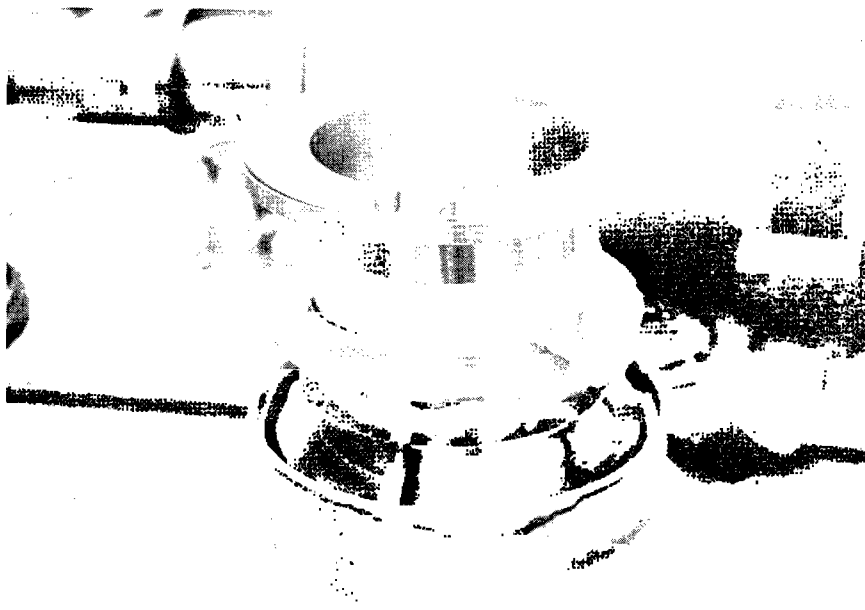


Fig. 11 — Superconducting Coil in Mould for Potting



Fig. 12 — Completed Superconducting Coil After Potting
and Removal of Bands and Excess Epoxy



Fig. 13 — Enlarged Cross Section of
Epoxy Potted Test Coil

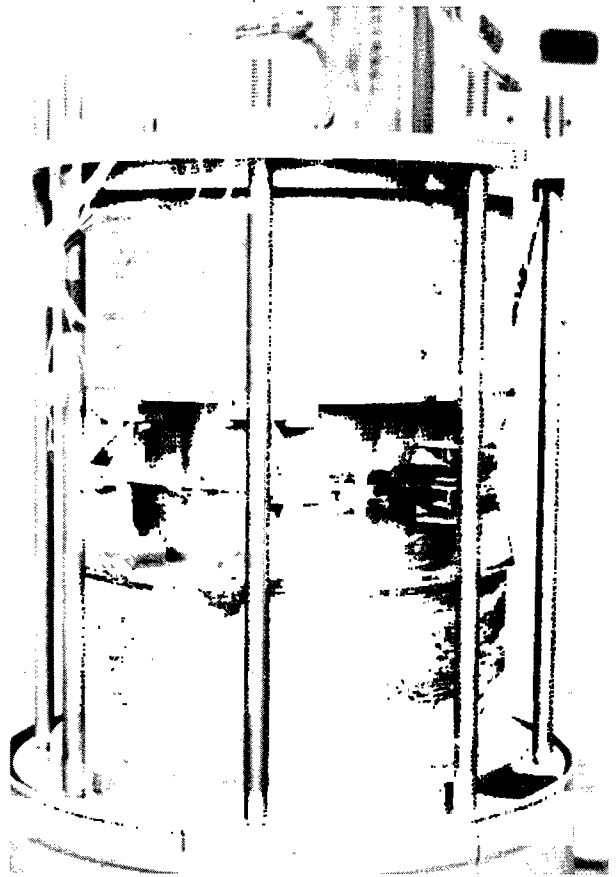


Fig. 14 — Completed Superconducting Magnet
for Acyclic Generator Prepared for Testing

allows excess epoxy to be chipped off the coil without damaging the windings. Figure 11 shows the coil in a potting mould. This is placed in a vacuum chamber and after evacuation, the epoxy is poured into the mould, without interrupting the vacuum. When the coil is completely immersed in the epoxy, gas pressure is applied to assist the epoxy flow into the winding, and heat is applied to cure the epoxy. Figure 12 shows the coil after potting, with the steel bands and excess epoxy removed. Figure 13 is a microphotograph of a test sample cross section indicating the excellent penetration and lack of voids in the composite structure. Figure 14 shows the completed generator coil ready for testing. The tie rods are used for testing in lieu of a welded cover which will be applied later to resist the repulsion forces between coils.

Test results indicate that the process described above is effective in providing the desired results, i.e., a superconducting coil capable of operating near the short sample characteristics of the wire itself. The generator coil was tested to 145 amps, limited by the structural integrity of the coil form. Short sample wire data indicates a quench current of 160 amps. Some training was experienced in the coil, but appears to be permanent in nature.

LIQUID METAL CURRENT COLLECTORS

As a part of the motor-generator development effort at NSRDC, an on-going program to develop suitable liquid metal current collectors for such machines has been undertaken. Reference 4 provides a review of the problems one faces in designing an optimum collectors configuration. The theoretical treatment of the turbulent flow hydrodynamic problem and Lorentz force interactions between current and field simultaneously is difficult to the extreme. The only reliable method for ascertaining the proper collector design is through experimental means. To this end, several test rigs simulating current collector operation have been designed, constructed, and used to provide the required information. In addition, methods have been developed for safely handling the liquid metal, and clean-up of the machines when required. Figure 15 is an overall view of a small test rig used to obtain frictional drag and contact resistance data. Results indicate that with proper surface treatment, contact drop between the liquid metal and solid surface in the collector can be reduced to negotiable values. Figure 16 is a close-up of the collector portion of this test rig which shows the channel in which the disc rotates or vice-versa. Over 2000 hours of continuous operation have been obtained on this device with a single charge of liquid metal.



Fig. 15 — Liquid Metal Current Collectors Test
Apparatus-Rotating Channel Life Test

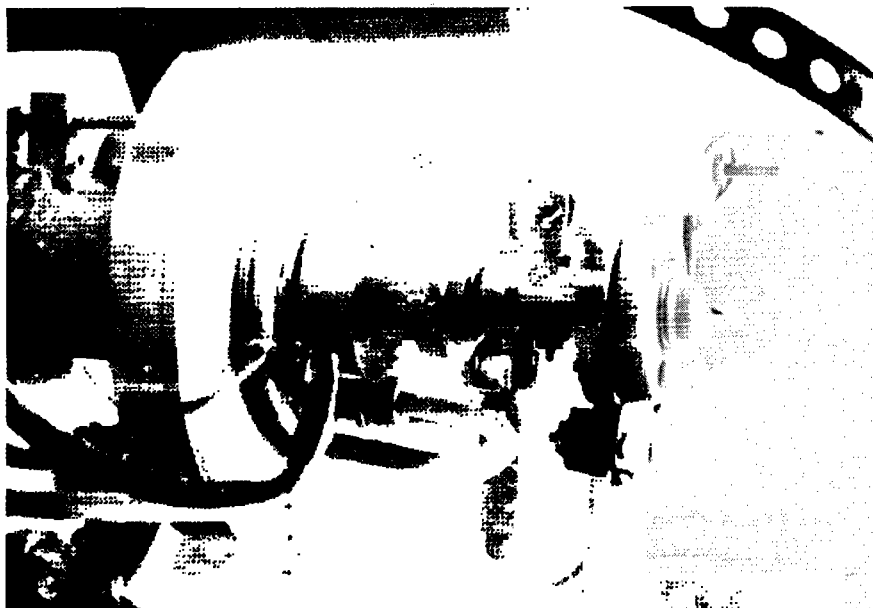


Fig. 16 — Liquid Metal Current Collector Under Test

Figure 17 shows the rotating disc and channel for a large test rig which approximates the dimensions of the current collectors used in the motor described earlier by Mr. Doyle. A second collector is incorporated near the inner radius of the disc to allow the passage of heavy currents through the collectors. Figure 18 is an assembled view of this test rig. Figure 19 shows the same apparatus with a field magnet installed to allow the study of field effects on collector operation. One preliminary result obtained from this test rig is that the viscous drag may be much less at high speeds than theoretically predicted, possibly due to a combination of hydrodynamic instabilities and gas entrapment in the liquid metal.

SUPERCONDUCTING MACHINERY TEST PROGRAM

In addition to the design and construction of 400 to 1000 HP superconducting machinery, the NSRDC program includes the test and evaluation of machinery systems in simulated and actual propulsion system configurations. The previously described motor and the generator described herein will undergo no-load testing to work out any "bugs" in their performance. The motor will then be tested, using a 400 KW power supply and water brake dynamometer load, up to 400 hp level. The generator will be tested to the 400 hp level with the LM 100 gas turbine prime mover and a load resistor. System tests will ensue, which will include operation of the motor and generator up to the 1000 hp level or until thermal limitations are met. Final testing of the motor and generator will be as the propulsion system in a 65 foot test craft as shown in figure 20. This craft will be capable of performing with propulsive power from 400 to 3000 hp, thus also allowing testing of 3000 hp systems now under development by contractors.



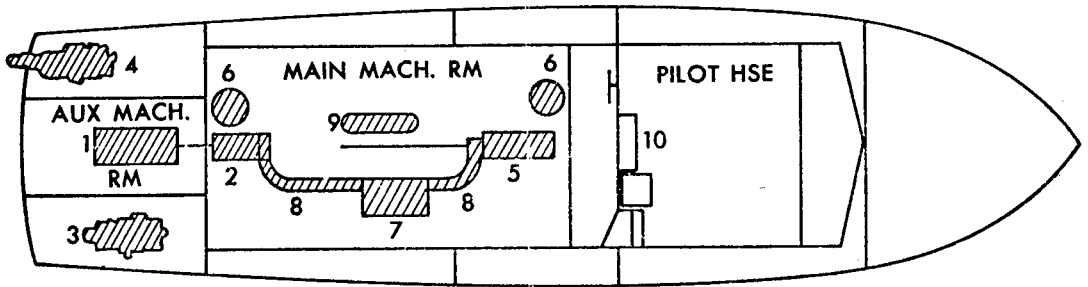
Fig. 17 — Disc and Channel for Rotating Disc Liquid Metal Current Collector Test Rig



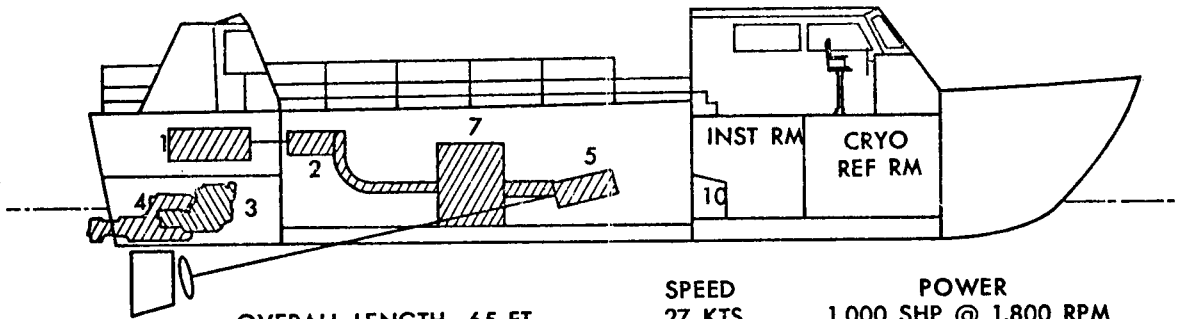
Fig. 18 — Liquid Metal Current Collector Test
Rig Assembly-Rotating Disc



Fig. 19 — Liquid Metal Current Collector Test Rig with Magnetic Field Coil in Place



- | | |
|-----------------------------|---------------------------------|
| 1 GAS TURBINE | 6 HELIUM STORAGE DEWAR |
| 2 SUPERCONDUCTIVE GENERATOR | 7 SWITCHGEAR & RHEOSTAT |
| 3 SHIP'S SERVICE GENERATOR | 8 ELECTRICAL TRANSMISSION LINES |
| 4 'TAKEHOME' POWER PLANT | 9 HEAT EXCHANGER |
| 5 SUPERCONDUCTIVE MOTOR | 10 CONTROL CONSOLE |



OVERALL LENGTH 65 FT
DISPLACEMENT 56,000 LB

SPEED
27 KTS
47 KTS

POWER
1,000 SHP @ 1,800 RPM
3,000 SHP @ 1,200 RPM

Fig. 20 — Superconductive Machinery Test Bed Vehicle

REFERENCES

1. M. J. Cannell, T. J. Doyle, S. M. Raphael, "Shaped Field Acyclic Motor Development," presented at CND-CNR Workshop on Naval Applications of Superconductivity, 29 Nov 1973.
2. G. Green, W. J. Levedahl, H. Robey, D. B. Steen, "Performance Advantages of Superconductive Ship Propulsion," presented at CND-CNR Workshop on Naval Applications of Superconductivity, 29 Nov 1973.
3. Appleton, A. D., "Motors, Generators, and Flux Pumps." Cryogenics, June 1969.
4. Rhodinizer, R. L., "Development of Solid and/or Liquid Metal Collectors for Acyclic Machines," Final Report 1 Jan 1970 to 30 September 1971, General Electric Co. NAVSHIPSYSCOM Contract NOOO-24-68-C-5415, 30 September 1971.

UNCLASSIFIED

PERFORMANCE ADVANTAGES OF SUPERCONDUCTIVE
SHIP PROPULSION

G. Green, W.J. Levedahl, H. Robey and D.B. Steen
Naval Ship Research and Development Center
Annapolis, Maryland 21402

Manuscript not available.

SUPERCONDUCTIVITY IN AIRBORNE MINESWEEPING

D. A. Ross
Naval Air Systems Command
Washington, D.C. 20360

UNCLASSIFIED

Manuscript not available